



International Committee for Future Accelerators

Sponsored by the Particles and Fields Commission of IUPAP

Beam Dynamics Newsletter

No. 50

Issue Editor:

J. Urakawa

Editor in Chief:

W. Chou

December 2009

Contents

1	FOREWORD.....	7
1.1	FROM THE CHAIR	7
1.2	FROM THE EDITOR	8
2	LETTERS TO THE EDITOR	9
2.1	BIG TOOLS FOR SCIENCE.....	9
3	THEME SECTION: ILC R&D STATUS.....	11
3.1	ILC DAMPING RINGS R&D AT CESR TA	11
3.1.1	Introduction	11
3.1.2	The CesrTA Research Program.....	12
3.1.2.1	<i>Machine Layout and Optics</i>	12
3.1.2.2	<i>Instrumentation and Feedback Systems</i>	13
3.1.2.2.1	Instrumentation for Low Emittance Tuning and Measurement	14
3.1.2.2.2	Feedback System.....	16
3.1.2.2.3	Electron Cloud Instrumentation	16
3.1.2.3	<i>Electron Cloud Measurements and Simulations</i>	17
3.1.2.3.1	Retarding Field Analyzer (RFA) Measurements and Simulations	17
3.1.2.3.2	Beam Dynamics Measurements and Simulations	20
3.1.2.4	<i>Low Emittance Tuning</i>	24
3.1.2.4.1	Machine Alignment and Beam Position Monitors	24
3.1.2.4.2	Low Emittance Tuning Procedure.....	24
3.1.2.4.3	BPM Upgrade and Systematic Effects	25
3.1.3	Plans for Further Investigations.....	27
3.1.3.1	<i>Mitigation Methods and Vacuum System R&D</i>	28
3.1.3.2	<i>Intrabeam and Touschek Scattering</i>	28
3.1.3.3	<i>Lifetime Measurements</i>	29
3.1.3.4	<i>Ion Effects</i>	30
3.1.3.5	<i>Cloud-Driven Emittance Dilution at Ultra Low Emittance</i>	30
3.1.3.6	<i>Instrumentation for Real-Time Monitoring of Machine Parameters</i>	30
3.1.3.7	<i>Role of Collaborators</i>	31
3.1.4	References	31
3.2	UPDATE ON THE ELECTRON CLOUD SIMULATIONS FOR DAΦNE	33
3.2.1	Introduction	33
3.2.2	Simulation of Single Bunch Instability	33
3.2.3	Conclusions	35

3.2.4	References.....	36
3.3	STATUS OF ATF R&D.....	36
3.3.1	Overview.....	36
3.3.2	Multi-Bunch Beam Injection/Ejection.....	37
3.3.2.1	<i>Cs₂Te Photocathode RF Gun</i>	37
3.3.2.2	<i>Multi-Bunch Beam Extraction from the Damping Ring</i>	38
3.3.2.3	<i>Fast Strip-line Kicker</i>	39
3.3.3	R&D Using the Damping Ring.....	40
3.3.3.1	<i>Low Emittance Tuning</i>	40
3.3.3.2	<i>Upgrade of the Readout System for the Damping Ring BPM</i>	42
3.3.3.3	<i>Study of the Fast Ion Effects</i>	43
3.3.3.4	<i>X-ray SR Monitor</i>	43
3.3.3.5	<i>SR Interferometer</i>	44
3.3.3.6	<i>Optical-Cavity Laser Wire Monitor</i>	44
3.3.4	R&D Using Extracted Beam	44
3.3.4.1	<i>Cavity Beam Position Monitors (BPM)</i>	45
3.3.4.1.1	Nano-BPM.....	45
3.3.4.1.2	ATF2-BPM.....	46
3.3.4.1.3	IP-BPM.....	48
3.3.4.1.4	Cold-BPM.....	49
3.3.4.2	<i>Pulsed Laser Wire System in the Extraction Line</i>	49
3.3.4.3	<i>Wire Scanners</i>	50
3.3.4.4	<i>Optical Transition Radiation Monitor</i>	50
3.3.4.5	<i>Optical Diffraction Radiation Monitor</i>	50
3.3.4.6	<i>Interference Fringe Monitor</i>	51
3.3.4.7	<i>FONT</i>	52
3.3.5	R&D for the Polarized Positron Source.....	53
3.3.5.1	<i>Cavity Compton</i>	53
3.3.6	Acknowledgements.....	54
3.3.7	References.....	55
3.4	ILC POLARIZED ELECTRON SOURCE DESIGN AND R&D PROGRAM.....	56
3.4.1	Introduction.....	56
3.4.2	Laser System Development	58
3.4.3	Photocathode R&D.....	58
3.4.4	Gun Development.....	58
3.4.5	Summary	59
3.5	POSITRON SOURCE R&D STATUS REPORT	59
3.5.1	Description of the Source	59
3.5.2	The Undulator.....	61
3.5.3	The Target.....	62
3.5.4	The Capture Magnet	63
3.5.5	Summary	64
3.5.6	References.....	64
3.6	DESIGN OF INJECTION KICKERS AT LNF	64
3.6.1	DAΦNE Kicker	65

3.6.2	ATF Kicker	66
3.6.3	Conclusions	68
3.6.4	References	68
3.7	STF STATUS 2009	69
3.7.1	Introduction	69
3.7.2	Cryomodule Test of STF Phase-1	70
3.7.3	STF Phase-1 Experiment Results	70
3.7.4	Infrastructure Developments	73
3.7.5	Phase-2 Developments	74
3.7.6	Acknowledgements	76
3.7.7	References	76
3.8	A FACILITY FOR ACCELERATOR RESEARCH AND EDUCATION AT FERMILAB	77
3.9	FINAL FOCUS TEST FACILITY ATF2 STATUS	79
3.9.1	Test Facility	79
3.9.2	Highlights of ATF2 First Results	84
3.9.3	ATF2 Outlook and Plans	87
3.9.4	Conclusion	88
3.9.5	Acknowledgements	88
3.9.6	References	89
3.10	FOURTH INTERNATIONAL ACCELERATOR SCHOOL FOR LINEAR COLLIDERS	90
4	WORKSHOP AND CONFERENCE REPORTS	93
4.1	47 TH ICFA ADVANCED BEAM DYNAMICS WORKSHOP ON <i>THE PHYSICS AND APPLICATIONS OF HIGH BRIGHTNESS ELECTRON BEAMS</i>	93
4.1.1	Introduction	93
4.1.2	Organization and Attendees	94
4.1.3	Scientific Program	94
4.1.4	Publications	95
4.1.5	References	96
4.2	WORKSHOP ON TOP-UP OPERATIONS AT SYNCHROTRON LIGHT SOURCES	96
5	RECENT DOCTORAL THESES	98
5.1	COUPLING IMPEDANCE AND COLLECTIVE EFFECTS IN THE RCS RING OF THE CHINA SPALLATION NEUTRON SOURCE	98
6	FORTHCOMING BEAM DYNAMICS EVENTS	99
6.1	46 TH ICFA ADVANCED BEAM DYNAMICS WORKSHOP: <i>HB2010</i>	99
6.2	48 TH ICFA ADVANCED BEAM DYNAMICS WORKSHOP ON FUTURE LIGHT SOURCES: <i>FLS2010</i>	99

6.3	2 ND ICFA MINI-WORKSHOP ON DEFLECTING/CRABBING RF CAVITY APPLICATIONS IN ACCELERATORS	100
6.4	NEW BOOKS ON ACCELERATORS	101
6.4.1	Innovation Was Not Enough – A History of the Midwestern Universities Research Association (MURA)	101
6.4.2	Reviews of Accelerator Science and Technology	101
7	ANNOUNCEMENTS OF THE BEAM DYNAMICS PANEL	102
7.1	ICFA BEAM DYNAMICS NEWSLETTER	102
7.1.1	Aim of the Newsletter	102
7.1.2	How to Prepare a Manuscript	102
7.1.3	Distribution	103
7.1.4	Regular Correspondents	104
7.2	ICFA BEAM DYNAMICS PANEL MEMBERS	105

1 Foreword

1.1 From the Chair

Weiren Chou, Fermilab
Mail to: chou@fnal.gov

At a meeting on August 19, 2009 in Hamburg, Germany, the International Committee for Future Accelerators (ICFA) and the International Committee on Ultra Intense Lasers (ICUIL) agreed to form a Joint Task Force. Its mission is “*to promote and encourage international collaboration between the accelerator and laser communities on future applications of laser acceleration.*” The task force consists of 16 members from ICUIL and two ICFA panels: the Beam Dynamics Panel and the Advanced Accelerators Panel. They are (in alphabetical order): Ralph Assmann (CERN), Chris Barty (LLNL), Paul Bolton (JAEA), Robert Byer (Stanford U.), Bruce Carlsten (LANL), Weiren Chou (Fermilab), Almantas Galvanauskas, (U. of Michigan), Dino Jaroszynski (Strathclyde U.), Ingo Hafmann (GSI), Wim Leemans (LBNL), Akira Noda (Kyoto U.), James Rosenzweig (UCLA), Wolfgang Sandner (MBI), Siegfried Schreiber (DESY), Mitsuru Uesaka (Tokyo U.) and Kaoru Yokoya (KEK). This task force includes leading physicists from both the laser and accelerator communities. It will start with a strategy planning workshop to take place from April 8 to 10, 2010 at GSI, Germany. Since this is the first joint task force between these two international committees, its success relies on the strong and continuous support of those communities. The task force welcomes comments and advice. Please feel free to contact any of these task force members and make suggestions.

The big news in November was that the Large Hadron Collider (LHC) came into operation and began an unprecedented journey in a deep and wide search for new physics. On November 30, the LHC reached 1.18 TeV, breaking the record held by the Tevatron and becoming the world’s highest energy particle accelerator. While the global high-energy physics community was cheering, Rolf Heuer, Director General of CERN, was quoted in *Time* magazine as saying “*I’m keeping my champagne on ice,*” refraining from celebrating. In the meantime, however, the first LHC physics paper “*First proton-proton collisions at the LHC as observed with the ALICE detector: measurement of the charged particle pseudorapidity density at $\sqrt{s} = 900$ GeV*” appeared on arXiv (arXiv:0911.5340 [hep-ex]), only a few days after the machine commissioning began. We believe Rolf will be unable to keep his champagne on ice for too long.

When one reads this LHC paper, the first impression is its long list of authors and their affiliations, occupying almost 6 pages. In the Acknowledgements section, it takes another half page to list the funding agencies. These already exceed the page limit for a *Physical Review Letters* (PRL) paper (maximum of 4 pages). The IUPAP C11 Commission (parent organization of ICFA) recognized this problem long ago. But an appropriate solution is yet to be found.

On October 26, the US DOE sponsored a public symposium entitled “*Accelerators for America’s Future.*” (<http://www.acceleratorsamerica.org>) About 400 people

attended and showed great interest in the potential of accelerators in areas such as basic science, medicine, industrial applications, energy, and homeland security, as well as in new accelerator technologies. Frederick Dylla, Executive Director and CEO of the American Institute of Physics, wrote a brief summary article “*Big Tools for Science.*” We have his permission to reprint it in Section 2 of this newsletter.

The Fourth International Accelerator School for Linear Colliders was held from September 7-18, 2009 at Hotel Jixian in Huairou near Beijing, China. It was a great success. Sixty-nine well-qualified students attended, selected from 244 applicants. They participated in an intensive 10-day program of lectures, homework assignments and a final examination. Nine students were honored and received awards based on their examination grades. The IHEP did a wonderful job in hosting this school. A report can be found in Section 3.10 of this newsletter.

The editor of this issue is Prof. Junji Urakawa, a panel member and senior physicist from KEK. Junji is the leader of the ATF Project of KEK. He chose *ILC R&D Status* as the theme of this newsletter and collected 10 excellent articles in the theme section. They give a comprehensive review of the status and future plans of the ILC, a leading candidate for the next large particle collider. On behalf of the panel, I thank Junji for editing a newsletter of great importance to the future of high-energy physics.

1.2 From the Editor

Junji Urakawa
High Energy Accelerator Research Organization (KEK)
1-1 Oho, Tsukuba, Ibaraki, Japan
Mail to: junji.urakawa@kek.jp

When in June I was invited to edit this issue, I considered future hard work related to preparation of the ILC TD (Technical Design) Phase 1 report and the on-going R&D at Test Facilities. As a member of the ILC GDE (Global Design Effort), and after correspondence with Weiren Chou, I chose as the theme for this newsletter “ILC R&D Status.” I asked my friends, members of the ILC GDE, and my colleagues at KEK-ATF to write reports on ILC R&D Status. Thanks to the much appreciated support of the authors, I received 10 excellent papers. They are arranged as follows:

- G.F. Dugan, M.A. Palmer and D.L. Rubin report on the detailed status of ILC damping ring R&D at the CESR Test Accelerator (CesrTA).
- Theo Demma, N. Terunuma, A. Brachmann, J. Clarke, F. Marcellini and D. Alesini report on “Update on the Electron Cloud Simulation for DAΦNE,” “Status of ATF R&D,” “ILC polarized electron source design and R&D program,” “Positron Source R&D Status Report,” and “Design of Injection Kickers at LNF” respectively.
- H. Hayano, M. Church and S. Nagaitsev wrote two articles: “STF status 2009” and “A Facility for Accelerator Research and Education at Fermilab.”
- Finally, the article on the “Final Focus Test Facility ATF2 Status” is given by P. Bambade, A. Seryi and T. Tauchi.
- Just before I completed editing, I received a report written by Barry and Weiren on the Fourth International Accelerator School for Linear Colliders. I added this as the last article in the theme section.

I appreciate very much the high quality of the papers from all the contributors.

There are also two workshop reports (47th ICFA ABDW *HBEB2009* and Top-Up Operations at Synchrotron Light Sources), three workshop announcements (46th ICFA ABDW *HB2010*, 48th ICFA ABDW *FLS2010*, and 2nd ICFA Mini-Workshop on Deflecting/Crabbing RF Cavity Applications in Accelerators) and an abstract of a recent doctoral thesis (N. Wang, IHEP, China).

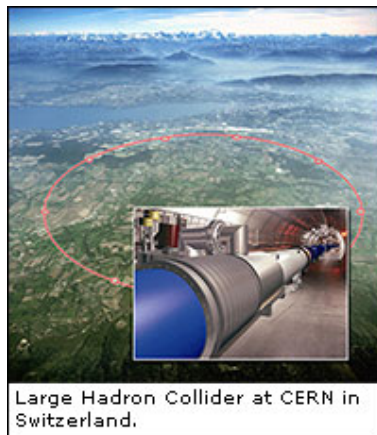
2 Letters to the Editor

2.1 Big Tools for Science

H. Frederick Dylla
Executive Director and CEO, American Institute of Physics
Mail to: dylla@aip.org

(This is an article published in the online magazine "AIP Matters," November 2, 2009. We have the author's permission to reprint it in this newsletter.)

On October 26, 2009 the Department of Energy sponsored a symposium entitled "[Accelerators for America's Future](#)" – a lofty title for a gathering to discuss the impact of investments in particle accelerators. These tools of science, which have existed for almost a century, have had considerable impact on both science and the economy in ways that many outside of the physics community are unaware.



These machines began as small tabletop devices in the 1920s, which were used to accelerate the newly recognized class of subatomic particles (electrons, protons, or charged atoms) to energies of many thousands of volts. As the technology of designing these tools progressed and the energy was boosted past a million volts, the machines became the basic workhorse for the new fields of nuclear and particle physics. In the 1930s, accelerators were first used in medicine as an instrument of radiation therapy for cancer treatment, and within the Manhattan Project in the 1940s, accelerators were essential for underpinning the nuclear physics for the development of the nuclear bomb and the large-scale industrial processes needed for separating uranium isotopes used to

fuel the bomb. Since World War II, the design and application of accelerators burgeoned for all three endeavors: science, industry, and medicine.

The science was driven by the push to higher energies—the Tevatron at Fermilab first broke the trillion-volt barrier, and the Large Hadron Collider (LHC) at CERN, which returns to operation next month, is designed to produce protons colliding at energies of 14 trillion volts. Coincident with this evolution for basic particle physics, families of accelerators built across the globe have nurtured other sciences. Numerous dedicated machines are installed in large user facilities for materials scientists to produce intense sources of x-rays and neutrons used to decode the structure of materials or to design new materials. This year's [Nobel Prize in Chemistry](#) was awarded to three scientists for unraveling the structure of a key macromolecule, the ribosome. This task required the capabilities of the dedicated x-ray light source at Brookhaven National Lab.

Beyond the science, small medical accelerators—the primary means of targeted cancer therapy—at many hospitals and large regional cancer centers now treat millions of patients every year. Industrial applications underpin the production of all the silicon wafers used in modern electronics and most large-scale sterilization methods for plastics and many foodstuffs. Last year, the manufacturers of small accelerators for medicine or industry generated over \$3.5 billion of revenue, which resulted in more than \$50 billion of valued products—not a bad spin-off from machines whose continued design and evolution are predominately confined to the rarefied academic halls of particle and nuclear physicists.

The scientists and engineers who gathered last week in Washington to consider these tools of science pondered several troubling issues. At one end of the spectrum, machines such as the Tevatron and LHC are the poster children of big science, yet the attainment of trillions of volts costs billions of dollars. At the other end, the machines that are used for medicine and industry are based on accelerators that were designed over a half century ago. On the horizon are new classes of accelerators based on boosting particles with plasmas or lasers, which could dramatically shrink the size and, hence, the cost of these machines. The scientists and engineers who have made a career as accelerator designers, and the Department of Energy, the agency that since its inception as the Atomic Energy Commission in 1946 has overseen accelerator development, used last week's symposium to make the case that these tools of science and contributors to the economy will be just as important in the 21st century as they were in the 20th century.

3 Theme Section: ILC R&D Status

3.1 ILC Damping Rings R&D at CEsrTA

G.F. Dugan, M.A. Palmer and D.L. Rubin for the CEsrTA Collaboration
 222 R.R. Wilson Laboratory, Cornell University, Ithaca, NY, USA
 Mail to: mark.palmer@cornell.edu

3.1.1 Introduction

Over the course of the last 1.5 years, the Cornell Electron Storage Ring (CESR) has been reconfigured as the CESR Test Accelerator (CesrTA) [1,2]. It now serves as the principal instrument of the CESRTA collaboration for the investigation of the physics of low emittance damping rings. Nearly three dozen multi-channel retarding field analyzers (RFAs) have been installed in the CESR vacuum system and used to measure the development of the electron cloud (EC) [3-5]. These electron detectors are being used to characterize the energy spectrum and spatial distribution of the cloud in dipole fields, quadrupoles, solenoids, and wigglers as well as in field free regions. Vacuum chambers with mitigating chemistry and geometry have been tested including grooved chambers, and chambers with TiN and amorphous carbon coatings, yielding direct comparison with bare aluminum and copper chambers. The chambers tested so far have been fabricated in collaboration with colleagues from CERN, KEK, LBNL and SLAC.

In order to achieve sufficiently low vertical emittance to test emittance diluting effects of the electron cloud and intra-beam scattering, a new network of survey monuments has been installed that permits regular efficient alignment of the magnetic guide field elements. Emittance tuning software has been interfaced to the CESR control system for real time optics analysis and correction [6]. This software takes advantage of an upgraded CESR beam position monitor (BPM) system with turn-by-turn readout capability that has just been deployed. An x-ray beam size monitor (xBSM) capable of providing single bunch-single pass measurements of vertical beam size at the level of a few microns has also been installed [7-9]. This device is being developed with the help of our colleagues from KEK. An emittance of 10pm corresponds to a beam size of 8 μ m at the xBSM source point. A key application of the xBSM is measurement of the vertical beam size of every bunch in a long train, thus illuminating emittance diluting effects of the electron cloud and allowing identification of electron cloud induced instabilities.

The collaboration has measured the tune shift of individual bunches along a train to characterize the ring-wide dynamical effects of the cloud, as well as its growth and decay times [10]. The phase shift of TE waves transmitted from a BPM electrode and received at another BPM electrode several meters away is a sensitive measure of the density of the intervening electron cloud. At CesrTA, TE wave measurements are being developed into a standard tool for characterizing the properties of the electron cloud in close collaboration with researchers from LBNL [11].

The experimental program is accompanied by a collaborative effort (involving researchers from the US, Europe and Asia) to simulate and model electron cloud related phenomena. A principal goal of the CEsrTA project is to validate simulation predictions with measurements, allowing one to build physics models of the cloud that can be used to predict with confidence its effects on the beam in the ILC damping rings [12,13]. There has been significant progress in understanding the experimental results in terms of cloud physics models.

During the remainder of the CEsrTA program period, we expect to complete a definitive set of measurements of electron cloud development and of the dynamics of the interaction of the electron cloud with the circulating beams of electrons and positrons. We will validate EC models by detailed comparison with measurements and will complete tests of several EC mitigation techniques. We will demonstrate reliable algorithms for tuning vertical emittance at the level of a few tens of pm and exploit our capability for single pass beam size measurements of vertical emittance with a few microns resolution.

We expect to have achieved reduction of the zero current vertical emittance to ~ 20 pm by mid-2010. Further reduction to 5-10 pm will require a continuing effort to exploit the enormous capability of the new BPM electronics and to minimize systematic errors in beam position measurements. As we continue to reduce residual dispersion and coupling, our sensitivity to emittance diluting effects will be enhanced. We have recently submitted a proposal to the U.S. National Science Foundation to continue our pursuit of these goals.

Coupled with the x-ray beam size monitors for electrons and positrons, and the flexibility to vary the beam energy over a broad range, we will measure the dependence of intrabeam scattering (IBS) emittance growth and lifetime limiting Touschek scattering on bunch current and beam energy, in various emittance coupling regimes.

We also plan to develop non-destructive techniques for monitoring in real time sources of emittance dilution including focusing errors, transverse coupling, and dispersion errors. Such techniques will be invaluable to the operation of future ultra-low emittance damping and light source rings.

3.1.2 The CEsrTA Research Program

3.1.2.1 Machine Layout and Optics

The layout of the storage ring was configured during the summer of 2008 for low emittance operation [1]. Damping wigglers were moved from the machine arcs to the 18m (L0) straight that became available with the removal of the CLEO HEP detector. The low beta final focus insert was replaced with standard FODO optics. The vertical separators were removed from the diametrically opposite straight (L3) to reduce longitudinal impedance and make space for instrumentation. The full complement of corrector magnets (56 vertical and 54 horizontal dipole correctors and 13 skew quadrupoles), essential for emittance tuning, has been preserved.

We have developed and tested optics for operation of the storage ring with beam energies of 1.8 GeV, 2.0, 2.3, 3.2, 4.0, 5.0 and 5.3 GeV. We achieve a horizontal emittance of 2.5 nm in our baseline lattice at 2 GeV beam energy using 12 damping wigglers. At 5 GeV the minimum emittance is 40 nm with 6 wigglers. All of the conditions are designed to be compatible with on energy injection of multiple bunches

so that experimental measurements can be performed efficiently. Figure 1 shows the optics functions of our 2.0GeV ultra low emittance optics while Table 1 summarizes the range of parameters spanned by the various CesrTA optics configurations.

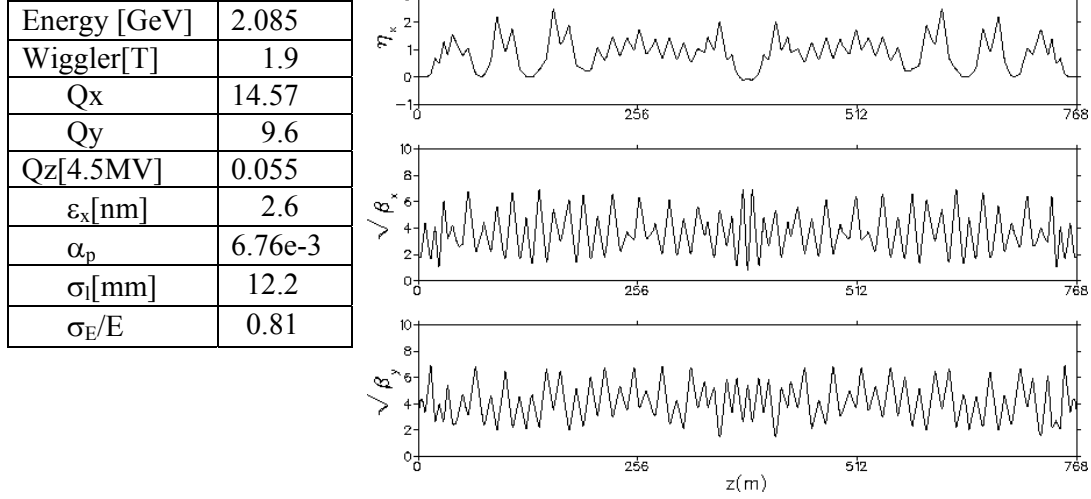


Figure 1: Low emittance lattice. 12 wigglers operating at 1.9T in zero dispersion straights increase radiation damping rate by a factor of 10 and reduce emittance by a factor of 4.

Table 1: CesrTA optics configurations.

Lattice	E[GeV]	Wigglers [1.9T]	ϵ_x [nm]
1800mev_20090607	1.8	12	2.3
2085mev_20090516	2.085	12	2.5
2300mev_20090608	2.3	12	3.3
3000mev_q0v_20090821	3.0	6	9.8
4000mev_23nm_20090816	4.0	6	23
5000mev_40nm_20090513	5.0	6	40
5000mev_pmwig_20090314	5.0	0	90

3.1.2.2 Instrumentation and Feedback Systems

The instrumentation requirements for the program fall into four principal categories:

- Beam instrumentation required to correct the machine optics for ultra low emittance operation,
- Beam instrumentation to characterize the beam emittance in these conditions,

- Local diagnostics to characterize the build-up of the electron cloud in the accelerator vacuum chambers, and
- Beam instrumentation to characterize the dynamics of the interaction between the beam and the cloud.

A feedback system capable of stabilizing bunch trains with similar parameters to those needed for the ILC damping rings is also required. We have implemented hardware to meet all of the above requirements over the course of the first 1.5 years and are presently beginning to take full advantage of our enhanced measurement capabilities for the R&D program.

3.1.2.2.1 Instrumentation for Low Emittance Tuning and Measurement

The key piece of instrumentation for optics correction is the beam position monitor (BPM) system. A new digital BPM system has been designed for turn-by-turn orbit measurements in CESR. The system is capable of simultaneous multi-bunch measurements in both single beam and dual beam (as used for CHESS) operation of the machine. A $10\mu\text{m}$ measurement resolution for successive measurements is necessary for our ability to correct the vertical dispersion around the machine at the $<10\text{mm}$ level (see Section 3.1.2.4). At present, preliminary measurements have been obtained with approximately 90% of the BPMs upgraded to digital modules with turn-by-turn readout capability. We have just deployed approximately a dozen additional readout modules with full multi-bunch capability for correction of the entire ring during our experimental run starting in November 2009.

In order to characterize the emittance of damping ring like beams, our efforts have focused primarily on the development of an x-ray beam size monitor (xBSM) which is capable of single pass measurements [7,8]. The present xBSM detector utilizes a 1-D InGaAs diode pixel array ($25\mu\text{m} \times 500\mu\text{m}$ pixels). With either Fresnel zone plate or coded aperture [9] x-ray imaging optics, this detector can resolve the $\sim 10\mu\text{m}$ vertical beam sizes that are expected when operating CESR in the damping ring configuration. Figure 2 shows the resolution capability with the Fresnel and the coded aperture optics, respectively. With the Fresnel optics in place, rotation of the detector array by 90 degrees allows for beam characterization in both vertical and horizontal planes.

Two CHESS x-ray lines, one looking at the positron beam and the second at the electron beam, have now been modified as “all vacuum” lines for xBSM use. Each line has insertable optics assemblies for flexible testing of a range of x-ray optics. At beam energies around 2GeV, the expected white beam flux on an xBSM detector, with no optics elements inserted, is approximately 550 photons/ma/pixel. With the coded aperture optics in place, this reduces to somewhat over 100 photons/ma/pixel in the 1keV to 5keV range which is quite adequate for single-pass imaging. In the case of the Fresnel zone plate, a monochromator is typically inserted in the beam path to provide optimum measurement resolution. The monochromator, however, reduces the flux by roughly two orders of magnitude, and this method is used for high resolution measurements which integrate over multiple beam passages. Single-pass measurements, with similar flux to that of the coded aperture case, can be made by using a Fresnel zone plate without a monochromator, at the price of somewhat degraded resolution. In multi-bunch mode, this allows for detailed characterization of emittance growth along ILC-like bunch trains. Figure 3 shows the results of some multi-turn averaged single-bunch measurements.

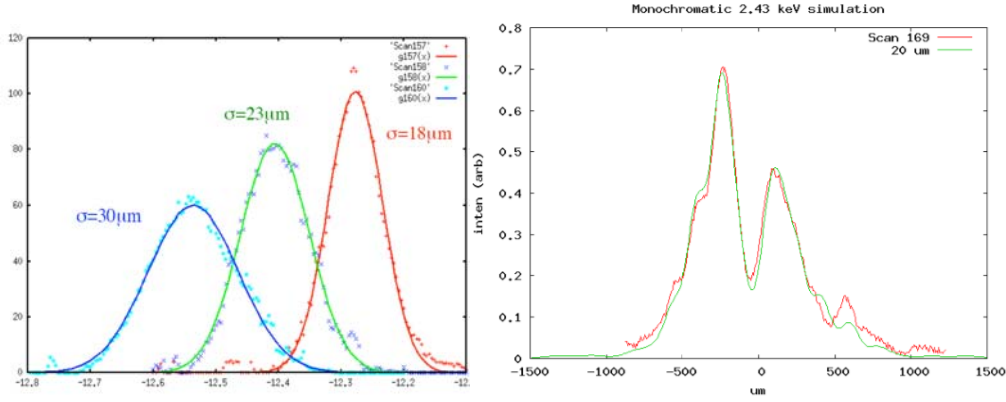


Figure 2: xBSM measurements using Fresnel zone plate imaging (left) where the x-y coupling in the machine was varied in the 2.085GeV optics. The right plot shows a measurement using the coded aperture optics with a monochromator centered on x-ray energies of 2.43 keV. The two curves are a simulation (green) of the expected image assuming a $20\mu\text{m}$ source size along with the data (red) which was obtained in the same conditions as the $18\mu\text{m}$ measurement with the Fresnel zone plate. The data is consistent with a vertical beam size which is slightly smaller than $20\mu\text{m}$. [Right plot courtesy of John Flanagan, KEK]

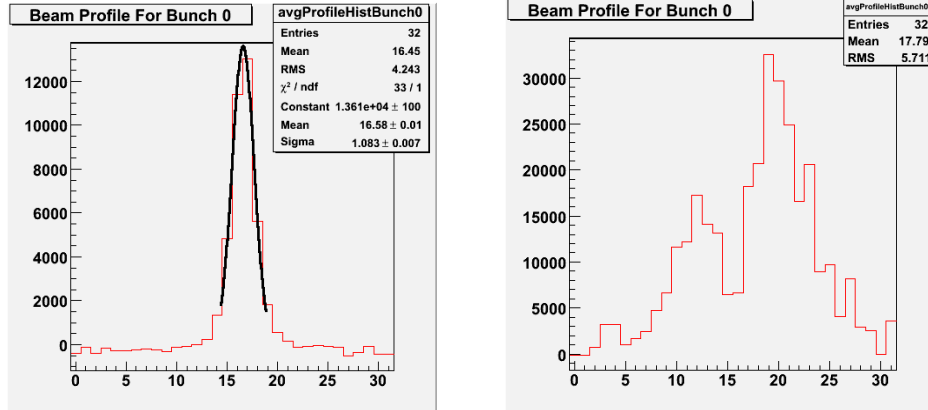


Figure 3: Single bunch beam profile measurements with the xBSM detector using the Fresnel zone plate optics (left) and coded aperture optics (right) for two different data runs. The horizontal axis shows the response of each pixel while the vertical axis is ADC counts for the bunch-by-bunch digitizer output. Both results are obtained in the 2.085GeV low emittance optics. The images correspond to measured vertical beam sizes of $19\mu\text{m}$ (left) and $17\mu\text{m}$ (right).

In addition to the xBSM, we are exploring ways to improve our visible light beam size monitor system (vBSM) in order to provide both a cross-check as well as an additional set of tuning tools for our low emittance operations. The vBSM system consists of direct imaging for beam sizes larger than the diffraction limit of the optics (~ 180 microns), a two slit interferometer with a slit spacing of 3 mm and 0.5 mm slit width (sensitive to vertical beam sizes between 50 to 200 microns), and a displaced imaging system for the vertically polarized component of the synchrotron light (sensitive to vertical beam sizes from 5 to 70 microns) [15]. We have two readout

methods available for the images: a conventional CCD TV camera feeding a frame grabber; and a 32 element linear photomultiplier with 1 mm photocathode spacing which is capable of resolving individual bunch passages. The vertical polarization method can provide beam size measurements for the range of emittances covered by the CEsrTA optics.

3.1.2.2.2 Feedback System

The ILC damping ring baseline design envisions operating the positron ring with bunch spacings of approximately 6ns [16]. In order to fully characterize electron cloud build-up in the relevant regime, the CESR feedback system has been upgraded for operation with bunch trains with spacings as small as 4ns. A feedback system from DIMTEL, Inc [17] was selected to provide the feedback in all 3 planes. A particular benefit of this system is the extensive diagnostics that come with it for characterization of the bunch trains [18]. This system has been in operation at CESR since mid-2009.

3.1.2.2.3 Electron Cloud Instrumentation

Instrumentation to characterize the electron cloud in CESR falls into two principal categories: local diagnostics measure surface properties and cloud build-up and beam diagnostics to measure the impact of the cloud on the beam dynamics.

A major component of the CEsrTA program has been to deploy retarding field analyzers in each of the major vacuum chamber types and magnetic field regions in CESR [3-5]. The CESR design relies on a very thin detector structure, ~3mm thickness, which can be inserted in magnets with extreme aperture constraints such as dipoles, wigglers, and quadrupoles. In these regions, detectors with single retarding grids and collector electrode structures generated with photolithography techniques on thin (0.006") polyimide substrates are employed. Figure 4 shows a schematic and assembly photo for a set of 3 such RFAs in a wiggler vacuum chamber. These detectors offer transverse segmentation in order to characterize the geometric distribution of electrons striking the vacuum chamber walls. As of summer 2009, approximately 30 RFAs have been deployed in CESR.

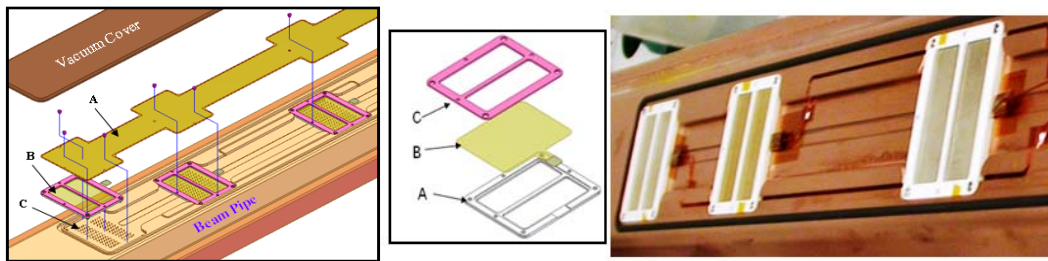


Figure 4: Retarding field analyzer structure utilized for the CEsrTA wiggler vacuum chambers. The drawing on the left shows the vacuum chamber assembly, the middle drawing shows the insulator and mesh layers that form the retarding grid, and the photo at the right shows the 3 RFAs during assembly. One RFA is located at the center of a wiggler pole, one at the boundary between two poles, and one in the field roll-off region at the edge of a pole.

In addition to the retarding field analyzers, we have also deployed instrumentation to allow characterization of the local cloud build-up via TE wave transmission through

the vacuum chambers [11,19]. In drift regions this method is sensitive to the density of the cloud in the center of the chamber. A major area of current effort is the application of this technique to magnetic field regions, particularly wigglers and dipoles.

Other elements of our local EC measurements program include ongoing R&D into obtaining direct time-resolved measurements of the EC build-up and decay via the RFAs, shielded pickups and TE wave measurements. We are also preparing to deploy an in-situ secondary electron yield measurement station which will allow us to characterize the SEY of various surface treatments before, during and after processing with synchrotron radiation. A companion (identical) setup is planned for the Main Injector at FNAL as part of a SLAC-FNAL-Cornell collaboration.

The integrated ring-wide impact of the EC on the beam is being studied with a variety of techniques. These include bunch-by-bunch measurements with the new BPM system, with the DIMTEL feedback system [17], with a gated spectrum analyzer and with the xBSM.

Bunch-by-bunch tune information has been obtained in several ways. Turn-by-turn data with the new BPM system has been recorded for cases where: 1) trains have been excited by a single-turn kick where the induced oscillations are then allowed to freely decay; 2) the feedback is turned off and the bunches in a train are monitored without excitation; and 3) the bunches are excited by a drive source (from a spectrum analyzer or the feedback system). The DIMTEL feedback system has also been used to obtain such information. Finally the gated spectrum analyzer measurements can also provide information on the bunch tunes.

Studies of multi-bunch instabilities are underway using mode spectra that can be obtained both via the BPM system and via the DIMTEL feedback system. The xBSM provides information on emittance growth along a train as well and experiments have begun to look for incoherent emittance growth effects as well as the onset of head-tail instabilities. A gated spectrum analyzer has also been configured to look for the presence of vertical synchro-betatron sidebands which are a signature of the head-tail instability [20].

3.1.2.3 Electron Cloud Measurements and Simulations

3.1.2.3.1 Retarding Field Analyzer (RFA) Measurements and Simulations

The RFA's described in section 3.1.2.2 have been used to make a variety of measurements, in CESR drift regions with aluminum and carbon-coated chambers, in CESR dipoles with aluminum chambers, in wigglers with copper, TiN coated, and grooved chambers, and in the PEP-II chicane dipoles with standard aluminum, with a TiN coated chamber, and with a grooved chamber. The measurements have been made with both positrons and electrons, at 2 and 5 GeV, with bunch trains from 45 to 145 bunches long, with bunch spacings as small as 4 ns, and bunch currents from a few tenths up to 2mA/bunch. In the PEP-II chicane, measurements have been made as a function of dipole field, and clear evidence of cyclotron resonances [23] has been observed. We have also installed a retarding field analyzer in a quadrupole in CesrTA to characterize the build-up of the cloud in this magnetic environment.

The data provide information on the energy and spatial differential current density of electrons which impact the chamber walls at the location of the RFAs. This information provides a direct measurement of the time-average electron cloud density

generated in the associated magnetic and vacuum chamber environment as a function of the generating beam conditions.

Three examples of data taken in the using the PEP-II chicane dipoles from SLAC installed in the CsrTA L3 region are shown in Figures 5-7. The total RFA current in the central collector, and in edge collectors, is shown as a function of the dipole field, measured in units of the cyclotron resonance field. The structure due to cyclotron resonances is evident. The suppression of the total current in the chambers with mitigations (coatings and grooves) is also evident. The overall cloud current suppression from the uncoated aluminum chamber to the coated, grooved chamber is approximately a factor of 300 at the chamber center (where multipacting dominates) and about a factor of 5-20 at the edges.

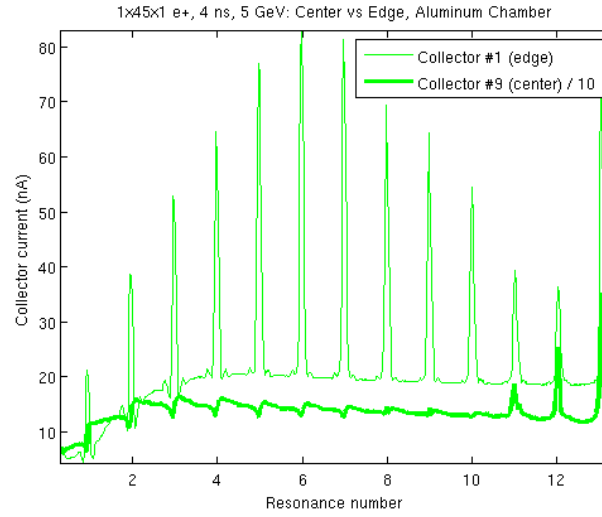


Figure 5: Total RFA current vs. chicane dipole field, as measured by the cyclotron resonance number, in an uncoated aluminum chamber.

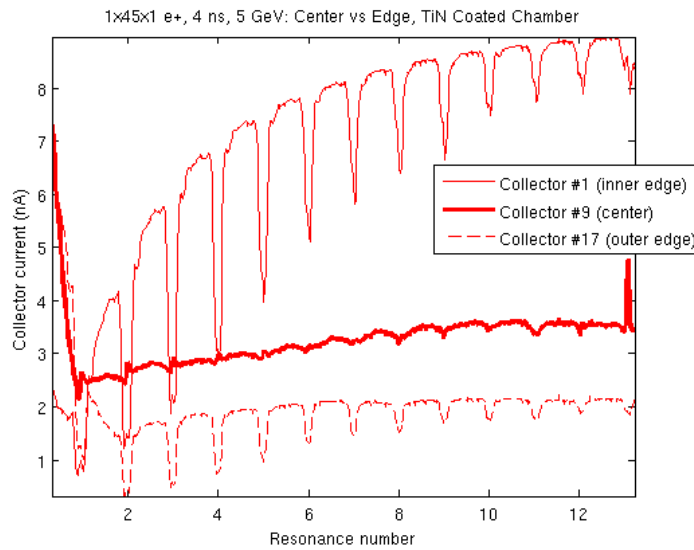


Figure 6: Total RFA current vs. chicane dipole field, as measured by the cyclotron resonance number, in a chamber with TiN coating.

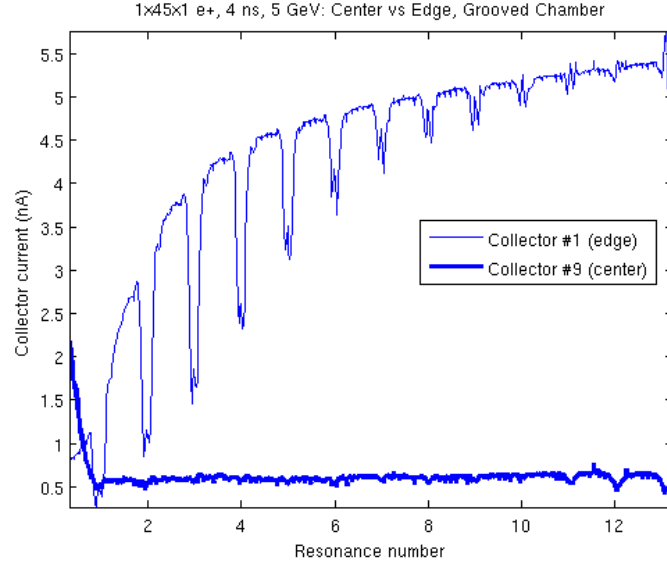


Figure 7: Total RFA current vs. chicane dipole field, as measured by the cyclotron resonance number, in a chamber with both TiN coating and grooves.

In order to interpret the data in terms of the physics models of the formation of the electron cloud, it is necessary to compare the observed differential current densities with the results of a simulation. The simulation needs to include all important features of the magnetic and vacuum chamber environment, as well as that of the generating beam.

In drifts and dipoles, most of the RFAs are located in regions in which a two-dimensional description of the electron cloud dynamics is sufficient for an accurate simulation of the development of the cloud. However, in the wigglers, the inherently 3D nature of the field may require a 3D simulation code. In collaboration with LBNL, we are developing a 3D code (WARP-POSINST) with the capability to model the cloud growth in wigglers. Several interesting features of the 3D wiggler results, such as trapping of electrons in the region of peak longitudinal fields, have been observed in the simulation, and work is underway to develop methods to verify this effect experimentally.

In dipoles, and particularly in the high-field wigglers, the confinement of the motion of the electrons to helical trajectories around the field lines, with cyclotron radii which are small compared to the vacuum chamber holes which define the RFA acceptance, means that the dynamics of the cloud electrons which are detected by the RFAs is strongly influenced by the RFA electric fields, and by secondary emission processes occurring within the RFAs themselves. For an accurate simulation, it is therefore necessary to include the RFA structure and its effect on the cloud within the electron cloud simulation program itself. In collaboration with LBNL, we are working on developing versions of both POSINST [24] and ELOUD [24] which include the RFAs.

An example of a comparison between RFA measurement and a simulation is shown in Figure 8. This figure compares POSINST and ELOUD simulations (using nominal cloud model parameters, and an overall SEY of 1.8) with the measured currents on central and outer collectors of the segmented RFA at 15E in CsrTA. This

region is a drift with an uncoated Al chamber. The data was taken with a 45 bunch train of positrons at 2 GeV, with a bunch spacing of 14 ns. A simple postprocessing script has been used to compute the RFA efficiency, supplemented with an empirical model to account for secondaries generated inside the beam pipe holes. The agreement with the simulations is satisfactory. Further improvements to the model are in progress.

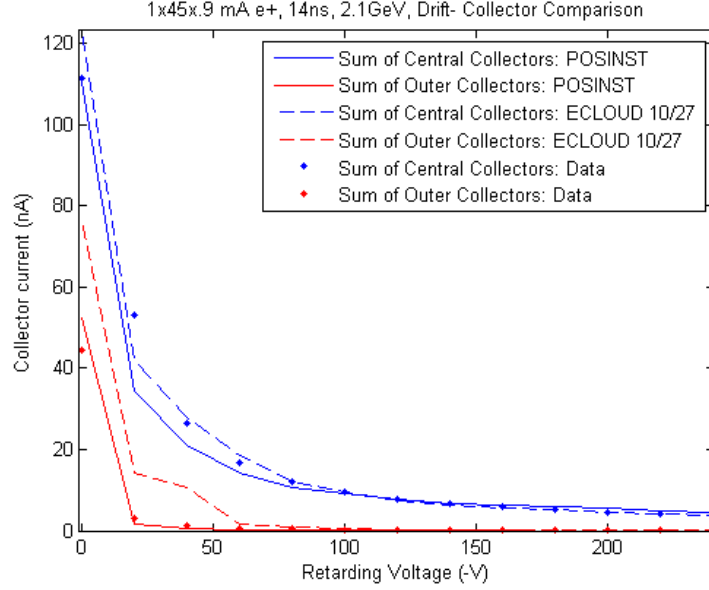


Figure 8: Comparison of RFA at location 15E in CsrTA with POSINST simulation. This region is a drift with an uncoated Al chamber.

Using the codes discussed in the previous section, we will generate simulations of the observable RFA differential current densities, and compare with the observations. These comparisons will be made for a range of magnetic environments, including the variable dipole field results from the SLAC chicane, and for a range of vacuum chamber environments including all the proposed mitigation techniques. The comparisons will allow us to tie the observations to cloud physics model parameters, which will establish confidence in our understanding of the cloud development in these environments and the suppression of that development by the mitigation techniques. Clearing electrodes are one of the most promising avenues for cloud mitigation. Significant suppression of the electron cloud by clearing electrodes has been measured at KEK and seen in simulations. At CsrTA, we will install a chamber with clearing electrodes and an RFA in a wiggler, and measure the resulting mitigation over a wide range of beam conditions.

3.1.2.3.2 Beam Dynamics Measurements and Simulations

Measurements of coherent tune shifts along long trains of bunches, and of “witness” bunches following these trains, can probe the growth and decay of the ring-wide average electron cloud in CESR. Tune shift measurements have been made with both positrons and electrons, at 2 and 5 GeV, with bunch trains of length varying from a few to 145 bunches, with bunch spacings as small as 4 ns, and with bunch currents from a few tenths up to 5 mA/bunch. The coherent tune shift of a bunch is determined by the effective force gradient experienced by the bunch. To exclude the effects of non-cloud-

related fields, we use a reference bunch at the start of the train and compute tunes relative to this bunch.

Ring-wide measurements of coherent tune shifts cannot differentiate between the drift and dipole contributions. To disentangle them, we have installed solenoids in a large fraction of the drift regions of the ring. We are planning on making ring-wide tune shift measurements with and without solenoids in place. Using our new BPM system, we will also attempt to measure betatron phase shifts as a function of bunch number over a dipole-dominated region of the ring.

Coherent tune shift measurements have been made both by inducing a coherent oscillation of the entire train and by exciting individual bunches. The dynamics of the beam-cloud interaction are different in these two conditions, and different tune shifts result. These differences have been observed in measurements. In order to properly simulate this situation, simulation runs with offset bunches and trains were used to compute effective field gradients. Runs were performed in both drifts and dipoles, in which the cloud was generated from photons with computed intensities appropriate to a ring-wide average in CESR. Simulations with the same cloud model parameters give relatively good agreement with data for both positrons and electrons, giving confidence that the measured tune shifts along the train are dominantly due to electron cloud effects. Some examples are illustrated in the following pages.

In Figures 9 and 10, plots of tune shift data and comparisons with simulations are shown for positrons and electrons with 10 and 20 bunch trains and witness bunches, with 14 ns spacing. In Figure 11, positron tune shift data is shown for a 30 bunch train with 4 ns spacing. The simulation parameters in the cloud physics model are the same in all cases; the variation with one simulation parameter, the chamber overall secondary emission yield, is also shown.

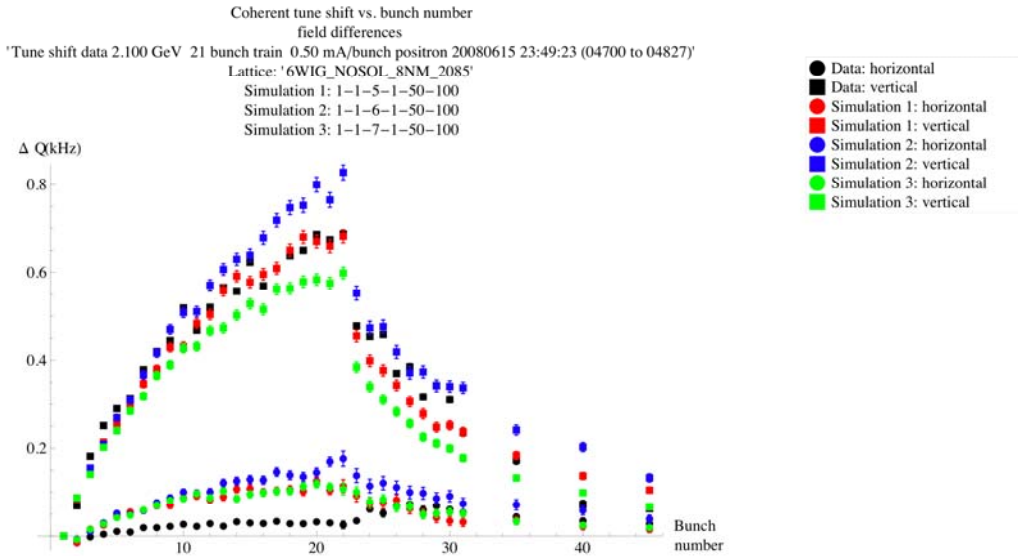


Figure 9: Measured and simulated coherent tune shifts for a 20 bunch train of positrons, with 0.5 mA/bunch and 14 ns spacing, at 2.1 GeV, followed by 11 witness bunches. The tunes were measured using a pinger to coherently excite the whole train. The simulation parameters in simulation 1 correspond to an SEY of 2.0 in an aluminum chamber; for simulation 2, SEY=2.2, and for simulation 3, SEY=1.8.

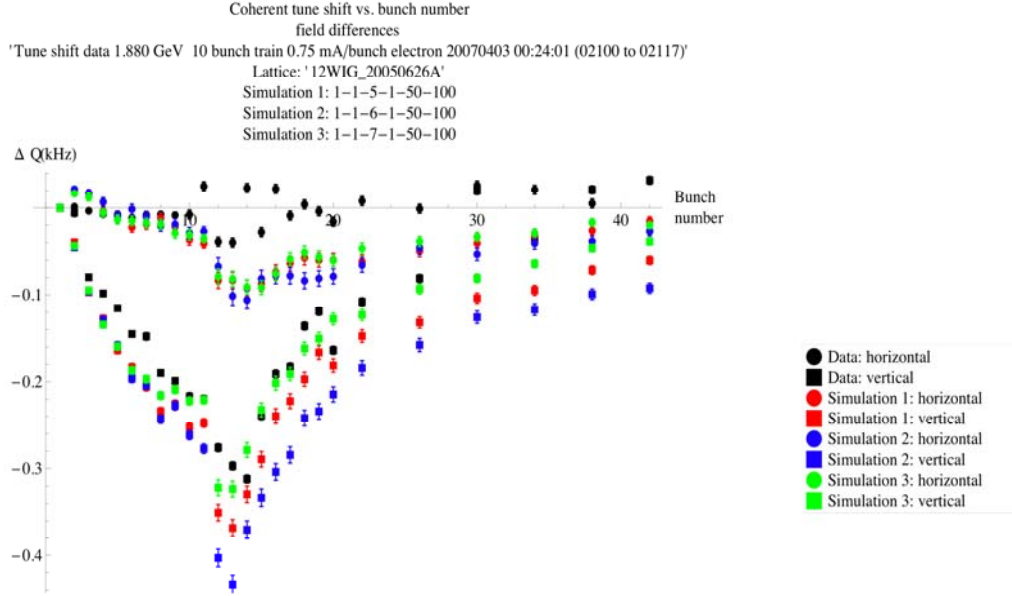


Figure 10: Measured and simulated coherent tune shifts for a 10 bunch train of electrons, with 0.75 mA/bunch and 14 ns spacing, at 1.9 GeV, followed by 13 witness bunches. The tunes were measured using a pinger to coherently excite the whole train. The simulations use the same input parameters as in Fig. 9.

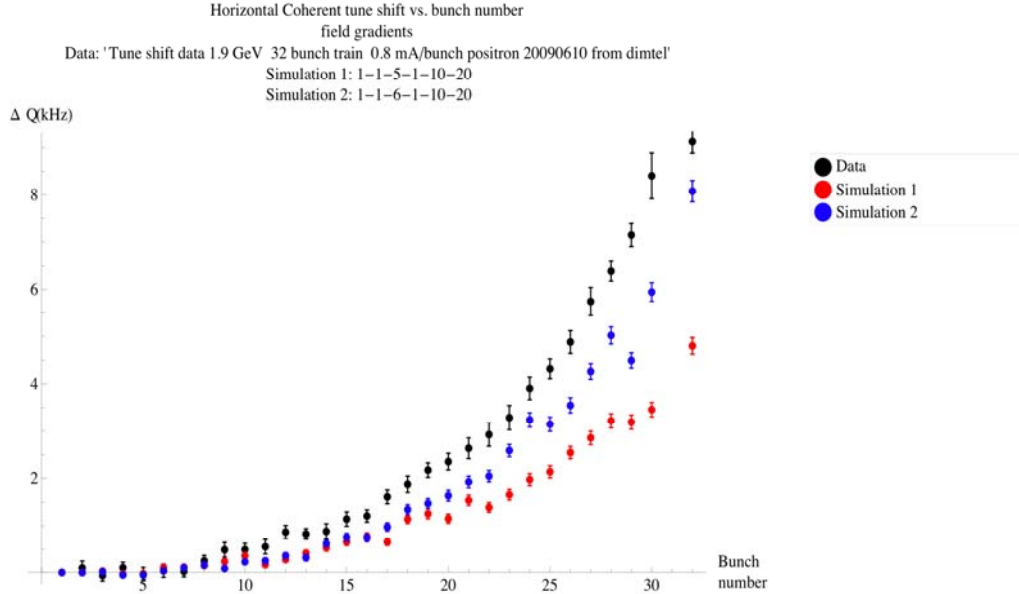


Figure 11: Measured and simulated horizontal coherent tune shifts for a 30 bunch train of positrons, with 0.8 mA/bunch and 4 ns spacing, at 1.9 GeV. The tunes were measured using the Dimtel feedback system. Same simulation parameters as in Fig. 9 for simulation 1; SEY increased to 2.2 for simulation 2.

The wide range of coherent tune shift data that we have taken and will take allows a comprehensive set of comparisons with cloud build-up simulations in both POSINST and ELOUD. These comparisons will allow us to characterize the cloud physics model parameters in a way that is complementary to the comparisons using the RFA data. For example, the time dependence of the cloud growth and decay, provided by the train and witness bunch-by-bunch tune measurements, provide access to information on the cloud dynamics not available from the RFA data. On the other hand, the RFA data provide a direct measurement of the electron energy spectrum. The combination of cloud and RFA data, and the requirement of consistency between these data, allows one to identify systematic errors in both measurements which might otherwise evade detection. This provides further confidence in our understanding of the physics of the formation of the electron cloud. This understanding is essential for a convincing extrapolation to the conditions expected in the ILC damping rings.

Our new feedback system will be used to make grow-damp measurements of the growth time and mode spectrum of electron-cloud-driven multi-bunch instabilities. The mode spectra are sensitive to details of the electron cloud growth. Measurements of the spectra over a wide range of beam conditions will both provide additional information on the build-up of the cloud and provide us with more information on the interaction of the cloud with the beam.

We plan to compare our observations of multi-bunch instability growth times and mode spectra discussed above with simulations. Although we do not have simulation capability for this at Cornell, our collaborators (from INFN and KEK) are very interested in this and have agreed to support these simulations using their well-developed codes.

The coherent tune shift measurements that we have made to date indicate that, at the highest bunch currents and with long trains, we can develop electron cloud densities which are sufficiently large that, for the last bunches in the train, we may be above the threshold for the head-tail single bunch instability. We will use gated tune measurements to look for the excitation of synchro-betatron sidebands, a signature of this instability. If observed, we will measure the threshold for the onset of the instability, which can provide information about the high frequency dynamics of the cloud.

Similarly, we plan to compare our observations of single bunch instability thresholds discussed above with simulations. Again, we will rely on the simulation capability of our collaborators (from SLAC and KEK).

In conjunction with the gated tune measurements described in the previous section, we will use our visible and X-ray beam size monitors to observe emittance growth associated with the onset of the head-tail instability.

The visible and X-ray beam size monitors will also be used to pursue a more elusive, but possibly more significant, effect: sub-threshold incoherent emittance dilution. Such dilution is driven by nonlinear phase space diffusion, whose origin is the nonlinear terms in the electron cloud fields experienced by the beam. While such effects may be small for low cloud densities, given the very small design emittance of the ILC damping ring, there is not much headroom for such effects. The sensitivity of searches for these effects will depend on the minimum vertical emittance which can be reached at CsrTA, and on the resolution of the beam size monitors.

Emittance dilution from coherent instabilities will be simulated using codes developed by our collaborators at SLAC and KEK. Sub-threshold emittance dilution

due to nonlinear phase space dilution resulting from the electron cloud can be modeled using single particle tracking codes. There is an interest in this work on the part of our collaborators at KEK. In addition, tracking codes available at Cornell may also be used.

3.1.2.4 *Low Emittance Tuning*

Low emittance tuning is the measurement and correction of sources of single particle vertical emittance, including vertical dispersion and transverse coupling. Transverse coupling is generated by tilted quadrupoles and vertically offset sextupoles. Vertical dispersion is generated by rolled bend magnets, vertically offset quadrupoles and by any mechanism that couples horizontal dispersion into the vertical plane. We measure coupling by resonant excitation of the normal betatron modes and measurement of the relative phase and amplitude of horizontal and vertical motion at each of the 100 beam position monitors. Dispersion is measured by taking the difference of off energy orbits. The quality of the measurement depends on the accuracy of the beam position monitors.

3.1.2.4.1 Machine Alignment and Beam Position Monitors

The coupling and dispersion that is generated by misaligned magnets is minimized with the help of dipole and skew quad correctors. A simulation study [22] shows that, using our upgraded tuning algorithm, the requirements for achieving 20pm vertical emittance are: quadrupole vertical misalignments $<150\mu\text{m}$; sextupole vertical misalignments $<300\mu\text{m}$; quadrupole and dipole rotations about the beam axis $<100\mu\text{rad}$; beam position monitor accuracy for orbit differences $<20\mu\text{m}$; and BPM rotations $<15\text{mrad}$. We have reduced vertical misalignments to well below the required specification for both quadrupoles and sextupoles. The rms dipole roll is presently $150\mu\text{rad}$. We continue to measure and level dipoles as time and manpower permits.

One of the major components of the CEsrTA upgrade is high bandwidth and high precision beam position monitor electronics. As of early September, 90% of the CESR BPMs were instrumented and commissioned with turn-by-turn readout electronics. We anticipate that the new system will routinely be used for low emittance tuning during the next CEsrTA running period that begins in November 2009. Tests of individual modules indicate that the new system readily meets the targets for accuracy and reproducibility required to achieve ultra low emittance.

3.1.2.4.2 Low Emittance Tuning Procedure

The strategy for minimizing vertical emittance begins with a beam based alignment of the beam position monitors with the centers of the adjacent quadrupoles. Using closed orbit bumps the trajectory of the beam is adjusted until the closed orbit is independent of a change in strength of the quadrupole. BPM resolution and systematics associated with the finite distance between the center of the quad and the BPM limit the precision of the offset measurement to 50-75 microns.

Having aligned the beam position monitors with respect to the quadrupoles the procedure is to:

1. Measure the closed orbit at each of 100 beam position monitors and correct (center in quadrupoles) using all 108 dipole correctors
2. Measure betatron phase and transverse coupling at each BPM by resonant excitation of the normal modes, and correct using all 100 quadrupoles and 14

skew quadrupoles. We typically achieve an rms phase error of less than 1.5 degrees and an rms coupling error of less than 0.6% in just a couple of iterations. A single iteration of measurement, analysis, and correction takes about 3 minutes.

3. Remeasure coupling and measure dispersion by orbit difference. Simultaneously fit dispersion and coupling using skew quadrupoles and vertical dipole correctors.

At the conclusion of the low emittance tuning procedure we typically measure an rms residual dispersion of about 2.4cm. According to our machine model, a residual dispersion of 2.4cm rms will generate vertical emittance of 80pm, assuming no coupling. Preliminary measurement of the vertical beam size with the x-ray beam size monitor indicates a vertical emittance of ~40pm which corresponds better to residual vertical dispersion of 1.7cm. We believe that the discrepancy is due to the limited accuracy of the beam position measurement (soon to be fully replaced). The dependence of the Touschek lifetime on bunch current is also consistent with a zero current vertical emittance of ~40pm [1].

Systematic effects limit the performance of the old analog/relay beam position monitor electronics. Reproducibility and resolution is compromised by the mechanical nature of the relays. In a tilted BPM, horizontal dispersion appears with a vertical component. We have developed BPM gain mapping techniques, orbit response measurement methods, and coupling measurements to identify BPM tilts and button to button gain errors.

Our ability to understand the systematics of the new BPM system depends on the resolution and reproducibility of the measurements. Critical for low emittance tuning are measurements of transverse coupling and dispersion. With 90% of the CESR BPMs configured with the new electronics we measured an rms resolution in the coupling measurement of $< 0.5\%$, and an rms resolution of the dispersion measurement of $< 5\text{mm}$, both well below the level required to achieve zero current vertical emittance of less than 10pm. We anticipate that with the complete characterization of the digital BPM electronics that we will be able to understand these systematic effects at the requisite level, but that the complete characterization will take considerable effort.

3.1.2.4.3 BPM Upgrade and Systematic Effects

As noted above, precision beam position measurement is essential to identifying and eliminating sources of residual vertical dispersion and transverse coupling. A vertical dispersion of 1cm corresponds to vertical emittance of about 10pm. We can change the beam energy by about 0.2% by varying the frequency of the storage ring RF. Then a vertical dispersion of 1cm corresponds to an orbit difference of $\Delta y = \eta \Delta E/E = 20\mu\text{m}$. Systematic errors such as BPM tilt, and button to button gain variation will contaminate the measurement of vertical dispersion. Typical horizontal dispersion in the CesrTA lattice is about 1m. Therefore we must determine BPM tilts (either physical or electronic) at the level of 10mrad in order that the contribution of measured vertical dispersion due to BPM coupling be less than the required 1cm. We use beam based gain mapping techniques to identify button to button gain errors [6]. Measurement of relative amplitude and phase of resonantly excited vertical and horizontal motion at each BPM gives coupling matrix elements \bar{C}_{12} , \bar{C}_{22} , and \bar{C}_{11} [22]. While \bar{C}_{11} and \bar{C}_{22} are sensitive to BPM tilt, \bar{C}_{12} is not. The true coupling of transverse motion can be eliminated by measurement and correction of \bar{C}_{12} . Then \bar{C}_{22} is a direct measure of

beam position monitor tilt [2]. Reproducibility of measured coupling and dispersion shows that the intrinsic resolution of the BPM is more than adequate to achieve our target emittance.

The data shown in Figure 12 were collected in the last two days of the August-September CsrTA run. The plots labeled horizontal and vertical dispersion are actually the difference of two dispersion measurements made roughly 20 minutes apart at each of 100 beam position monitors. The machine optics is nominally unchanged. Detectors 1-87 and 98-100 are part of the new digital system. Detectors 88-97 have yet to be converted. Note that the RMS of the vertical dispersion is 5mm.

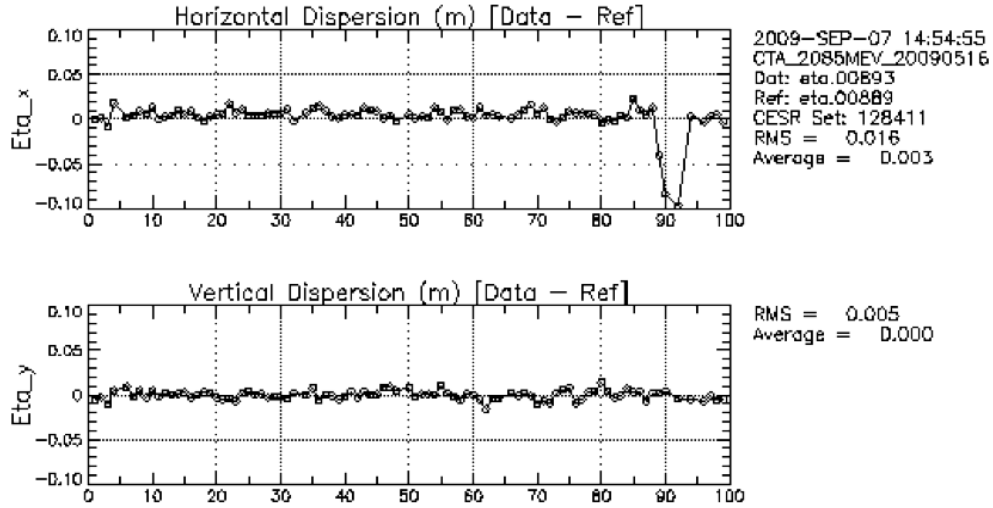


Figure 12: Difference of dispersion measurements at each of 100 beam position monitors. The two sets of measurements were made twenty minutes apart. The machine optics is not changed between measurements. Detectors 1-87 and 98-100 are part of the new digital system. Detectors 88-97 have yet to be converted. The RMS of the vertical dispersion is 5mm.

Coupling data are shown in Figure 13. The \bar{C} -matrix elements are based on measurements of the relative amplitude and phase of vertical and horizontal motion at each of the normal mode frequencies. In the plot Data and Ref correspond to measurements of coupling taken ~20 minutes apart in a machine that is nominally unchanged. Again, detectors 1-87 and 99-100 are instrumented with the new digital electronics. Detectors 88-97 are part of the old relay system. The superior performance of the new system is evident. The residual for the new system detectors in the measurement of \bar{C}_{12} is much less than 0.1% (note that $\bar{C}_{12}=1\%$ corresponds to an 0.01% emittance coupling).

A single measurement of coupling matrix elements is shown in Figure 14. Again detectors 1-87 and 97-100 are part of the new system. \bar{C}_{12} (the middle plot) is insensitive to BPM tilt, whereas \bar{C}_{22} , in the absence of real coupling of horizontal-vertical motion, is a direct measure of BPM tilt and button to button gain errors. We will exploit this distinction to better understand BPM systematics and improve the quality of our measurement of vertical dispersion.

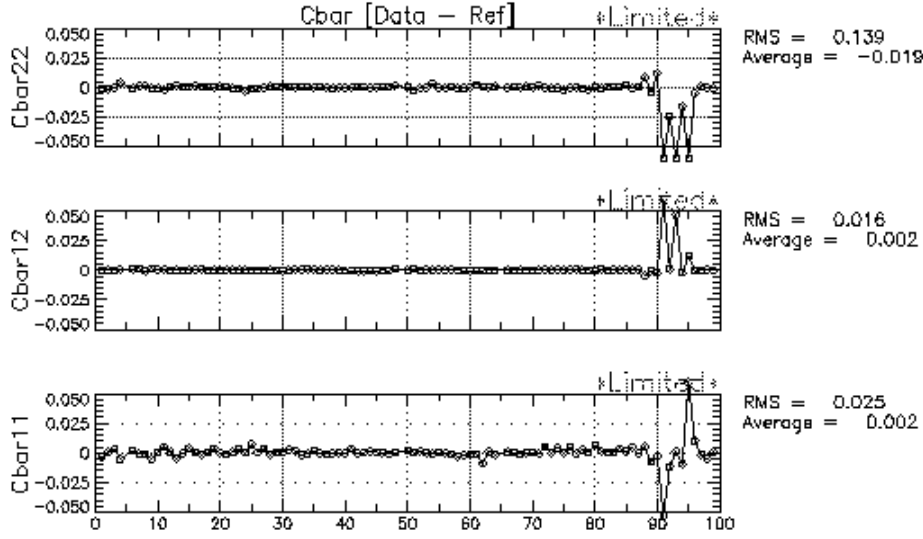


Figure 13: Difference of coupling measurements at each of 100 beam position monitors. The two sets of measurements were made twenty minutes apart. The machine optics is not changed between measurements. Detectors 1-87 and 98-100 are part of the new digital system. Detectors 88-97 have yet to be converted. The residual is less than 0.01%.

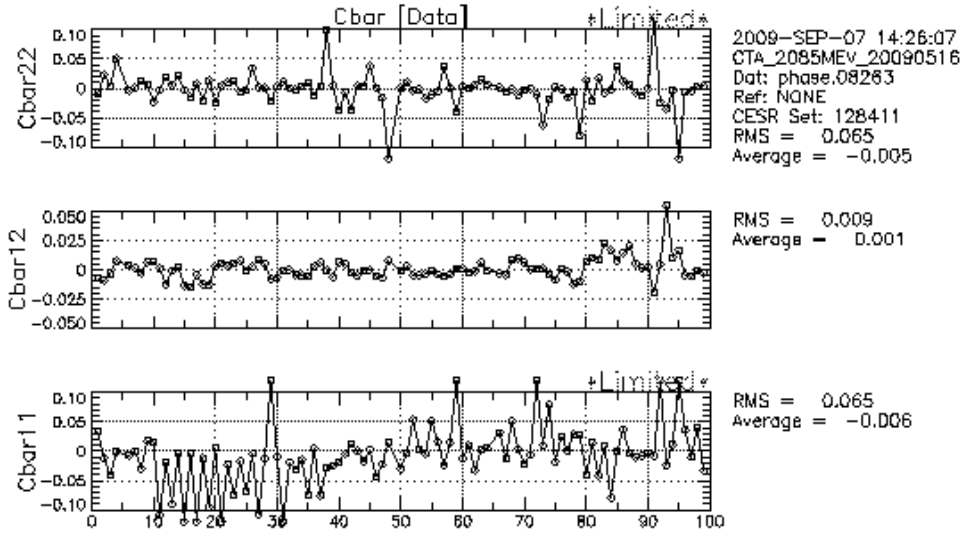


Figure 14: Measurement of the coupling matrix elements at each of 100 beam position monitors. \bar{C}_{12} (middle plot) is insensitive to BPM tilt and button to button gain errors. If \bar{C}_{12} is zero, then \bar{C}_{22} is a direct measure of BPM tilt.

3.1.3 Plans for Further Investigations

Measurement of emittance diluting effects is a critical component of the CsrTA program. Our sensitivity to such effects depends on our ability to achieve ultra low zero current emittance. The digital BPM electronics that has recently been commissioned has the intrinsic measurement resolution necessary to identify guide field errors and to reach

vertical emittance in the ILC damping ring regime. With further effort to understand systematic measurement errors, to develop our low emittance tuning algorithms, and to identify time dependent sources of emittance dilution (power supply ripple, magnet vibration, etc.), we expect to reproducibly achieve 5-10pm zero current vertical emittance. This will permit us to measure emittance diluting effects with exquisite sensitivity. We will continue to advance our x-ray and visible beam size monitor designs to exploit this experimental regime.

3.1.3.1 Mitigation Methods and Vacuum System R&D

Ongoing R&D on mitigation methods forms a significant part of our proposed research program during the remainder of the ILC Technical Design Phase. We plan to maintain an operating schedule during this time frame that will allow detailed evaluation of the aging effects of the mitigations proposed for the damping rings. The CESR operations model, which will include two running periods per year with intervening downs, is well-suited to tests of new and refined mitigation methods as they are developed. The duration of the R&D program is also commensurate with the time required to design and test prototype ILC-like vacuum chambers incorporating EC mitigations. In regions such as the wigglers, these designs are challenging and such tests will ensure that a robust design exists. Details of the designs will then be incorporated into the overall impedance model for the damping rings.

3.1.3.2 Intrabeam and Touschek Scattering

The fully instrumented CesrTA offers a unique laboratory for the investigation of intra-beam scattering. With the combination of the low emittance and the low beam energies that typify CesrTA optics, effects of intrabeam scattering are evident. The wide range of beam energies accessible to CESR will permit detailed characterization of the energy dependence of IBS. Flexibility of the optics allows for straightforward variation of the zero current emittances. We will use the low emittance tuning techniques and instrumentation for real time measurement of vertical beam size (xBSM and vBSM) that are now being developed to minimize vertical emittance. Ultimately we will measure the current and energy dependence of horizontal and vertical emittance for both electron and positron beams, allowing a complete characterization of intra-beam scattering and electron cloud induced emittance dilution.

Calculations suggest that as we approach our design zero current vertical emittance we will observe a strong current dependent emittance growth [2]. In particular we find a strong dependence of horizontal emittance on bunch current as shown in Figure 15. The sensitivity of horizontal emittance to intra beam scattering is due to the relatively large horizontal dispersion in the CesrTA optics. The dynamic range of the xBSM will permit measurements of bunch size from 0.4mA to 5mA. In order to measure the very significant energy dependence of the IBS emittance growth, we have developed and tested optics for operation from 1.8GeV to 5.0GeV beam energy, with a range of zero current horizontal emittances from 2.5nm to 100nm. The essential parameters of each lattice are summarized in Table 1.

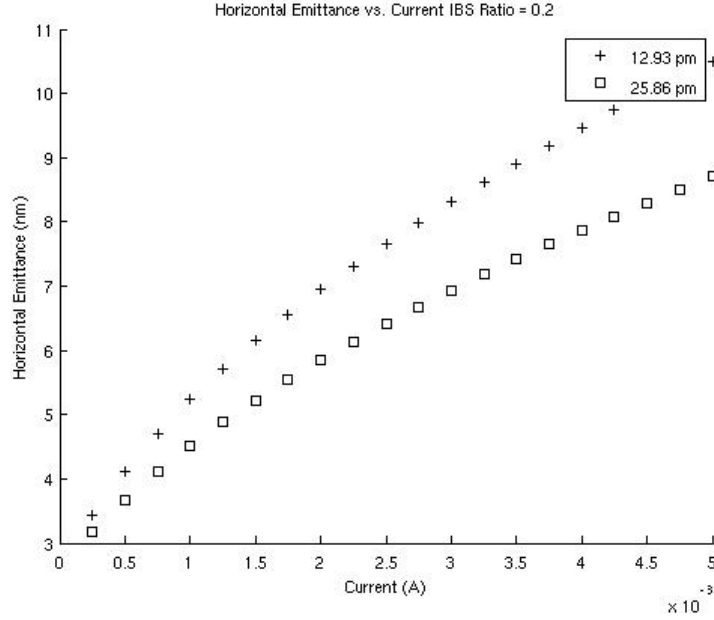


Figure 15: Calculated horizontal emittance as a function of bunch current for zero current horizontal emittance of 2.6nm and zero current vertical emittances of 12.93pm and 25.86pm respectively. We assume that the fraction of the vertical emittance due to transverse coupling is 0.2, the remainder coming from vertical dispersion.

We plan to measure horizontal and vertical beam size, and beam lifetime as a function of bunch current over the range of energies from 1.8GeV to 5.0GeV. We will repeat the measurements for positrons and electrons. This data will provide a unique test of models of emittance growth and particle loss due to intrabeam scattering and interaction with the electron cloud.

3.1.3.3 Lifetime Measurements

Sensitivity of beam lifetime to emittance provides a powerful tool for studying collective effects. The Touschek effect is characterized by the dependence of lifetime on beam current. ($dI/dt = -I/\tau_0 - I^2/b$) If the Touschek b-parameter is small, Touschek scattering will significantly degrade the lifetime. The effect of Touschek scattering on lifetime depends on particle density (emittance) and the energy acceptance of the lattice.

Determination of the effective energy acceptance is non-trivial. If the energy acceptance is limited by the RF overvoltage, then the tolerance of a particle to an energy change due to scattering is independent of where in the lattice that energy change occurs. However, if the limiting energy acceptance is dynamic, then that acceptance does depend on local lattice functions. In a lattice with strongly varying dispersion and beta functions, like the CsrTA optics, energy acceptance cannot be characterized by a single number. We are developing algorithms to locally compute dynamic acceptance and then to incorporate that information into the calculation of the Touschek lifetime.

3.1.3.4 Ion Effects

An electron beam is subject to the effect of the fast ion instability (FII). Ions are created by interaction of the beam with the residual gas molecules. The ions may dilute the emittance of the electron bunch in an electron beam by a mechanism similar to the effect of the electron cloud on the positron bunch in a positron beam [7]. Similarly, ions may couple bunches within a train. The instability threshold depends on the beam configuration, bunch charge density, and residual gas pressure. The FII can dilute the emittance of the electron beam and ultimately limit the bunch and current density of the electron damping ring if not controlled. For example, it is anticipated that the ion density will increase along the length of the train of bunches. We will measure individual bunch size, frequency, and tune shift to further characterize the effect. We plan to use CEsrTA to explore the fast ion instability in the emittance, charge density, and beam current regime that is characteristic of the ILC electron damping ring. Comparison of the data with the theoretical expectations and simulations can be used to benchmark the models used in the design of the ILC damping rings.

3.1.3.5 Cloud-Driven Emittance Dilution at Ultra Low Emittance

The single bunch instabilities which the electron cloud can generate, such as the head-tail instability, will lead to a growth in the emittance, and cannot in general be controlled by conventional feedback systems. While the density of the cloud generated by a beam is not expected to depend substantially on the emittance of the beam, the strong electric fields generated near a low emittance beam will cause rapid oscillations of the electrons in the cloud near the beam. These rapid oscillations are expected to drive the development of the head-tail instability. Thus, the threshold for the instability may be lower for low emittance beams, even for fixed cloud density. Since this phenomenon is not well understood, it is important to study it experimentally, which should be possible in CEsrTA with ultra low emittance beams, using the extensive suite of beam-size-monitoring instrumentation which is coming on line.

Even at cloud densities well below the threshold for coherent single-bunch instabilities, emittance dilution may be driven by phase space diffusion from the nonlinear terms in the EC fields experienced by the beam. Given the very small design emittance of the ILC damping ring, there is not much headroom for such effects. Simulations at KEK have indicated that such growth can occur, but on very long time scales. Hence, it is important to look for such effects in long-term experiments carried out using the lowest possible emittance beams. Moreover, at CEsrTA, the level of cloud density experienced by a particular bunch can be controlled by placing the bunch in a “witness” position at a variable distance from the end of a bunch train. Thus, carefully controlled studies of the effects of low levels of cloud density on the emittance of ultra low-emittance test bunches can be carried out. Such studies are needed to establish how important this effect may be for the ILC damping ring.

3.1.3.6 Instrumentation for Real-Time Monitoring of Machine Parameters

The high bandwidth beam position monitor electronics provide the capability of continuous and nondestructive measurement of machine parameters such as the betatron phase, coupling, dispersion and beam emittance. We plan to drive a witness bunch at the normal mode tunes (horizontal, vertical and longitudinal) and to measure phase and amplitude of horizontal and vertical motion at each BPM. From this data we can extract

betatron phase and amplitude, transverse coupling parameters, and vertical and horizontal dispersion at each beam position monitor. Real time analysis of the measurements will drive the correction scheme.

3.1.3.7 *Role of Collaborators*

Collaborators have played and will continue to play a fundamental role in the CEsrTA program, including the design and fabrication of hardware and instrumentation, loan of existing equipment, contribution to the development of modeling software, and participation in CEsrTA machine studies. Physicists and engineers from KEK, LBNL and SLAC have collaborated in the design and fabrication of wiggler vacuum chambers with electron cloud mitigation and retarding field analyzers. Accelerator physicists from KEK and INFN-Frascati have participated in the experimental programs to characterize e-cloud induced instabilities, and to identify and correct sources of residual vertical emittance in CESR. Physicists from KEK have made very important contributions to the development of the CEsrTA xBSM.

There is a close LBNL-Cornell collaboration to develop the electron-cloud simulation and modeling codes to interpret the data that is emerging from CEsrTA. SLAC and Argonne are also contributing to e-cloud code development and investigation of e-cloud dynamics. Both FNAL and CERN are taking advantage of the Test Accelerator to characterize electron-cloud mitigating surface treatments, physicists from CERN have been able to test aspects of the proposed CLIC magnet stabilization system in CEsrTA, and physicists from BNL have utilized CEsrTA for beam position monitor tests. The use of TE microwaves to measure cloud density at CEsrTA has relied heavily on the involvement of our LBNL colleagues.

The instrumented dipole chicane, that was first implemented at PEP II and, on loan from SLAC, is now installed in CEsrTA, is being used to measure the field dependence of electron cloud development. Also on loan from SLAC is equipment for in-situ measurement of secondary emission yield. CalPoly is collaborating on the visible light beam size monitor, on instrumentation for measurement of bunch by bunch tune shifts, and on streak camera instrumentation.

Accelerator physicists at the Cockcroft Institute have contributed to the development of the low emittance tuning program, participated in LET machine studies, and analyzed the data that has come from those studies. Technician is helping to create phenomenological models of electron-cloud dynamics.

CesrTA is fundamentally a group effort and we would like to take this opportunity to express our gratitude to all of those who are participating in the research program.

3.1.4 **References**

1. M.A. Palmer, *et. al.*, The Conversion and Operation of the Cornell Electron Storage Ring as a Test Accelerator (CesrTA) for Damping Rings Research and Development, Proceedings of 2009 Particle Accelerator Conference, 2009
<http://www.lns.cornell.edu/~dlr/papers/pac09/FR1RAI02.pdf>.
2. D. Rubin, *et. al.*, CesrTA Layout and Optics, Proceedings of 2009 Particle Accelerator Conference, <http://www.lns.cornell.edu/~dlr/papers/pac09/WE6PFP103.pdf>.
3. Y. Li, *et. al.*, CesrTA Vacuum System Modifications, Proceedings of 2009 Particle Accelerator Conference,
<http://www.lns.cornell.edu/~dlr/papers/pac09/MO6RFP005.pdf>.

4. Y. Li, *et al.*, Design and Implementation of CsrTA Superconducting Wiggler Beampipes with Thin Retarding Field Analyzers, Proceedings of 2009 Particle Accelerator Conference.
5. M.A. Palmer, *et al.*, Design, Implementation and First Results of Retarding Field Analyzers Developed for the CsrTA Program, Proceedings of 2009 Particle Accelerator Conference.
6. J. Shanks, *et al.*, CsrTA Low-Emittance Tuning -- First Results, Proceedings of 2009 Particle Accelerator Conference, http://www.lns.cornell.edu/~dlr/papers/pac09/PAC09-LET_first_results.pdf.
7. J. Alexander, *et al.*, CsrTA X-Ray Beam Size Monitor Design, Proceedings of 2009 Particle Accelerator Conference.
8. J. Alexander, *et al.*, First Results from the CsrTA x-Ray Beam Size Monitor, Proceedings of 2009 Particle Accelerator Conference.
9. J. Flanagan, *et al.*, Performance of Coded Aperture X-Ray Optics with Low Emittance Beam at CsrTA, Proceedings of 2009 Particle Accelerator Conference.
10. J.A. Crittenden, *et al.*, Studies of the Effects of Electron Cloud Formation on Beam Dynamics at CsrTA, Proceedings of 2009 Particle Accelerator Conference, <http://www.lns.cornell.edu/~dlr/papers/pac09/FR5RFP044.pdf>.
11. S. De Santis, *et al.*, The TE Wave Transmission Method for Electron Cloud Measurements at CsrTA, Proceedings of the 2009 Particle Accelerator Conference.
12. J. Calvey, *et al.*, Electron Cloud Modeling Considerations at CsrTA, proceedings of 2009 Particle Accelerator Conference.
13. J. Calvey, *et al.*, Simulations of Electron-Cloud Current Density Measurements in Dipoles, Drifts and Wigglers at CsrTA, proceedings of 2009 Particle Accelerator Conference http://www.lns.cornell.edu/~dlr/papers/pac09/FR5RFP043_RFA_Simulations.pdf.
14. ILC Project Managers Report: ILC Research and Development Plan for the Technical Design Phase, July 2009, http://ilc-edmsdirect.desy.de/ilc-edmsdirect/file.jsp?edmsid=D0000000*813385.
15. A. Andersson, *et al.*, Determination of a small vertical electron beam profile and emittance at the Swiss Light Source, Nuclear Instruments and Methods A, March, 2008, http://www.sciencedirect.com/science?_ob=MImg&_imagekey=B6TJM-4S0PK3J-2-16&_cdi=5314&_user=492137&_orig=search&_coverDate=07%2F01%2F2008&_sk=994089996&view=c&wchp=dGLzVzz-zSkzV&md5=dd871c1062b5b71ff7a9dfc0a4f145d3&ie=/sdataicle.pdf.
16. ILC Reference Design Report http://ilcdoc.linearcollider.org/getfile.py?docid=182&name=ILC_RDR_Volume_3-Accelerator&format=pdf.
17. DIMTEL, Inc. <http://www.dimtel.com/>.
18. A. Drago, *et al.*, Commissioning of the IGP Feedback System at DAFNE, Proceedings of the 2008 European Particle Accelerator Conference, Genoa, Italy, <http://cern.ch/AccelConf/e08/papers/thpc116.pdf>.
19. S. De Santis, *et al.*, Measurement of Electron Clouds in Large Accelerators by Microwave Dispersion, PRL 100, 094801 (2008).
20. J.W. Flanagan, *et al.*, Vertical synchro-betatron sideband measurement at KEKB, PRL 94, 054801 (2005), <http://prola.aps.org/pdf/PRL/v94/i5/e054801>.
21. D. Sagan, *et al.*, Betatron Phase and Coupling Measurements at the Cornell Electron/positron Storage Ring, Phys. Rev. ST Accel. Beams 3, 059901 (2000).
22. R. Helms, Studies for Csr-TA: A Low-Emittance Test Accelerator at the Cornell Electron Storage Ring, PhD thesis, Cornell, January 2008.
23. C.M. Celata, M.A. Furman, J.-L. Vay, and J.W. Yu, Electron cloud cyclotron resonances in the presence of a short-bunch-length relativistic beam, Phys. Rev. ST Accel. Beams 11, 091002 (2008).

24. F. Zimmermann and G. Rumolo, Electron Cloud Effects in Accelerators, ICFA Beam Dynamics Newsletter No. 33, eds, K. Ohmi and M.A. Furman (2004).

3.2 Update on the Electron Cloud Simulations for DAΦNE

Theo Demma, INFN Laboratori Nazionali di Frascati, Italy
 Mauro F. T. Pivi, SLAC, USA
 Mail to: Theo.Demma@lnf.infn.it

3.2.1 Introduction

A strong horizontal instability, limiting the positron current at $I \approx 500\text{mA}$, has been observed at DAΦNE since the installation of the FINUDA detector in 2003. Experiments and simulations seem to provide evidence that the electron cloud build-up in the wigglers and bending magnets of the DAΦNE positron ring induces coupled bunch instability with features compatible with observations [1-5]. Recently the installation of a new horizontal feedback system allowed to control the instability for value of the positron current as high as possible ($I \approx 1000\text{mA}$) [6].

To better understand the electron cloud effects and possibly to find a remedy, a detailed simulation study is undergoing. In this communication we present recent simulation results relative to the single bunch instability induced by an electron cloud interacting with the beam.

3.2.2 Simulation of Single Bunch Instability

In positron storage rings, where an electron cloud is created by photoemission and secondary emission, single-bunch instability due to a coherent oscillation of both electrons and positrons can occur [7]. If the electron cloud density near the beam is sufficiently large the oscillations grow from any small initial perturbation of the bunch distribution, e.g., from the statistical fluctuations due to the finite number of beam particles.

To study the coupled motion of a positron bunch and the electron cloud we used the code CMAD (M.P. SLAC) [8]. The code accepts in input the files “sectormap” and “optics” previously generated by running MAD (mad8 or madx) with the ring lattice. Sectormap and optics files respectively include the information on the first and second order transfer maps and the Twiss lattice parameters for each element of the ring. The beam is then tracked along the ring by first order R and second order T transfer maps. Typically, the interaction between the beam and the electron cloud is simulated at every element of the ring. The bunch and the cloud are modeled by macroparticles and allowed to move in 3 dimensions (3D). During the beam-cloud interaction, the 2D forces from the beam and the cloud are computed. The bunch is typically sliced longitudinally and a number of kicks are applied to the electron cloud which is pinched by the positive beam potential. The electron cloud space charge force is computed at each bunch slice. The cloud experiences both the electric fields from the beam and the cloud. The dynamics of the electron is computed including the magnetic fields of the element and their position is updated with a Leap-frog and Boris rotation integrator scheme. Finally, the code makes use of parallel simulations to reduce the computation time when dealing with a large number of ring elements.

The input parameters for CMAD are collected in Table 1 and in Figure 2 are reported the DAΦNE beta functions, used in the simulation, as obtained by a MADX model that matches quite well beam measurements [9]. To take into account the suppression of the cloud in the drift regions of DAΦNE, where solenoids are installed, the interaction between the bunch and the cloud is computed only in the bending and wiggler sections of the ring.

Figure 2 shows emittance growth due to the fast single-bunch instability caused by the electron cloud effect in the DAΦNE e^+ ring. Each line shows an emittance growth for various cloud densities. The threshold density is determined by the density at which the growth starts. From this numerical simulation, we determine that the instability starts at a value of the electron density that is between $\rho_e = 2$ and $5 \times 10^{13} \text{ m}^{-3}$. This threshold is well above the simulated e-cloud density in wigglers and bending magnets [6].

Figure 3 shows the turn by turn evolution of the bunch population for different values of the cloud density. Above the instability threshold the bunch oscillation become large enough to lead to beam losses. In these simulations the bunch population is reduced to about the 50% of the initial value after 2500 turns.

Table 1: DAΦNE beam parameters used as input for CMAD simulations.

<i>Parameter</i>	<i>Value</i>
Beam energy E[GeV]	0.51
circumference L[m]	97.58
bunch population Nb	2.1×10^{10}
bunch length σ_z [mm]	12
horizontal emittance ϵ_x [um]	0.56
vertical emittance ϵ_y [um]	0.035
hor./vert. betatron tune Q_x/Q_y	5.1/5.2
synchrotron tune Q_z	0.012
hor./vert. avg. beta function	6/5
Momentum compaction α	0.019

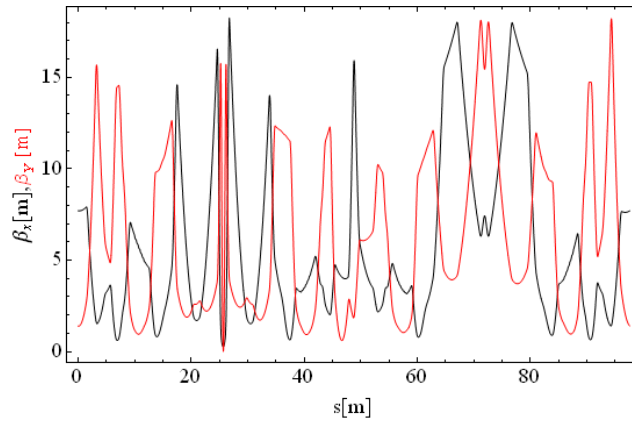


Figure 1: Horizontal (black) and vertical (red) beta functions as obtained by an accurate MADX model of the DAΦNE e^+ ring.

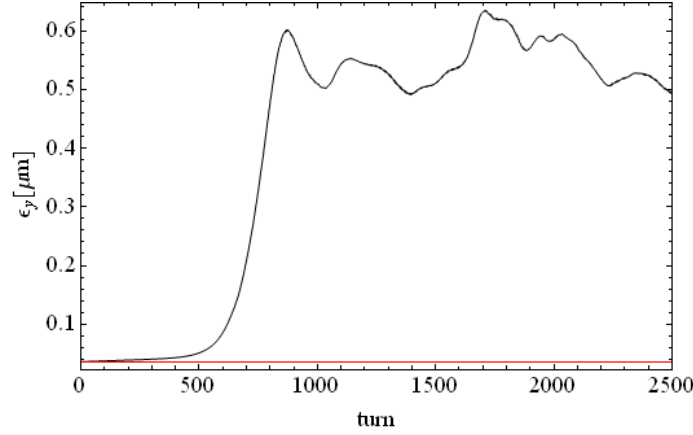


Figure 2: Vertical emittance growth due to single-bunch instability. The interaction between the beam and the cloud is evaluated in bending and wiggler sections of the DAΦNE e+ ring for an electron density $\rho_e=2\times 10^{13}\text{m}^{-3}$ (red) and $\rho_e=5\times 10^{13}\text{m}^{-3}$ (black).

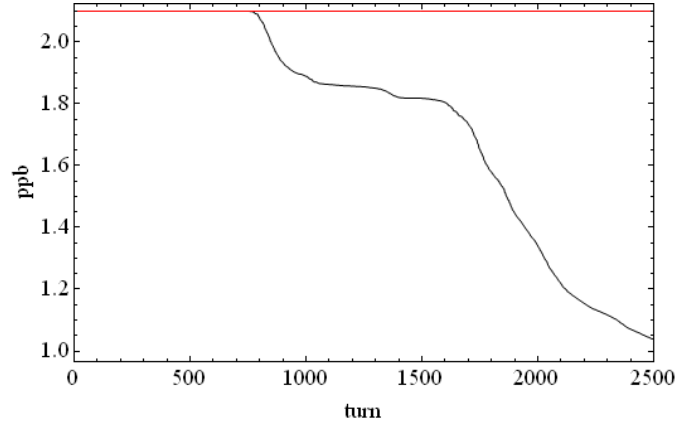


Figure 3: Number of particles per bunch as a function of turn number for an electron density $\rho_e=2\times 10^{13}\text{m}^{-3}$ (red) and $\rho_e=5\times 10^{13}\text{m}^{-3}$ (black).

3.2.3 Conclusions

We used the code CMAD to track the electron cloud induced single-bunch instability in the DAΦNE positron ring. Results show that, in agreement with experimental observation, the single bunch instability threshold is well above the value of the electron density estimated by the build-up simulations for the wiggler and bending section of the DAΦNE positron ring with the actual beam current. However the foreseen increase of the positron current and/or a further reduction of the beam emittances in DAΦNE may lead to a value of the cloud density close to the predicted instability threshold. For this reason, the installation of clearing electrodes to suppress electron cloud in the magnetic field regions of DAΦNE is under study [10]. A more detailed study of both coupled and single bunch instability, taking into account also the presence of clearing electrodes, is undergoing.

3.2.4 References

1. C. Vaccarezza, et al, ECLLOUD04, Napa Valley proc.
2. A. Drago et al., Proceedings of PAC05, p.1841.
3. C. Vaccarezza et al., Proceedings of PAC05, p.779.
4. A. Drago et al., proc. of the 40th ICFA Beam Dynamics Workshop on High Luminosity e⁺e⁻ Factories.
5. T. Demma, ICFA Beam Dyn.Newslett. **48**, pp. 64-71, 2009.
6. A. Drago, Proceedings of PAC09, p.1779.
7. K. Ohmi and F. Zimmermann, Phys. Rev. Lett. **85**, 3821 (2000).
8. M. T. F. Pivi, Proceedings of PAC07, p. 3636.
9. C. Milardi, Proceedings of EPAC08, p.2599.
10. D. Alesini, A. Battisti, T. Demma, V. Lollo, R. Sorchetti, M. Zobov, DAΦNE Tech. Notes, (in preparation).

3.3 Status of ATF R&D

N. Terunuma, K. Kubo, S. Kuroda and T. Naito for the ATF Collaboration
 High Energy Accelerator Research Organization (KEK)
 1-1 Oho, Tsukuba, Ibaraki, Japan
 Mail to: Nobuhiro.Terunuma@kek.jp

3.3.1 Overview

The Accelerator Test Facility (ATF) [1] in KEK is a research center for studies on

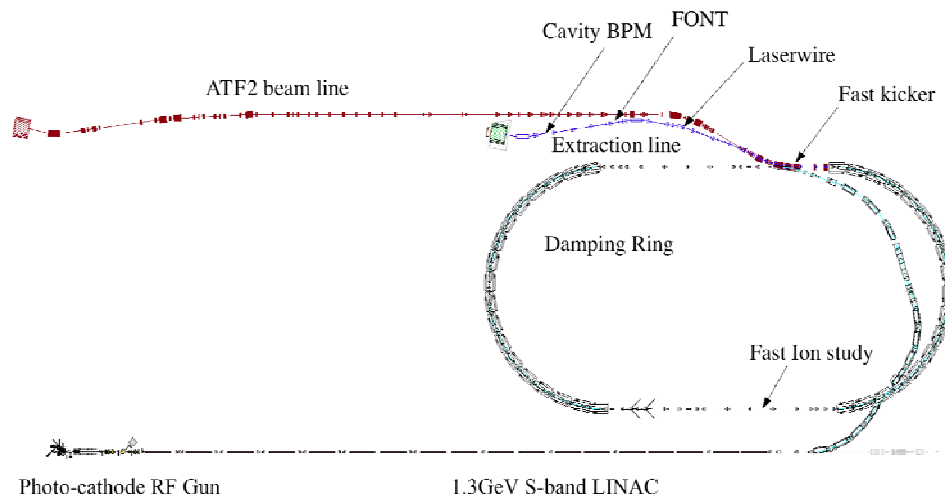


Figure 1: Schematic view of the ATF. Extraction line was modified to the ILC final focus test line (ATF2) in 2008.

issues concerning the injector, damping ring, and beam delivery system for the ILC. Figure 1 shows a schematic plan view of the ATF. It comprises a multibunch-capable RF gun (with up to 20 bunches, spaced by 2.8 ns, per pulse), a 1.3 GeV electron linac, a damping ring, and a beam extraction line. The extraction line has been modified, in

2008, as a test beam line for ILC final focus system (ATF2 [2]). Nominal electron beam in the ATF has an energy of 1.3 GeV, beam charge of 1×10^{10} e/bunch, and pulse repetition rate of 1.56 Hz. There are three types of operational modes, a single bunch mode, a multi-bunch mode of 20-bunches with 2.8 nsec bunch spacing, and a 3-bunches mode with 150 nsec spacing. The damping ring reduces transverse emittances of the beam down to 1.5 nm-rad and 6 pm-rad in horizontal and in vertical plane, respectively. Emittance tuning procedures are routinely performed applying corrections to reduce dispersion and couplings based on beam orbit measurements around the DR. The typical dimensions of the damped beam are 100 μm in horizontal, 10 μm in vertical, and 8 mm in longitudinal directions. After beam reaches equilibrium in the DR, it is kicked out to the extraction line. The emittance in the extraction line is measured with multiple wire-scanners. The extracted low-emittance beam has been used to develop various devices, such as cavity BPMs, laser-wire, ODR/OTR and intra-train feedback system (FONT) etc. In the ATF2 beam line started in end of 2008, the cavity BPMs are installed as a main beam position monitors and other monitors under developing are also installed.

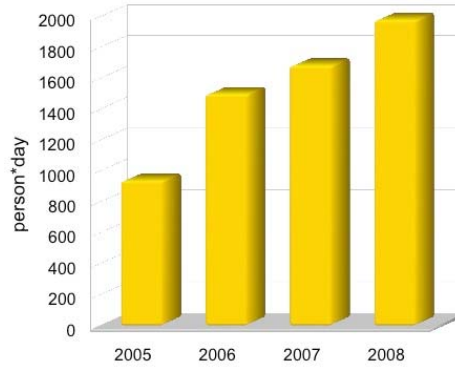


Figure 2: Numbers of visitors from overseas institutions that participated in the R&D programs at the ATF. The unit is person-days.

To continue providing vital opportunities for accelerator development for the ILC with the world community a set of Memorandum of Understandings (MoU) was signed by representatives of a number of institutions in the three regions, and definitive definitions were established for the organization of the international collaboration [3].

The beam operation at the ATF is scheduled for totaling 21 weeks per year, interlaced by regular maintenance and shutdown periods in the summer and in the winter. A large number of accelerator scientists from SLAC, LBNL, FNAL, Oxford University, DESY, CERN, UCL, LLNL, IHEP, PAL, RHUL and other institutions participated in research programs at the ATF (Figure 2).

3.3.2 Multi-Bunch Beam Injection/Ejection

3.3.2.1 *Cs₂Te Photocathode RF Gun*

The efficiency with which the electron beam is injected into the damping ring is a key issue for the research programs at the ATF. The electron source should supply the

electron beams with a bunch structure ranging from 1 bunch to 20 bunches per pulse with a 2.8 ns bunch spacing. Before 2002, the electron beam was generated by an injector based on a thermionic gun. The research activities at the ATF, especially those with the multi-bunch electron beam, were limited by a small amount of beam loss caused by an energy jitter and a beam tail. In 2001, experiments were conducted to solve these problems by temporarily replacing the above system and testing a conventional laser-driven S-band (2856 MHz) RF gun [4] in single-bunch operation. The injection performance of the damping ring was vastly improved. The conventional RF gun had produced an injection efficiency of almost 100 %, while the injection efficiency was about 60 % for 3.2 nC when the injector based on the thermionic gun was used.

To obtain the intensity required by the multi-bunch electron beam at the ATF, typically 1.6 nC per bunch and 20 bunches per pulse, the Cesium Telluride (Cs_2Te)

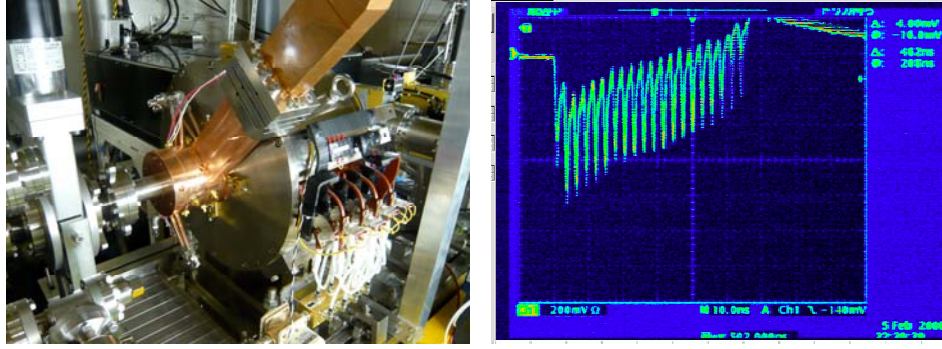


Figure 3: New photocathode RF gun (left) and the example of the multi-bunch beam stored in the damping ring (right).

photocathode [5] was selected for operation together with a laser system of a conventional scale. Cs_2Te is a well-known photocathode with a high quantum-efficiency (QE) (on the order of 1%). A conventional S-band RF gun with a modification to mount the Cs_2Te photocathode was produced for the ATF and installed in September 2002. The stored multi-bunch intensity was increased to 1.6 nC/bunch while that was 0.6 nC/bunch for the injector based on the thermionic gun. Further improvement on the design of RF gun was carried out and a newly manufactured RF gun was installed in September 2008 [6]. Figure 3 shows the RF gun and the example of the multi-bunch beam stored in the damping ring.

3.3.2.2 Multi-Bunch Beam Extraction from the Damping Ring

A double kicker system that extracts the low emittance multi-bunch beam stably from damping ring was developed at the ATF. It consists of two identical kicker magnets with single pulse power supply and compensates the kick angle jitter of the first kicker by tuning optics between two kickers. The kick angle jitter was reduced as 3×10^{-4} while that of single kicker scheme was 1×10^{-3} [7].

The upgrade of the double kicker system with a flattop of pulse length 340 ns was done by SLAC and KEK. It allows us to extracting 3 bunches at 154 ns duration and 2 bunches at 336 ns duration as shown in Figure 4. This ILC-like beam extraction is

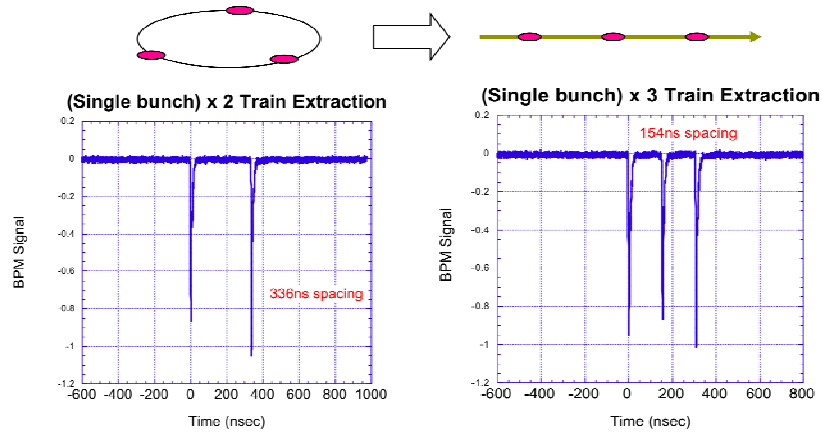


Figure 4: ILC-like beam extraction at ATF.

applied to the hardware development, such as FONT and Cavity BPM, described in later.

3.3.2.3 Fast Strip-line Kicker

In the ILC reference design report (RDR), the damping rings must store up to ~ 5120 bunches in a ~ 6 km circumference and provide the main linacs with bunches spaced apart by ~ 190 ns or ~ 370 ns. Thus, the injection and extraction kickers have to realize 3.0 nsec rise and fall times at a repetition rate of 3 MHz or 6 MHz. A collaboration was formed among KEK, SLAC, DESY, LBNL and LLNL in the fall of 2004 to address this issue. In spring, 2005, three flavors of pulse circuits (built by DESY, SLAC/LLNL and KEK) were used to test-drive a strip-line kicker (prepared by KEK), which was installed at the ATF damping ring. Two strip line kicker system demonstrates the rise and fall times of 2.2 ns and 3.0 ns, respectively, as achieved [8] with two commercially available 5 kV fast pulses and with two 32.7 cm long strip line kickers as shown in Figure 5. This R&D program has been continued to demonstrate the beam extraction from the damping ring [9], to check the stability and reliability, and to check the effects on previous and following bunches. The first beam extraction by the fast kicker system

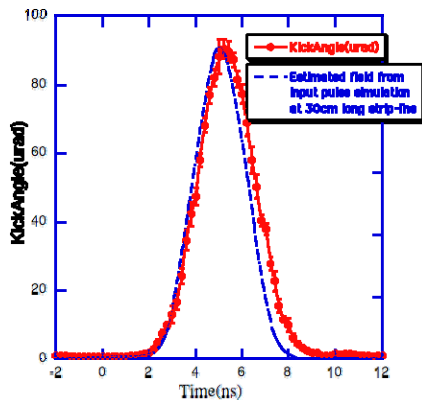


Figure 5: Timing scan of the kick angle by fast kicker. Amplitude of a beam oscillation excited by fast kicker was scanned by changing timing between a beam and a fast pulser.

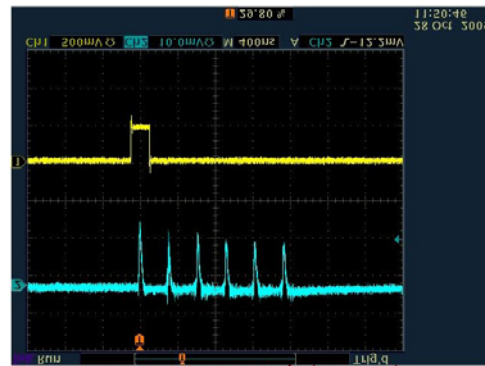


Figure 6: Multi-bunch beam extraction by a fast kicker. Extraction of six bunches at 308 ns duration was demonstrated on October 28, 2009.

was successfully demonstrated on October 2009. Multi-bunch extraction system was also tested. Figure 6 shows an example of the six bunches extraction. Improvements on the pulsers and the extraction system will be continued for the routinely application of the fast kicker for the ATF operation. Realizing the stable multi-bunch beam extraction will enable the R&Ds to make efficient, using ILC-like 30 bunches with a bunch spacing of 308 ns, for the ATF2 project.

3.3.3 R&D Using the Damping Ring

3.3.3.1 *Low Emittance Tuning*

One of the goals of ATF is to demonstrate ultra-low vertical emittance for linear colliders. Highly precise correction of the vertical dispersion and betatron coupling will be needed to achieve the target of 2 pm (which is the specification for the ILC). Optics correction and tuning must be supported by an accurate model, which can be developed from a variety of beam measurements, including orbit response to dipole kicks, beta functions at the quadrupoles, etc.

Our usual tuning procedure for low emittance in the ATF damping ring consists of three consecutive corrections: orbit correction, vertical orbit-dispersion correction, and coupling correction. The performance of the tuning with misalignment of magnets and errors in the BPMs was studied by simulations [10]. Using this procedure, we had achieved and confirmed very low emittance beam, of around 4 pm [11,12] in 2004. Over the past year, renewed efforts have been made to achieve very low emittance once again [13]. In April and May 2009, the vertical emittance after tuning was less than 10 pm. Three items of studies were performed for the low emittance: Beam based alignment measurement (BBA), beta-beat correction and analysis of orbit response matrix (ORM).

Simulations have shown that the vertical emittance after tuning depends strongly on vertical offset errors of BPMs with respect to the nearest magnet field centre (magnet to BPM offset) [10]. For reducing these errors, we perform beam based alignment measurement (BBA). BBA is performed with each pair of quadrupole (or sextupole) magnet and the nearest BPM, one by one. Since the vertical position is more important than the horizontal position for the vertical emittance tuning, we first concentrated on the vertical offsets of BPMs.

For each quadrupole-BPM pair, vertical local bump orbits of several different amplitudes are set, where the beam position change at the magnet should be the same as at the BPM. Then for each bump setting, the response of the vertical orbit in the whole ring (beam position at all BPMs) to the strength change of the magnet is measured. If the beam is at the field center of the magnet, there should be no orbit response. The procedure is similar for a sextupole magnet-BPM pair. Each sextupole magnet has trim windings to produce a skew quadrupole field, and BBA is performed for that skew quadrupole field. So, for each vertical bump setting, the response of the horizontal orbit to the strength change of the magnet is measured. The typical error of the measured offset, estimated from fluctuations of the BPMs, is about 30 micron for quadrupole magnets and about 80 micron for sextupole magnets.

Our experiences have shown that optics matching can be important for achieving low emittance. There were obvious beatings in the arc sections in a case when we could not achieve low emittance. Effects of the optics mismatch were studied by applying the

same simulation of low emittance tuning to different matching conditions. The results suggest that the mismatch will enhance the sensitivity to errors (misalignment of magnets and BPMs).

Recently, we set a new optics that, in calculation, has no beta-beat. Then, the beta functions at every quadrupole magnet were measured, by observing the betatron tunes as functions of the strength of each magnet. Since there are errors in the optics model, there remained some beta-beat. We tried to correct the residual beta-beat based fully on model calculations. However, we found that the fitted beta-function had some difference from the measurement. The model was not good enough for predicting the beta function after quadrupole strengths change.

We still could reduce the beta-beat by a somewhat empirical technique, though the results are not completely satisfactory. In this correction, we concentrated on the beta function at magnets of one family in the arc sections (magnets named QF1R). Then, using model calculations, we looked for quadrupole magnets whose change would partly correct the beta-beat in that region. More systematic methods of beta-beat correction and the effect of such corrections on the performance of low emittance tuning are still under investigation.

Orbit response matrix (ORM) analysis is a well-established technique for identifying and correcting optics errors [14]. Briefly, one measures changes in the closed orbit with respect to changes in strength of a number of orbit correctors, and then fits a machine model to the data, by adjusting parameters such as quadrupole strengths, BPM gains and couplings, and corrector magnet strengths and tilts. At ATF, the orbit response matrix is measured using all BPMs in each plane, and all steering magnets. This procedure effectively projects the betatron coupling sources onto the skew quadrupoles, and thus allows the determination of skew quadrupole strengths required to cancel the coupling sources. Previous studies [15] have validated the ORM analysis technique by showing that known changes in skew quadrupole strengths can be identified from fitting ORM data taken immediately before and after the changes were made. We obtained similar success during more recent attempts at coupling correction.

After recent efforts using a variety of techniques to reduce the emittance in the ATF damping ring, a vertical emittance less than 10 pm was constantly achieved in April and May 2009. Figure 7 shows the recent history of the low emittance achievement, measured using three different beam size monitors. Emittance is evaluated from the beam size and beta-function at each monitor, which is fitted from beta-function at quadrupole magnets around the monitor. Our experiences suggest the laser wire monitor is the most reliable for small beam size measurements.

In order to achieve even smaller emittance (2 pm is the target), more studies on the tuning procedure and analysis of beam measurements will be necessary. In addition, it is planned to upgrade all BPM electronics and to carry out a re-alignment of the magnets.

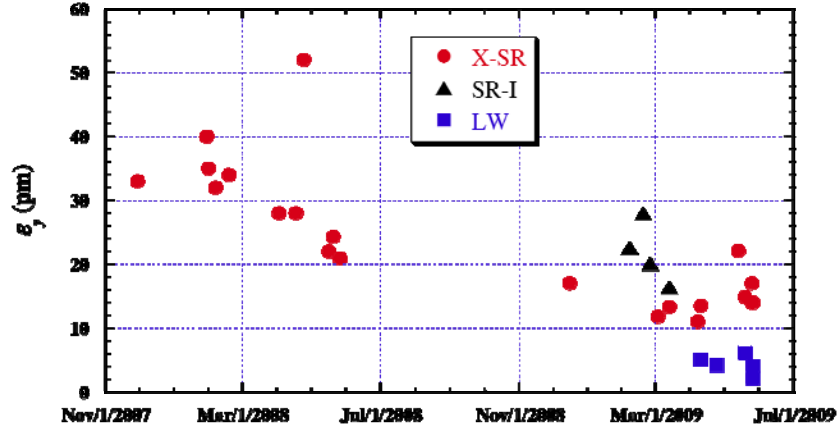


Figure 7: Achieved low vertical emittance as function of date. Measured using X-ray synchrotron radiation profile monitor (X-SR), synchrotron radiation interferometer (SR-I) and laser wire (LW)

3.3.3.2 Upgrade of the Readout System for the Damping Ring BPM

In frame of the International Linear Collider (ILC) R&D program, the goal of the beam studies at the KEK ATF damping ring is to generate and extract a beam with an ultra-low vertical emittance < 2 pm. This requires various optimization methods to steer the beam along an optimum (“golden”) orbit with minimum disturbance of non-linear field effects. A high resolution BPM system is one of the important tools to achieve this goal, which requires a resolution in the 100 nm range in a “narrowband” mode.

New read-out system based on analog and digital down-conversion, digital signal processing, and a gain error correction schema (see Figure 8) was installed in May of 2007, by the team of FNAL, SLAC and KEK [16]. New circuits are distributed along the arcs and cover 20 (out of 96) of damping ring BPMs. Figure 9 shows the improvements of the beam position read-out. Revising of the read-out circuit for remaining BPMs is planned in FY2010.

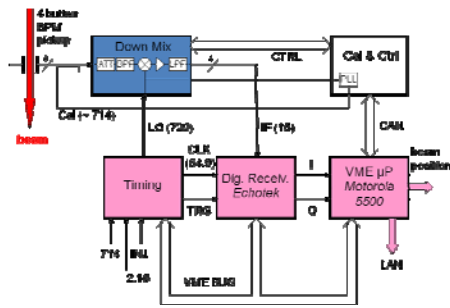


Figure 8: Upgraded BPM hardware.

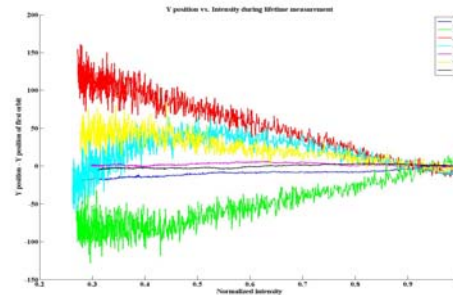


Figure 9: Position data of the stored beam, as a function of the bunch intensity. Data from BPMs with the old, existing readout circuits and with new test circuits are overlaid.

3.3.3.3 Study of the Fast Ion Effects

Fast ion instability is one of the highest priority R&D issues for the ILC damping rings. In low emittance and high intensity rings, the growth rate of the instability is particularly high [17,18].

The vertical emittance of the multi-bunch beam was measured at ATF in 2004 and it showed the emittance growth for later bunches under the smaller vertical emittance of 4 pm. The simulation including fast ion instability suggested that the emittance growth at ATF was caused by a fast ion effect. Therefore, the fast ion experiment at the ATF damping ring is planned to (1) distinguish the two ion effects, beam size blow-up and dipole instability, (2) quantify the beam instability growth time, tune shift and vertical emittance growth, (3) provide detailed data to benchmark simulations. The instruments

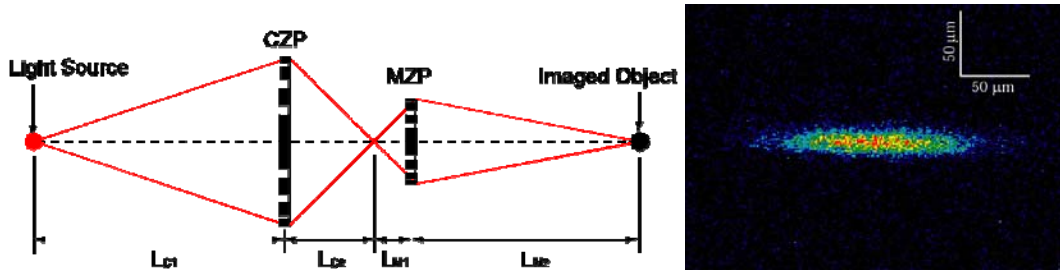


Figure 10: Schematic of the X-Ray Telescope using Zone Plate (left) and the beam profile measured by a X-ray CCD camera (right).

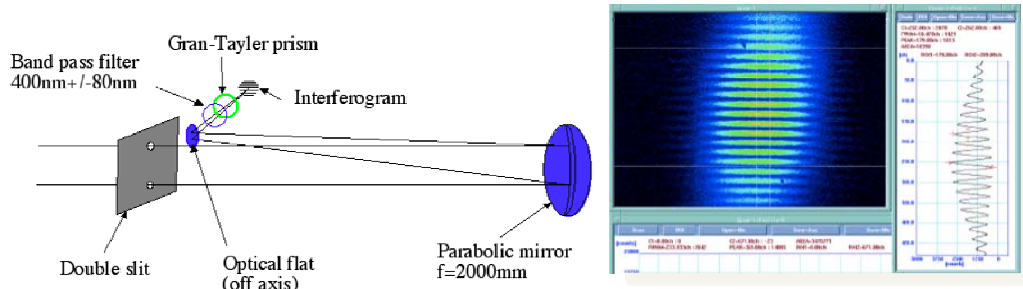


Figure 11: Schematic of the SR interferometer (left) and the interferogram measured by CCD camera (right).

to measure the bunch-by-bunch position, N_2 gas injection system to vary the vacuum pressure are installed in the damping ring [19]. The study was started in 2009 after confirming a small vertical emittance beam.

3.3.3.4 X-ray SR Monitor

Imaging its source point on a screen, synchrotron radiation (SR) can be used to measure the beam profile. Since the beam size in the arc sections of the DR is too small to image with a visible light due to the diffraction limit, we have developed an X-ray optical system [20]. SR from a bending magnet is first reflected by a monochromator of Si crystal to choose 3.24 keV X-ray, then transported through a magnification optics

which consists of two Fresnel Zone Plates (FZP). It was designed to realize a 20 times magnified image of the source on an X-ray CCD camera as shown in Figure 10. This monitor can measure beam size as small as $5\ \mu\text{m}$ with $1\ \mu\text{m}$ resolution, and is now routinely used in beam operation, especially for the tuning of the low emittance beam.

3.3.3.5 SR Interferometer

Spatial coherence of SR can be used to estimate its source size. SR of visible light region is transported to a double-slit interferometer as explained in Figure 11. Visibility of the interferogram is a good measure to tell the beam size, as the smaller the beam size and the larger the visibility. This monitor can measure $5\ \mu\text{m}$ beam size with a carefully tuned system [21].

3.3.3.6 Optical-Cavity Laser Wire Monitor

To reliably measure beam emittances in DR, a direct way to measure the beam size was developed [22]. This monitor uses a thin laser beam to scan the electron beam in the transverse direction. Compton scattering produces gamma rays in the forward direction of the electron beam. Since the flux of the gamma ray is proportional to the convolution of the beam profile and the laser profile, the beam profile can be obtained by scanning the laser across the beam. To be able to measure a small beam size, laser

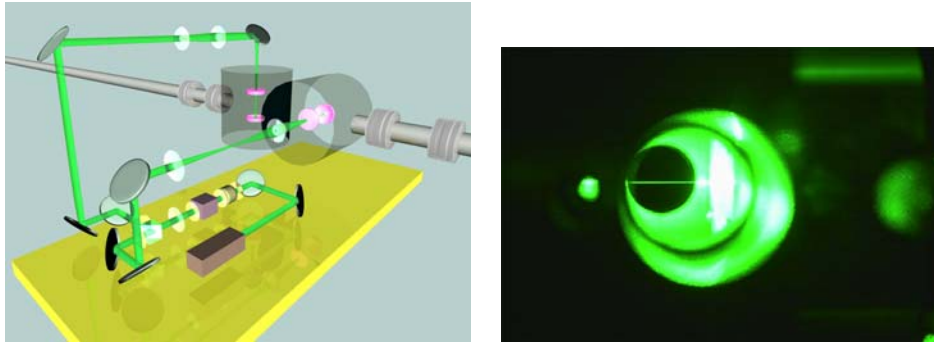


Figure 12: Schematic of the laser wire system in the damping ring (left) and a photo of the laser wire in the vacuum chamber (right).

beam has to be well focused. A CW laser of 532 nm wavelength is injected into a high finesse optical cavity of nearly concentric configuration to stably realize such a small spot while enhancing the effective laser power by 1000 times. By identifying the bunch number with the incoming timing of the scattered gamma rays, this monitor can separately measure each bunch of the multi-bunch beam at the same time. This monitor can measure $5\ \mu\text{m}$ beam size with a good accuracy since the laser spot size is known precisely. Since it takes 5 minutes to complete a scan, accurate beam orbit monitoring to remove the effects of beam position drift is necessary to further improve the system. Figure 12 shows the laser wire system in the damping ring.

3.3.4 R&D Using Extracted Beam

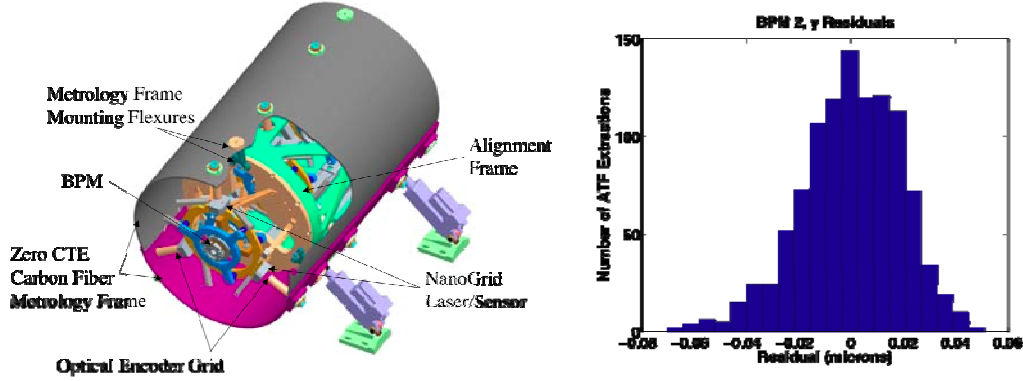


Figure 13: Schematic of the nano-BPM triplet with Nanogrid system (left). Typical distribution for the residuals at second BPM from the predicted position by the first and third BPMs (right).

3.3.4.1 Cavity Beam Position Monitors (BPM)

Transverse dipole modes are useful to measure the beam positions because their field strength are proportional to the product of beam charge and the beam offset with respect to the electrical center. The beam signal is read out through a rectangular waveguide coupler that selectively couples only with the dipole mode. The strong and narrowband signal enables us to measure the beam position with order nano-meter resolution. Mechanical rigidity and reliability of the electric center are also advantages of cavity BPMs. These types of BPMs are expected to play important roles in ATF-II and future accelerators. Problems of these cavities are the calibration, stability and turnkey operation, a problem that will be studied at ATF2 as a prototype for the ILC-BDS.

3.3.4.1.1 Nano-BPM

Developments of a nanometer resolution cavity BPM were carried out in ATF extraction line. Signal strength depends on the choice of cavity frequency. Considering the relatively long bunch length, C band frequency (~ 6 GHz) was estimated to be the most sensitive in ATF, and it was a basis of the following development at ATF.

Three-BPM method is a usual technique to study very high resolution BPMs. A triplet of BPMs is supported by a rigid frame so that the relative position of the three is mechanically stable. A precise mover system is needed to align the BPMs in a straight line within $10\ \mu\text{m}$. Two of the three are used to monitor the beam orbit and they predict the beam position at the remaining BPM. Comparing the actual measurement with the prediction, resolution of the BPM can be estimated. Two sets of BPM triplet systems, based on the different stabilization ideas, were developed in the extraction line.

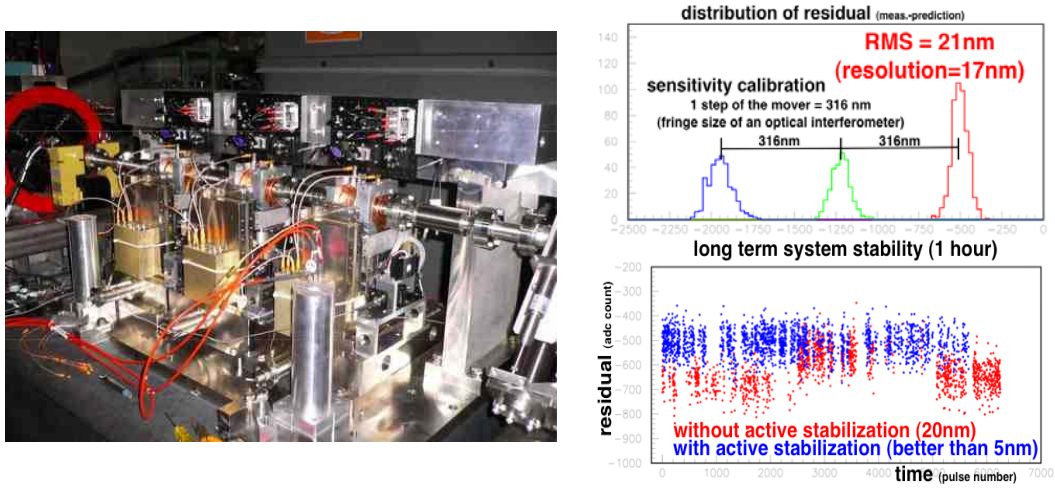


Figure 14: The nano-BPM triplet with an active stabilization system (left). Distribution of residuals by moving BPM (right-top). The long-term stability with(out) the active stabilization (right-bottom).

One triplet was designed by a US group, based on a Budker Institute for Nuclear Physics (BINP) design, the three BPMs were rigidly mounted inside an alignment frame on six variable-length struts, so called Nano Grid, which allowed movement in position and angle as shown in Figure 13. The RF signals from the cavities were down converted in two-stage mixer-amplifier circuit, yielding an IF of approximately 20 MHz. The down converted signal was sampled using a fast digital waveform recorder, operating at 100 MHz. Using an analysis procedure of fitting or digital down-conversion, the data was converted to beam positions. The demonstrated position resolution was 15.6 nm and a tilt resolution was 2.1 μrad , over a dynamic range of approximately 20 μm [23].

The other triplet was designed by KEK with an active stabilization system by movers and optical interferometers. As for the electronics, this system used a fast analogue electronics that directly rectified the signal into beam positions. Calibrating the scale by moving one of the BPM with known amount, the residual between the measurement and prediction can be estimated as shown in Figure 14. The position resolution smaller than 17 nm was also shown by this BPM triplet. Further, an active stabilization system had improved the long-term stability.

3.3.4.1.2 ATF2-BPM

Based on the results of the prototype cavity BPM, described in above, further improvements were done by the collaboration between KEK, SLAC and PAL [24]. The resonant frequency of the cavity and the isolation between horizontal and vertical modes were tuned efficiently using tuning pins brazed on the cavity rim instead of the conventional tuning plunger. Offset between electrical and mechanical centers could be reduced by tuning within $\pm 5 \mu\text{m}$, the isolation tuned better than 50 dB, and the 100 nm resolution of the cavity BPM has been proved through the beam tests in the ATF extraction beamline. Cavity BPMs for the ATF2 beam line, 39 in total, were fabricated by PAL as shown in Figure 15.

Cavity BPMs for the final doublet magnets were also fabricated by the collaboration between KEK and the Kyungpook National University (KNU, Korea). These BPMs

have an inner diameter of 40 mm for the enlarged beam size before the focal point of ATF2. Therefore, the resonant frequency of BPM is selected as S-band 2.872 GHz [25].

The readout and controls of the ATF2 BPM system has also been improved using the experience of the ATF systems described above. All BPMs S and C band are processed using a single stage image-rejection mixer and amplifier circuits constructed by JAI and SLAC respectively. The resulting IF is approximately 20 MHz for all cavities, which is subsequently digitized by 100 MHz, VME system. The waveforms are processed in real-time to produce position signals using an EPICS software package developed by the JAI.



Figure 15: C-band cavity BPM in the ATF2 quadrupole (left) and S-band cavity BPM in the final doublet quadrupole (right).

The readout and controls of the ATF2 BPM system has also been improved using the experience of the ATF systems described above. All BPMs S and C band are processed using a single stage image-rejection mixer and amplifier circuits constructed by JAI and SLAC respectively. The resulting IF is approximately 20 MHz for all cavities, which is subsequently digitized by 100 MHz, VME system. The waveforms are processed in real-time to produce position signals using an EPICS software package developed by the JAI.

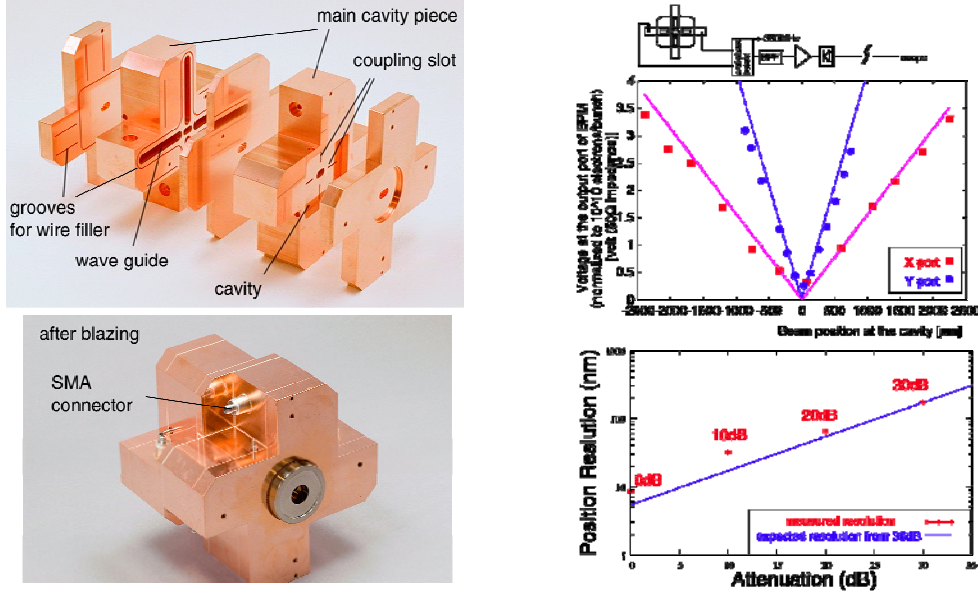


Figure 16: Structure of IP-BPM (left), the position sensitivity (right-top) and the resolution evaluation (right-bottom). At the highest sensitivity 0dB, the position resolution of 8.7 nm was obtained.

3.3.4.1.3 IP-BPM

The main goal of the ATF2 project are to prove a possibility of focusing a beam down to nanometer size at the focal point (the virtual IP) while stabilizing beam position to within nanometers. It provides a direct demonstration of beam position stability at the IP, tracks the beam trajectory during beam size measurements to correct the effects of position jitter, and produces a feedback signal to stabilize the beam orbits of the following bunches. Development of the ultra-fine resolution cavity BPM (IP-BPM), the goal resolution of 2 nm, for the focal point of ATF2 had been carried out by KEK, Tokyo University and KNU (Korea) as shown in Figure 16. The rectangular shape isolates two dipole modes in the orthogonal direction and the thin gap reduces the sensitivity to trajectory inclination. A highly sensitive analog processor with phase-sensitive detection was also developed. The characteristics of the cavity were checked in the previous ATF extraction line [26]. Results show the achieved position resolution of 8.7 nm for a beam intensity of 0.7×10^{10} e/bunch with a dynamic range of $5\mu\text{m}$. Low-Q type IP-BPM for multi-bunch beam operation was also developed by KNU and KEK [27,28]. Figure 17 shows results of low-Q IP-BPM tested in the extraction line and the beam signals well separated for the three bunches with a bunch spacing of 154 ns.

3.3.4.1.4 Cold-BPM

The development of the cavity BPM for ILC main linac and for STF has been started under the collaboration of Pusan National University (Korea) and KEK. Performance of the BPM is evaluating with a beam at the end of the ATF linac [29].

3.3.4.2 Pulsed Laser Wire System in the Extraction Line

The ILC and other electron accelerators require beam size measurements of order μm for emittance measurement. The need to avoid invasive methods leads to a requirement for micron size laser wire systems [30]. The aim of the ATF extraction line laser-wire project is to develop a system capable of reliably measuring an electron beam of order one micron in vertical size. A laser beam is focused with a specially designed f/2 lens system to have an order μm spot size, and is used to scan across the electron beam.

To obtain enough Compton signal in single collision, a pulsed laser of high peak power is necessary, typically peak pulse powers exceeding 100 MW. A passive mode locked seeded regenerative Nd:YAG laser combined with a high power linear amplifier is used to generate laser pulses of 0.4 J with a duration of approximately 300 ps at a wavelength of 532 nm. With these short pulses a precise timing system is also important to establish stable collisions.

The various optical focusing and operation schemes have been tested on the prototype system located at the ATF extraction line. The beam line device to realize and test the collision of a laser is shown in Figure 18. In addition to the focusing lens and beam pipe, a specialized interaction chamber [31], knife-edge target with vacuum manipulator to establish collision timing [31-32] are required. The custom lens is directly fixed to the interaction chamber to minimize optical aberrations as the optical device. The interaction chamber itself can be moved in two orthogonal directions with respect to the beam direction, allowing collision optimization and laser focus scanning. The smallest convoluted beam size was obtained as $4.0 \mu\text{m}$, shown in Figure 18, while the estimated laser size was between 1.9 and $2.3 \mu\text{m}$.

A detailed study of the factors which limit the beam size measurement [33] reveals

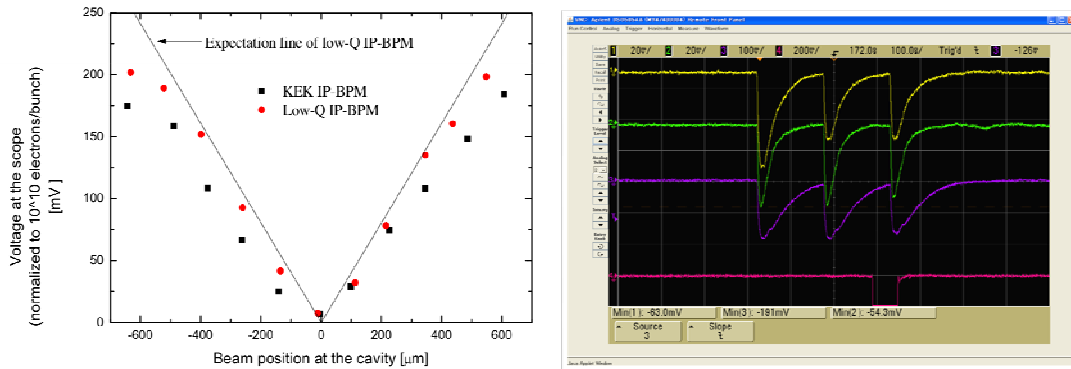


Figure 17: Beam test results of the low-Q IP-BPM. Position sensitivity (left) and the signal separation for three bunches with a bunch spacing of 154 ns (right).

that the custom lens was probably over-filled with laser light, increasing the focused laser beam size and dispersion was increasing the electron beam size. Further improvement to achieve a μm laser-wire system will be continued at the ATF2 beam line. The relocation of the system into the ATF2 beam line is already complete and the system will be re-available in early 2010.

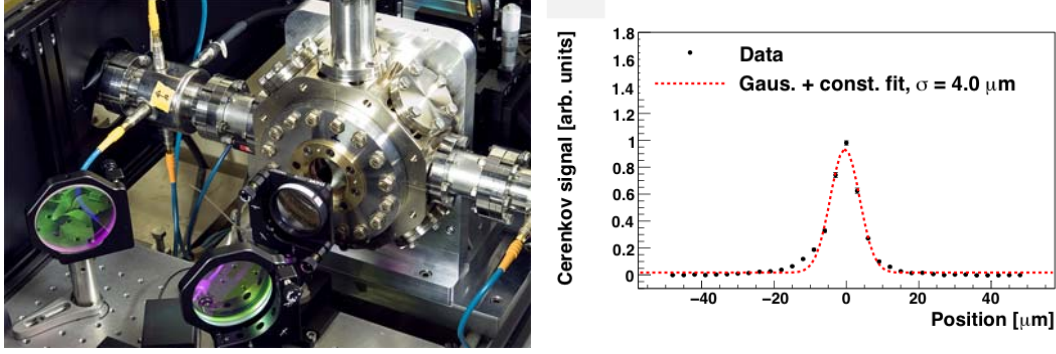


Figure 18: The beam line device of the pulsed laser wire at the collision point (left). The smallest convoluted beam size was obtained as $4.0 \mu\text{m}$ (right).

3.3.4.3 Wire Scanners

The emittances of the extracted beam are usually measured by a wire scanner system. Tungsten wires of $10 \mu\text{m}$ diameter are installed in horizontal, vertical, 45 degree and 10 degree direction in a scanning system [34]. The horizontal (vertical) wires are used to measure the vertical (horizontal) beam size, and the angled wires to estimate the beam tilt. An air-Cherenkov detector placed downstream measures the flux of the gamma ray produced in the collision of the wire and the beam. There are 5 sets of the wire scanners in the dispersion-free section of the extracted line to calculate emittances by measuring development of the beam size along the phase advance. Although it can measure beam size as small as $3 \mu\text{m}$, the resolution of the emittance measurement is limited by residual dispersions in the extraction line.

3.3.4.4 Optical Transition Radiation Monitor

A beam profile monitor to be able to measure beam spots as small as $5 \mu\text{m}$ with the optical transition radiation (OTR) was developed in the extraction line [35]. Visible light is emitted from a polished plane of a beryllium target when intercepted by the electron pulse. In order to image the radiation that has an opening angle of $1/\gamma$ without aberrations, a high NA lens system to magnify the source image is needed. Although it successfully verified the expected resolution, the target could not tolerate the high intensity beam for a long enough time.

3.3.4.5 Optical Diffraction Radiation Monitor

An experiment on the investigation of optical diffraction radiation (ODR) from a slit target as a possible tool for non-invasive electron beam-size diagnostics has been performed at the KEK accelerator test facility. The experimental setup has been installed at the diagnostics section of the extraction line [36]. The first observation of

the incoherent ODR from a slit target has been performed. The measured angular distributions are in reasonable agreement with the theoretical expectation. The beam-size effect onto the ODR angular pattern has been observed. Moreover, the sensitivity to the beam size as small as $14\text{ }\mu\text{m}$ has been achieved. The experiment was performed with a photomultiplier that excludes a possibility for single shot diagnostics. In a next stage experiment a single shot electron beam size measurements using a low-noise cooled CCD camera was done. The resolution for the beam size measurements of about $15\mu\text{m}$ was confirmed. Also the observation and detailed investigation of the pre-wave zone effect (PWZ) effect in optical transition (OTR) and diffraction (ODR) radiation phenomena [37] has been done. And as an option to correct a distortion caused by PWZ effect in beam size monitors another proof-of-principle experimental comparison of OTR and ODR generated by the flat and the spherical target in the pre-wave zone were done [38].

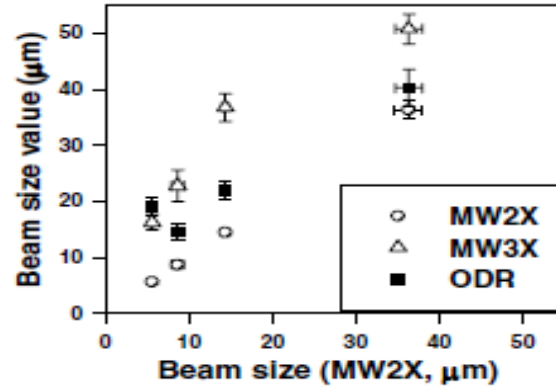


Figure 19: The correlation between the beam size measured with ODR (black squares) and two wire scanners installed upstream (open circles) and downstream (open triangles) of the target.

3.3.4.6 Interference Fringe Monitor

To measure 37 nm vertical beam size to be realized at ATF2, a beam size monitor based on the laser interference fringes is prepared. It was used at the Final Focus Test Beam (FFTB) experiment at SLAC [39]. There 70 nm vertical beam size was measured. The beam size monitor at ATF2 focal point is an upgrade from the one used at FFTB. The major modification is the wavelength of the laser. To have a sufficient sensitivity of the beam size measurement at ATF2, the second harmonics of Nd:YAG laser, 532 nm [40], is used while the wavelength of 1064 nm of Nd:YAG laser was used at FFTB.

The layered CsI(Tl) scintillation detector [41] was developed to detect the signals of scattered laser photons. Figure 20 shows the interferometer system at ATF2 focal point. The commissioning of the monitor with the laser wire mode has been started from the end of 2008. The interferometer mode will be started in November 2009.

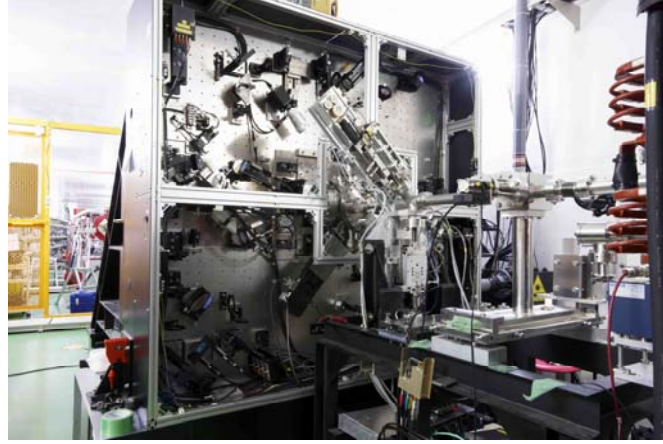


Figure 20: The interferometer system at the ATF2 focal point.

3.3.4.7 FONT

FONT (Feedback on Nanosecond Timescales) is an experimental program being pursued by a team comprising Oxford University, KEK, and SLAC to test a very fast orbit feedback which is applied within a bunch train. This technology is vital in order to realize stable beam collisions in ILC, as well as stabilization in the virtual IP of ATF2.

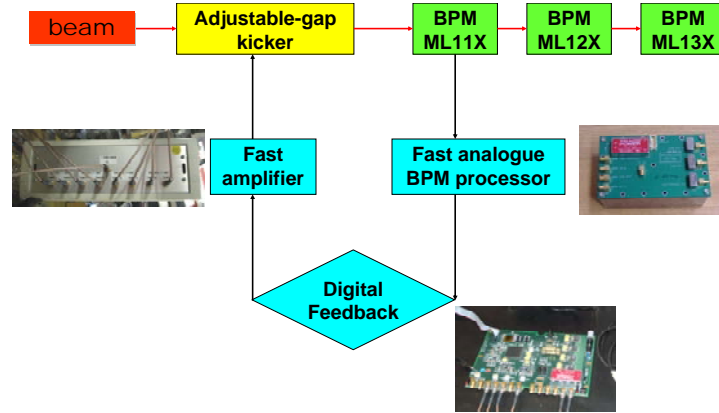


Figure 21: Schematic of FONT4 at the ATF extraction beamline showing the elements of the feedback system.

Critical issues for the intra-train feedback performance include the latency of the system, as this affects the number of corrections that can be made within the duration of the bunch train, and the feedback algorithm. Previously we have reported on all-analogue feedback system prototypes in which our aim was to reduce the latency to a few tens of nanoseconds. We achieved total latencies (signal propagation delay + electronics latency) of 67ns (FONT1) [42], 54ns (FONT2) [43] and 23ns (FONT3) [44].

The use of a digital processor will allow for the implementation of more sophisticated algorithms which can be optimized for possible beam jitter scenarios at ILC. This approach is now possible for ILC given the long, multi-bunch train, which includes parameter sets with c. 3000/6000 bunches separated by c. 300/150ns respectively. Initial results were reported previously [45,46].

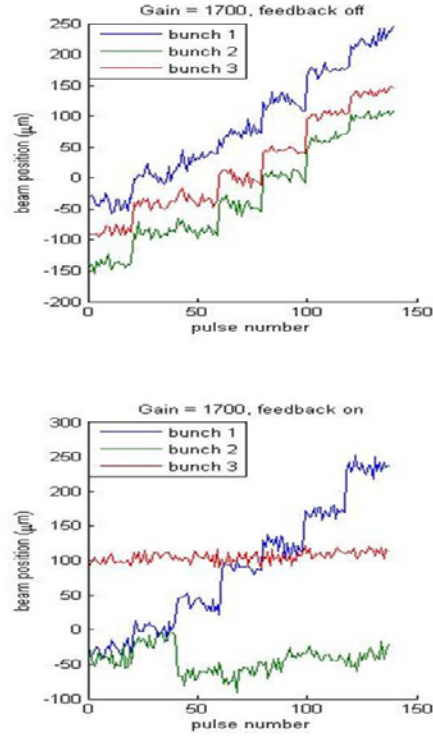


Figure 22: Beam position vs. pulse number: feedback off (top) and on (bottom) for sequential changes in the incoming beam orbit.

The ATF damping ring can be operated so as to provide an extracted train that comprises 3 bunches separated by an interval that is tunable in the range 140 - 154 ns. FONT4 has been designed [45] as a bunch-by-bunch feedback with a latency goal of less than 140ns. A schematic of the FONT4 feedback system prototype and the experimental configuration in the ATF extraction beamline is shown in Figure 21. The layout is functionally equivalent to the ILC intra-train feedback system. This allows measurement of the first bunch position and correction of the second and third bunches. The correction to the third bunch is important as it allows test of the ‘delay loop’ component of the feedback, which is critical for maintaining the appropriate correction over a long ILC bunch train. Figure 22 shows the system operation with the gain set approximately optimally and bunch 3 steered to an arbitrary vertical position.

Although current operation is with only 3 bunches in a train, it is planned in future to operate ATF with the fast kicker system which extracts trains of 30 bunches with a bunch spacing of 154 or 308 ns; the design allows for this upgrade.

3.3.5 R&D for the Polarized Positron Source

3.3.5.1 Cavity Compton

The International Linear Collider (ILC) seeks to provide polarized electron beams for precise measurements of physics phenomena. In addition to the electron beam, there are hopes that polarizing positron beams as well will further improve the performance of the ILC as a machine for making precise measurements. The ILC baseline design

adopts the helical undulator scheme in which 150 GeV electrons are fed into the helical undulator with a length of more than 150 m to create photons.

One option for polarized positron generation is to use laser-Compton scattering for photon generation (the Compton scheme). The advantage of the Compton scheme is that the required energy of the electron beam to generate 10 MeV photons is about 1 GeV, which is low enough to develop positron sources using the existing small electron beam facilities. The proof of the principle of generating polarized positrons with the Compton scheme has been demonstrated by a series of experiments performed at the ATF [47]. The next step toward the positron source will be to increase the intensity of photons required by the ILC. For this purpose, we adopt a scheme to increase the intensity of the laser pulses by accumulating them in an optical resonant cavity in the ATF damping ring [48], and performed an experiment to generate photons by laser-Compton scattering.

The laser power was enhanced up to 250 times that of injection power by the accumulation. The generated photons were 26.0 ± 0.1 photons/train, which corresponds to 10^8 photons /second. The results demonstrated the feasibility of using the optical resonant cavity for effective photon generation by laser-Compton scattering. The photon yields were almost consistent with expectations but appreciable deviation was observed for larger number of bunches per train. The effect of synchrotron oscillation on the bunch in the ATF may be a cause but further investigation is necessary [49].

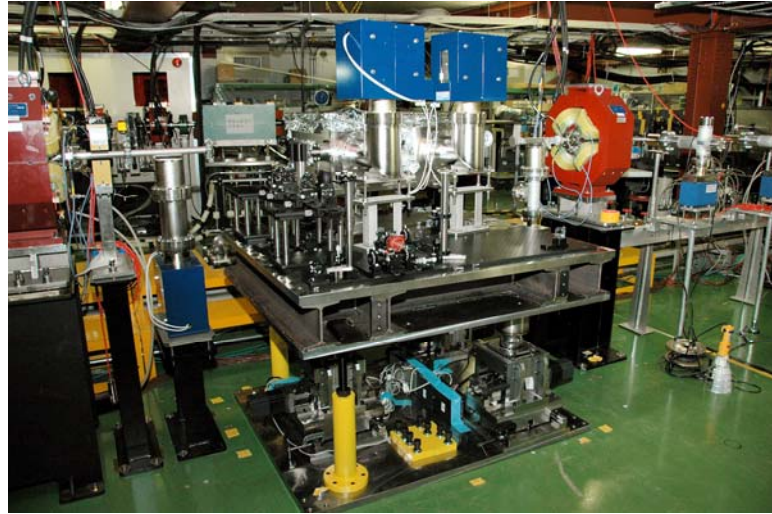


Figure 23: The optical resonant cavity is installed in the straight section of the KEK-ATF damping ring.

3.3.6 Acknowledgements

The authors would like to express our gratitude to all members of the ATF international collaboration for their activities on the R&Ds at the ATF. We are also grateful to Prof. Philip Burrows, Dr. Stewart Boogert, Dr. Pavel Karataev and Dr. Alexander Aryshev for their helps preparing this report.

3.3.7 References

1. F. Hinode et al., ATF Design and Study Report - KEK Internal 95-4.
2. ATF2 Proposal, Volume 1, CERN-AB-2005-035, CLIC note 636, DESY 05-148, ILC-Asia-2005-22, JAI-2005-002, KEK Report 2005-2, SLAC-R-771, UT-ICEPP 05-02 (2005), Volume 2, KEK Report 2005-9, CERN-AB-2006-004, DESY 06-001, ILC- Asia-2005-26, JAI-2006-001, SLAC-R-796, UT- ICEPP-05-04.
3. The ATF international collaboration, <http://atf.kek.jp/collab/>
4. X.J. Wang, et al., Proceedings of PAC97, Canada, 1998, p. 2793.
5. P. Michelato, Nucl. Instrum. Methods Phys. Res., A 393 (1997) 455.
6. N. Terunuma et al., To be published in Nucl. Instrum. Methods Phys. Res., A.
7. T. Imai, et al., "Highly Stable Beam Extraction by Double Kicker system", KEK-Preprint 2002-16, May 2002.
8. T. Naito et al., "Development of a 3ns rise and fall time strip-line kicker for the international linear collider.", Nucl. Instrum. Methods Phys. Res., A571, p.599 (2007).
9. T. Naito et al., "Design of the Beam Extraction by Using Strip-line Kicker at KEK-ATF", Proceedings of EPAC08, p.MOPP025 (2008)
10. K. Kubo, "Simulation study of low emittance tuning of the Accelerator Test Facility damping ring at KEK" Physical Review ST-AB, vol. 6, 092801 (2003)
11. ATF Collaboration, "Extremely low vertical emittance beam in accelerator test facility at KEK", Phys. Rev. Lett. 88:194801, 2002.
12. Y. Honda et al., "Achievement of ultralow emittance beam in the ATF damping ring", Phys. Rev. Lett. 92:054802, 2004.
13. K. Kubo *et al.*, Proceedings of PAC09, FR1RAC05
14. J. Safranek, "Experimental determination of storage ring optics using orbit response measurements," Nucl. Instrum. Methods Phys. Res., A388 (1997) 27-36.
15. A. Wolski, M.D. Woodley, J. Nelson, M.C. Ross, "Analysis of KEK-ATF optics and coupling using LOCO," proceedings of EPAC 2004, Lucerne, Switzerland.
16. P. Priet, et al., "High resolution upgrade of the ATF damping ring BPM system", Presented at 13th Beam Instrumentation Workshop (BIW08), Lake Tahoe, California, May 2008.
17. T. Raubenheimer and F. Zimmermann, Phys. Rev. E52, no.5, p.5487 (1995).
18. G.V. Stupakov, T. Raubenheimer and F. Zimmermann, Phys.Rev.E52, no.5, p.5499 (1995).
19. N. Terunuma et al, Proceedings of EPAC08, p.MOPP066.
20. H. Sakai et al., Phys. Rev. ST Accel. Beams, vol. 10, 042801 (2007)
21. T. Naito et al., Phys. Rev. ST Accel. Beams, vol. 9, 122802 (2006).
22. Y. Honda et al., Nucl. Instrum. Methods Phys. Res., A 538 (2005) p.100.
23. S. Walston et al., "Performance of a high resolution cavity beam position monitor system", Nucl. Instr. and Meth. A578 (2007) 1-22.
24. J. Y. Huang et al., Proceedings of APAC07, Indor, India (2007).
25. H. S. Kim, Report on the 6th ATF2 project meeting, Nanobeam-2008 (2008), <http://ilcagenda.linearcollider.org/conferenceOtherViews.py?view=standard&confId=2320>
26. Y. Inoue et al., "Development of a high-resolution cavity-beam position monitor", Physical Review ST-AB, vol. 11, 062801 (2008).
27. S. H. Shin et al., Proceedings of PAC07, DOI 10.1109/PAC.2007.4439968 (2007).
28. Y. Honda, Report on the 7th ATF2 project meeting (2008), <http://ilcagenda.linearcollider.org/conferenceDisplay.py?confId=3003>
29. H. Hayano, Report on the 7th ATF2 project meeting (2008),

30. I. Agapov, G. A. Blair, and M. Woodley, Phys. Rev. ST Accel. Beams 10, 112801 (2007)
31. S. T. Boogert et al, Proceedings of EPAC06
32. A. Aryshev et al, Proceedings of EPAC08
33. L. Deacon, Thesis (PhD), University of London (Royal Holloway), 2009
34. H. Hayano, Proceedings of Int. Linac Conf., Monterey (2000) p146.
35. M. Ross et al., Proceedings of 10th Beam Instrumentation Workshop (BIW 02), Upton, New York, (2002)
36. P. Karataev, et al., Physical Review Letters 93, 244802 (2004).
37. P. Karataev et al., Phys. Rev. ST Accel. Beams 11, 032804 (2008).
38. L. Sukhikh et al., Phys. Rev. ST Accel. Beams 12, 071001 (2009).
39. T. Shintake et al., Proceedings of PAC 95, Dallas, USA, Vol.4, pp.2444
40. T. Yamanaka et al., Proceedings of PAC09
41. M. Oroku et al., IEEE NSS Conference Record 2008, Dresden, Germany, pp. 2330-2334
42. FONT1: P.N. Burrows et al, Proceedings PAC03, Portland, Oregon, May 2003, p. 687.
43. FONT2: P.N. Burrows et al, Proceedings EPAC04, Lucerne, July 2004, p. 785.
44. FONT3: P.N. Burrows et al, Proceedings PAC05, Knoxville, TN, May 2005, p. 1359.
45. FONT4: P.N. Burrows et al, Proceedings EPAC06, Edinburgh, UK, June 2006, p. 849.
46. A. Kalinin, P.N. Burrows, Proceedings PAC07, Albuquerque, NM, June 2007, p. 419.
47. T. Omori et al., Phys. Rev. Letts 96 (2006) 114801
48. H. Shimizu et al., J. Phys. Soc. Jpn. 78 (2009) 074501
49. S. Miyoshi et al., Preprint submitted to TIPPO9 Proceedings in NIMA.

3.4 ILC Polarized Electron Source Design and R&D Program

A. Brachmann, J. Sheppard, F. Zhou, M. Poelker
 SLAC, Menlo Park, California
 Mail to: brachman@slac.stanford.edu

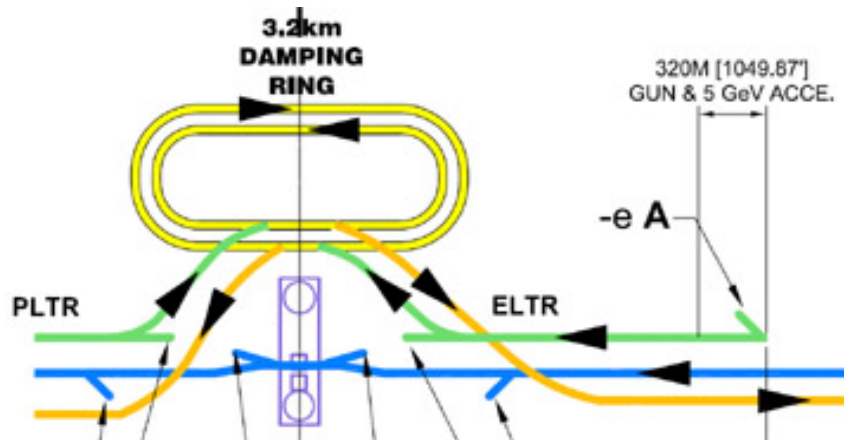
3.4.1 Introduction

The R&D program for the ILC electron focuses on three areas. These are the source drive laser system, the electron gun and photo cathodes necessary to produce a highly polarized electron beam. Currently, the laser system and photo cathode development take place at SLAC's 'ILC Injector Test facility', which is an integrated lab (laser & gun) that allows the production of the electron beam and is equipped with a set of diagnostics, necessary to characterize the source performance. Development of the ILC electron gun takes place at Jefferson Lab, where advanced concepts and technologies for HV DC electron guns for polarized beams are being developed. The goal is to combine both efforts at one facility to demonstrate an electron beam with ILC specifications, which are electron beam charge and polarization as well as the cathode's lifetime. The source parameters are summarized in Table 1.

Table 1: Source parameters

Parameter	Symbol	Value	Unit	Comments
Electrons per bunch (at gun exit)	n_e	$4 \cdot 10^{10}$	Number	RDR
Electrons per bunch (at DR injection)	n_e	$2 \cdot 10^{10}$	Number	RDR
Number of bunches	N_e	~ 3000	Number	RDR
<i>Number of bunches</i>	N_e	~ 1500	<i>Number</i>	<i>Low-P option</i>
bunch repetition rate	$F_{\mu b}$	3	MHz	RDR
bunch repetition rate	$F_{\mu b}$	1.5	MHz	<i>Low-P option</i>
bunch train repetition rate	F_{mb}	5	Hz	RDR
bunch length at source	Δt	$\sim 1\text{ns}$	ns	RDR
Peak current in bunch at source	I_{avg}	3.2	A	RDR
Energy stability	$\sigma E/E$	< 5	% rms	RDR
Polarization	P_e	80 (min)	%	RDR
Photocathode Quantum Efficiency	QE	0.5	%	RDR
Drive laser wavelength	λ	780-810	nm	RDR
single bunch laser energy	E	5	μJ	RDR

The current schematic design of the ILC central complex is depicted in Figure 1. The electron and positron sources are located and laid out approximately symmetric on either side of the damping rings.

**Figure 1:** Central ILC region

3.4.2 Laser System Development

The source laser system must provide sufficient peak power to produce the required number of electrons at a 3 MHz rate. The wavelength must be tunable for a range of 80 – 100 nm centered at 800 nm to exactly match the band gap of GaAs to obtain the maximum of electron polarization. This limits the choice of the laser system's gain material to Ti:Sapphire. The system under development consists of a mode locked Ti:Sapphire oscillator, which is further amplified using a regenerative amplifier cw pumped by frequency doubled Yb:YAG laser. The regenerative amplifier's input/output switch operates at a rate of 3 MHz, thereby providing the pulse trains repetition rate. For stability reasons, the 3 MHz pulses are generated as a cw train with subsequent switching at 5 Hz to provide the macro-bunch pulse train format. The ILC low power option will not change the technological approach for the laser system. The longer intra-bunch pulse separation leads to a lowered demand for pump power, which will result in a less demanding amplifier pump laser. At this time, we anticipate to complete the source laser system approximately within a year.

3.4.3 Photocathode R&D

The main objective of photocathode R&D is to demonstrate the ability to produce an electron beam with at least 80% polarization using GaAs based photo cathodes. Currently, strained layer super lattice GaAs/GaAsP with a doped surface layer is the most promising material for an ILC polarized photocathode. Although such materials have been and are used at almost every polarized source, it is unclear if the surface charge limit will be an issue for the long pulse trains required for the ILC. We will be able to answer this question with confidence when the laser system development is completed and a pulse train can be extracted from the cathode.

Efforts are underway to develop new activation techniques to improve the robustness of the cathode. Robust cathodes will lessen the demand on the gun vacuum condition, increase operational up-time by increasing the time between re-activation requirements. In addition to this research, new promising materials such as AlInGaAs/AlGaAs are being investigated, however GaAs cathodes are still the most promising candidates for a future polarized source.

3.4.4 Gun Development

Although DC gun for electron accelerators are well established, new advances in the high voltage technology have been developed in a variety of fields. Some examples are new cathode materials such as niobium and single crystal niobium and new ceramics for insulating structural components. Their combined application allows reduction of dark currents and increase of HV breakdown limits, thereby leading to higher possible field gradients at the electrodes, which is desirable from a beam dynamics standpoint (reduced space charge forces, improved electron beam emittance). A comparison of typical field emission characteristics for various electrode materials is given in figure 2. Currently, the gun development program at Jlab applies these new technologies.

Furthermore, new electrode surface preparation techniques are being developed to further push the limits of achievable gradients.

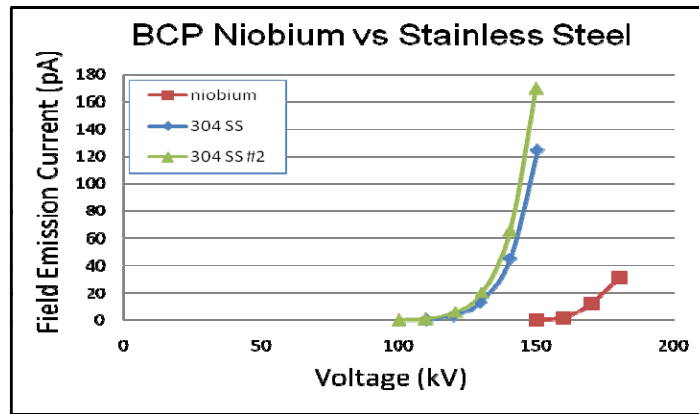


Figure 2: Comparison of field emission characteristics for stainless steel and niobium electrodes.

3.4.5 Summary

The current main activities of the ILC polarized electron source development are predominantly of an R&D nature and focus on resolution of technical issues. The goal is to demonstrate the baseline parameters at either SLAC's Injector Test lab or the Jlab source development facility. A significant challenge will be the integration of efforts carried out at different locations into one test facility. We anticipate completion of this program within a 2 year period.

3.5 Positron Source R&D Status Report

Jim Clarke on behalf of the ILC Positron Source Group
 STFC Daresbury Laboratory, Daresbury, Warrington, Cheshire WA4 4AD, UK
 Mail to: jim.clarke@stfc.ac.uk

3.5.1 Description of the Source

The positron source is a highly challenging subsystem of the ILC. The intense luminosity requirements imply positron numbers per macropulse approximately three orders of magnitude beyond that delivered by any previous positron source. Another requirement of the ILC is that the source design must allow for a future upgrade to provide highly-polarized positrons (up to 60%) and this imposes restrictions on the possible solutions available. In the solution adopted the electron main linac beam passes through a long helical undulator to generate a multi-MeV photon beam which then strikes a thin metal target to generate positrons in an electromagnetic shower. The positrons are captured, accelerated, separated from the shower constituents and the unused photon beam and then are transported to the Damping Ring. Although the baseline design only requires unpolarized positrons, the positron beam produced by the

baseline source will have a polarization of $\sim 30\%$, and beamline space has been reserved for an eventual upgrade to $\sim 60\%$ polarization.

A recent proof of principle experiment at SLAC has demonstrated the feasibility of this technique by generating 6 MeV positrons with $>80\%$ polarisation [1, 2].

The positron source must perform three critical functions:

- generate a high power multi-MeV photon production drive beam in a suitable short period, high K-value helical undulator;
- produce the needed positron bunches in a metal target that can reliably deal with the beam power and induced radioactivity;
- capture and transport the positron bunch to the ILC Damping Rings with minimal beam loss.

The key parameters of the Positron Source are listed in Table 1 and Figure 1 shows the major elements of the positron source. The photon beam is produced by passing the main electron linac beam through a long undulator. This photon beam is transported ~ 500 meters to the positron source target hall where it hits a 0.4 radiation length thick Ti-alloy target producing showers of electrons and positrons. The resulting beam is captured using a Capture Magnet (CM) and normal conducting (NC) L-band RF with solenoidal focusing and accelerated to 125 MeV. The electrons and remaining photons are separated from the positrons and dumped. The positrons are accelerated to 400 MeV in a NC L-band linac with solenoidal focusing. They are transported ~ 5 km to the central damping ring complex, where they are boosted to 5 GeV in a linac using superconducting (SC) L-band RF and injected into the positron damping ring.

The positron source system also includes an auxiliary source to generate a low intensity positron beam that can be injected into the SC L-band linac. This will be used for commissioning and also to allow various beam feedbacks to remain active if the main electron beam, and hence the undulator based positrons, is lost. This source uses a 500 MeV electron drive beam impinging on a tungsten-rhenium target to produce positrons which are then captured and accelerated to 400 MeV similar to the main positron source. The auxiliary source is presently designed to produce 10% bunch intensity for the full 2625 bunch ILC pulse train at 5 Hz though this specification is currently under review.

Table 1: ILC Positron source main parameters.

Parameter	Value
Positrons per bunch	2×10^{10}
Bunches per pulse	2625
Pulse repetition rate	5 Hz
Electron drive beam energy	150 GeV
Electron beam energy loss in undulator	3.0 GeV
Positron polarization	30%, upgradeable to 60%
Undulator period	11.5 mm
Undulator field strength	0.86 T
Photon Energy	10 MeV (1 st harmonic)
Target Material	Ti-6%Al-4%V
Target Thickness	14 mm (0.4 Rad Lengths)

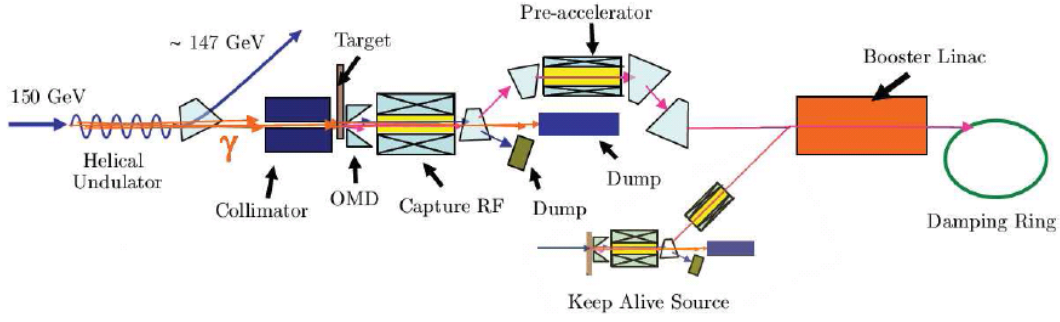


Figure 1: Schematic layout of the undulator-based positron source showing the key components.

3.5.2 The Undulator

The undulator must be superconducting to achieve the required parameters of high field and short period [3] (see Table 1). Two interleaved helical windings of NbTi spaced half a period apart generate the transverse helical field. The undulator will consist of 4 m long cryomodules containing two separate undulators with an active undulator length per cryomodule of 3.5 m. A number of short superconducting prototypes have been constructed by a joint collaboration between Daresbury Laboratory and Rutherford Appleton Laboratory (RAL) to help select the optimum undulator parameters. A full scale 4 m long cryomodule has been manufactured at RAL and is now in the final stages of commissioning [4].

The 1.75 m long undulators have been successfully measured magnetically in a vertical cryostat. The tests show that both magnets can deliver the nominal design current of 216A corresponding to 0.86 T. The maximum observed quench current was 301 A and 306 A for magnets 1 and 2 respectively (see Figure 2). A photo of the full cryomodule is given in Figure 3.

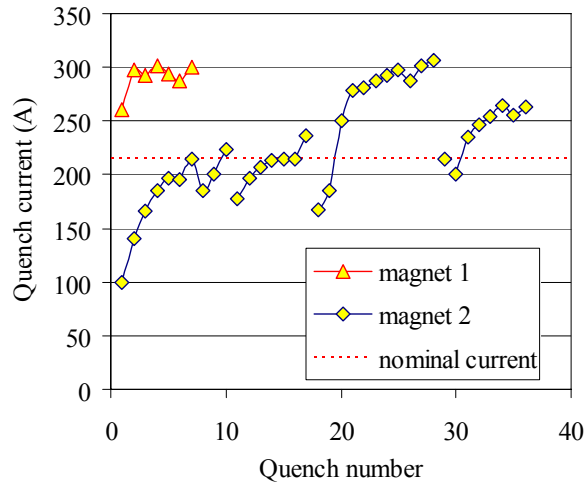


Figure 2: Magnet quench behaviour for the two nominally identical undulators, showing the current required to quench the magnets on successive occasions.



Figure 3: The 4m long cryomodule under commissioning at RAL.

A serious concern for the ILC is the impact of the undulator on the electron beam that travels through it since this electron beam later takes part in the collisions at the Interaction Point. Clearly the emission of synchrotron radiation within the undulator leads to a loss in energy by the electrons. On average the electrons will lose about 3 GeV of their 150 GeV at the undulator and this energy has to be made up in the linac that follows the undulator. The emission of synchrotron radiation also increases the energy spread of the electron bunches, in this case from a relative value of 0.16% to 0.23% at 150 GeV. The narrow bore of the undulator vacuum vessel (5.85mm diameter) means that strong wakefield effects will be generated. Fortunately these effects are relatively small so long as a smooth copper beam tube is utilised [5].

3.5.3 The Target

The positron production target is a rotating wheel made of titanium alloy. The photon beam is incident on the rim of the spinning wheel, whose diameter is 1 m and thickness is 14 mm. During operation the outer edge of the rim moves at 100 m/s. This combination of wheel size and speed offsets radiation damage, heating and the shock-stress in the wheel from the ~ 130 kW photon beam. A shaft extends on both sides of the wheel with the motor mounted on one shaft end, and a rotating water union on the other end to feed cooling water. The target wheel sits in a vacuum enclosure at 10^{-8} torr (needed for the adjacent NC RF operation). The rotating shaft penetrates the enclosure using two vacuum feed-throughs, one on each end. The CM is mounted on the target assembly, and requires an additional liquid nitrogen cooling plant. The motor driving the target wheel is sized to overcome forces due to eddy currents induced in the wheel by the CM.

Several numerical eddy current simulations of the wheel moving in the field of the CM have been carried out using alternative codes and techniques. Whilst broad agreement is found between these studies, showing power loading on the target of ~ 10 kW for a static 1 T field, it has been decided that this is such a crucial issue that a target prototype has been developed at the Cockcroft Institute and this is being used for eddy current benchmark measurements [6]. A view of the target test stand is shown in Figure

4. Whilst understanding of the exact eddy current losses is important, equally vital will be the demonstration of stable full speed operation. The experiment is currently taking data and comparison is being made against the numerical models. At present the wheel has operated successfully at up to 1800 revolutions per minute (94 m/s at the rim), no attempt has been made to go beyond this speed at present.

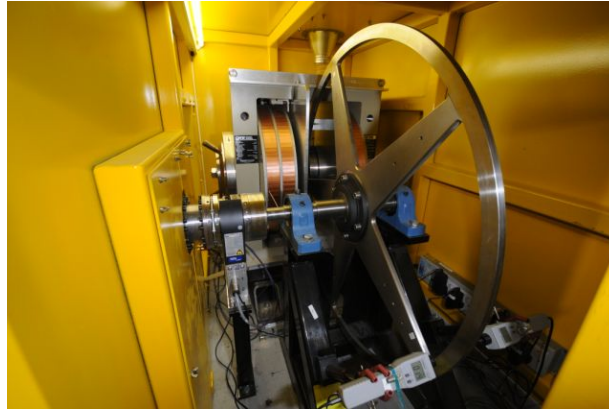


Figure 4: Photo of the 1m target wheel manufactured from Ti passing through the poles of the dipole test magnet. This eddy current experiment is housed inside a solid personnel safety enclosure due to the high rotation speeds being used.

3.5.4 The Capture Magnet

Immediately after the target wheel is the CM and a normal conducting RF linac that are jointly optimised to capture as many of the positrons as possible. The magnetic field profile of the CM has a strong impact on the positron yield and, broadly speaking, the higher the magnetic field on the target, the higher the capture efficiency. The baseline CM is a simple solenoid arrangement but the number of positrons captured would increase significantly if a different design were possible. One possibility is a normal conducting pulsed flux concentrator which generates a solenoidal magnetic field which peaks in strength at 4 T close to the target and falls off to 0.5 T to match the solenoidal field at the entrance of the RF capture section. This flux concentrator increases the capture efficiency by a factor of two. The design of such a flux concentrator is being pursued by LLNL. The key difference between this flux concentrator and the many examples that already operate successfully on accelerators around the world is the pulse length. For the ILC the macropulse is ~ 1 ms and so the flux concentrator must generate a field that will match this requirement. Other examples typically operate for a few μ s only although there is an example from the 1960's which operated successfully with a pulse length of 40 ms and a peak field of 10 T [7], albeit with a reduced pulse rate of 0.3 Hz compared with the 5 Hz required by the ILC.

A promising alternative to the flux concentrator solution is the use of a lithium lens [8], a technique which is presently used by CERN and FNAL for antiproton collection. Such a system could improve the positron capture efficiency by up to another factor of two, if it can be shown to be feasible. The main concern is the survivability of the windows which separate the lithium from the RF system vacuum. The full power photon beam and secondary positrons and electrons will traverse the windows so they

will suffer some level of radiation damage, thermal cycling, and have to cope with the shock waves. In addition cavitation within the lithium might also be an issue. However, the benefit of such a lens system is significant (effectively halving the required length of undulator) and so further studies on this system are essential and are presently being pursued by Cornell.

3.5.5 Summary

This report has highlighted three areas of intense R&D for the ILC positron source. The areas highlighted are those which have been identified as being of highest priority in terms of establishing the source as feasible and relatively low risk. All other areas of the positron source contain challenging features and these are being actively studied also. The construction of prototypes and the detailed simulations that have been carried out so far have shown the ILC positron source to be challenging but feasible with state of the art solutions required in several areas. The undulator based positron source was selected for the ILC as it was judged to be the lowest risk option in comparison with other positron generation techniques and that remains the case today.

3.5.6 References

1. G. Alexander et al, PRL 100, 210801 (2008).
2. G. Alexander et al, NIM A 610 (2009) 451-487.
3. D.J. Scott et al, PR-STAB, 10, 032401 (2007).
4. J. Rochford, "The Superconducting Undulator for the ILC Positron Source", PAC 09.
5. D. J. Scott, PhD Thesis, University of Liverpool
6. I.R. Bailey et al, "A Prototype Target Wheel for the ILC Positron Source", EPAC 08
7. H. Brechna, "150 K Liquid Nitrogen Cooled Pulsed Flux-Concentrator Magnet", Rev. Sci. Inst. (1965).
8. A. Mikhailichenko, "Lithium Lens for Positron Production System", EPAC 08

3.6 Design of Injection Kickers at LNF

Fabio Marcellini, David Alesini
INFN- Laboratori Nazionali di Frascati, Via E. Fermi 40, 00044 Frascati, Italy
Mail to: Fabio.Marcellini@lnf.infn.it

At LNF the injection system of the Φ -factory DAΦNE was upgraded in 2007. The main features of the new system, compared to the previous one, are [1]:

- a) much shorter pulse (≈ 12 ns instead of ≈ 150 ns);
- b) better uniformity of the deflecting field;
- c) lower impedance of the kickers.

The new kickers can operate with very fast pulsers, perturbing only the injected bunch and the two adjacent ones. This improvement can increase the current threshold of the transverse instability in the DAΦNE rings.

The better uniformity of the deflecting field can increase the injection efficiency at high currents and reduce the background to experiments during injection.

The broadband impedance, according to calculations and measurements, is reduced by a factor 3 with respect to the previous kickers. Moreover, since the new kickers have been designed with the same beam pipe cross section of the dipoles, no taper transition are needed between the dipoles and the kicker and this also contributes to the reduction of the machine impedance.

The new injection system at DAΦNE is, at the same time, a test and an R&D activity of one of the most challenging issues of the International Linear Collider (ILC): the injection/extraction kickers for the damping rings (DR) [2],[3]. The bunch distance in the DR and therefore the choice of the DR circumference are related to the kicker pulse duration; moreover the stability of the beam position at the IP depends also on the kicker pulse stability. Common requirements of ILC DR kickers and DAΦNE kickers are: ultra short rise and fall times, high integrated strength, good uniformity of the deflecting field, and impedances of the structure as low as possible.

Therefore the operation of these new kickers at DAΦNE is an important test for the ILC project, since it should demonstrate with beam measurements the achievement of the system performances.

3.6.1 DAΦNE Kicker

The kicker has been designed as a two stripline structure (see Figure 1).

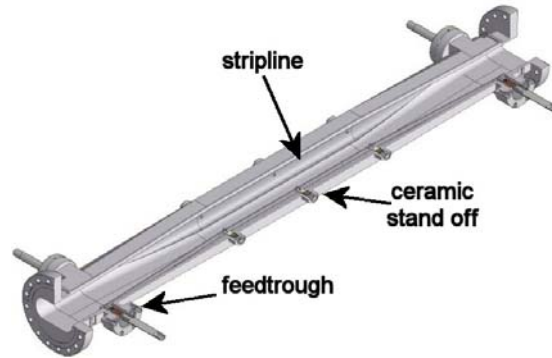


Figure 1: Cut-view of the DAΦNE injection kicker

The stripline and the surrounding vacuum chamber are properly tapered and each transverse section has constant 50Ω impedance to match the output impedance of the high voltage pulse generator. Coupling and transfer impedance reduction and optimized deflecting field uniformity in the transverse plane have been obtained mainly thanks to the proper stripline tapering.

The longitudinal and transverse beam coupling impedances have been calculated simulating the wire method technique of measurement. The longitudinal and the transfer impedance are reported in the Figures 2a and 2b. From the transfer impedance it is possible to evaluate the peak voltage and the average power induced by the beam into the kicker ports for a given beam current. The maximum induced peak voltage on the upstream (output) ports is of the order of 100 V with a 6 nC bunch while the average

power induced on the ports is of the order of few tens of Watts with a 2A beam. In longitudinal and horizontal planes there is no evidence of trapped HOMs and the longitudinal loss factor is $\sim 5 \cdot 10^{-3}$ V/pC for 1 cm bunch length. In vertical plane four trapped HOM (TE_{11n}) are found having impedance of the order of few tens of kV per meter. These modes could give, in the worst case of full coupling with beam spectrum lines, growth rates of the order of 1 ms^{-1} at a total current of 2A that are about two orders of magnitude lower than the damping rates provided by the DAΦNE vertical feedback system.

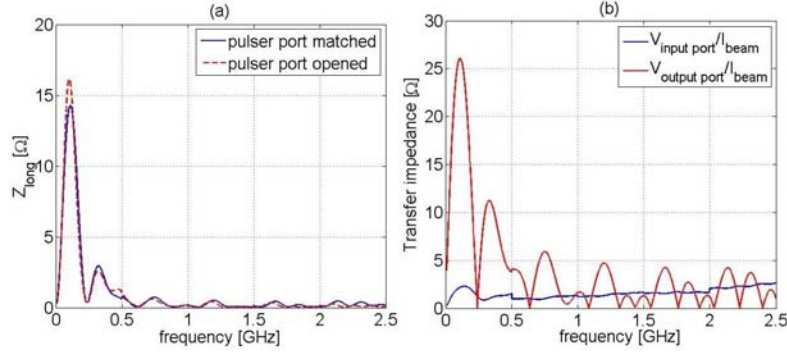


Figure 2: Longitudinal beam coupling impedance (a) and transfer impedance (b) calculated by HFSS [5].

Moreover, reducing the stripline section and placing it very close to the kicker vacuum chamber in the coaxial-stripline transition region improves the matching between the pulse generator and the kicker structure. This also contributes to reduce the longitudinal and transfer impedance of the kicker [4].

Concerning the flatness of the deflecting field in the transverse plane, the results are summarized in the following plots, where the field variation as a function of the horizontal and vertical coordinates is shown. It is within $\pm 2\%$ over the kicker horizontal aperture (± 2.7 cm) and less than 10 % over ± 1 cm along the vertical axis.

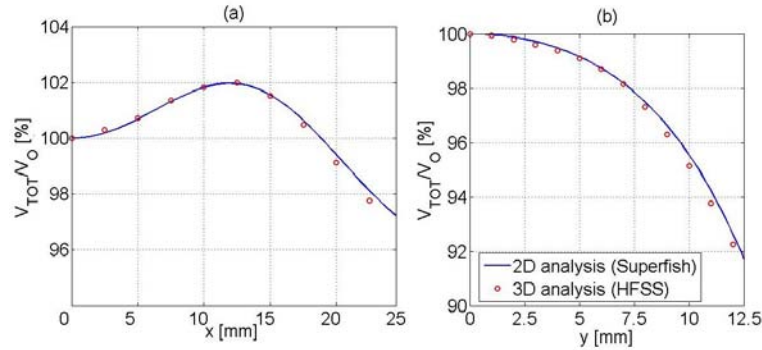


Figure 3: Deflecting field as a function of the horizontal (x) and vertical (y) coordinates.

3.6.2 ATF Kicker

A stripline kicker prototype has been designed and realized for ATF. After some lab tests at LNF it will be sent to KEK. The design has followed the same considerations and criteria adopted for the DAΦNE kicker. ATF is at the moment operating with a

conventional stripline kicker. It can be easily replaced by the LNF prototype, being the length and the flanges of the two devices identical. They are also made in the same material (stainless steel) and use the same feedthroughs. They just differ for the shape of the stripline, which has a constant section in the case of the ATF kicker while is tapered in the case of the LNF kicker.

The figure below shows a drawing of the kicker and in particular the shape of the tapered striplines.

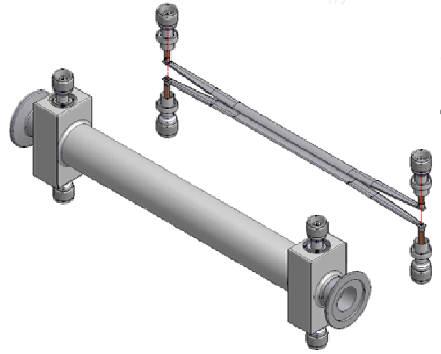


Figure 4: Drawing of the kicker for ATF

A full characterization of the two structures has been done by means of HFSS simulations. The following figure summarizes the results of this analysis. In each plot the blue line refers to the present ATF kicker and the red line to the new kicker with tapers. In plot (a) is represented the deflecting field along the kicker axis normalized to the voltage applied to the striplines. The tapered structure is less efficient in correspondence of the ends and more efficient in the central region of the stripline. In any case the tapered structure was designed to have the same integrated field of the conventional one.

The advantages of the new kicker are evident looking at the other plots. Plot (b) and plot (c) shows respectively the deflecting voltages along the horizontal and the vertical axis, so they indicate how flat is the deflecting field in the transverse plane. The new kicker shows a much flatter curve especially in the horizontal axis.

The reflection coefficient at the kicker input port is plotted in (d). Due to the smoother transition between stripline and coaxial line, reflections are smaller for the new kicker.

The beam coupling impedance is shown in plot (e) while in plot (f) the transfer impedances of the input (solid lines) and output (dotted lines) kicker ports are pointed out. The impedance of the new kicker is much smaller particularly at high frequency. A consequence of that is that the beam releases less power to the structure and less power flows through the kicker ports and reaches the pulse generator.

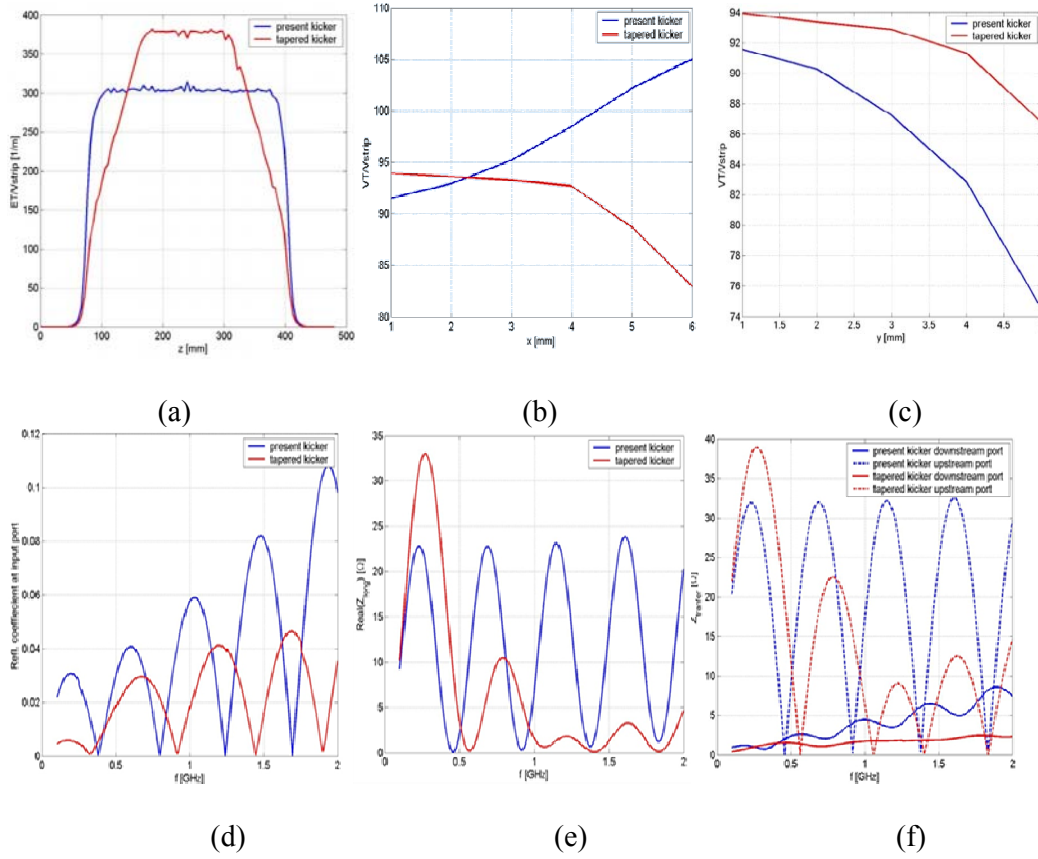


Figure 5: Comparison between present (blue) and tapered (red) ATF kickers: (a) deflecting field along the kicker beam axis; (b) deflecting voltage variations for horizontal position offsets; (c) deflecting voltage variations for vertical position offsets; (d) reflection coefficient at the input ports; (e) beam coupling impedance; (f) transfer impedance of input (solid) and output (dashed) ports.

3.6.3 Conclusions

The design of the new, fast stripline kickers for the injection upgrade of the DAΦNE Φ -factory is based on stripline tapering to simultaneously obtain low impedance and an excellent uniformity of the deflecting field.

These characteristics are essential also for the Damping Ring of the ILC, then the experience done with the new DAΦNE injection system is and will be, at the same time, an R&D on the Damping Ring injection system.

A kicker for ATF has been designed and built as well. Now it is ready to be installed. The comparison with the ATF present kicker indicates they have the same efficiency (kick vs. applied voltage) but the field uniformity and the beam impedances are better in the case of the tapered structure.

3.6.4 References

1. D. Alesini, et al, DAΦNE tech. note I-17, EUROTeV-Report-2006-025, 2006.

2. S. Guiducci, PAC05, Knoxville, (USA), May 2005.
3. A. Wolski, et al., LBNL-59449, 2006.
4. D.A. Goldberg and G.R. Lambertson, LBL-31664 ESG-160, 1992.
5. <http://www.ansoft.com>

3.7 STF Status 2009

Hitoshi Hayano
High Energy Accelerator Research Organization (KEK)
1-1 Oho, Tsukuba, Ibaraki, Japan
Mail to: Hitoshi.Hayano@kek.jp

Abstract

The superconducting RF test facility (STF) in KEK is aiming to promote R&D of superconducting linear accelerator to be used in the International Linear Collider (ILC) (Fig.1). The development was subdivided into phase-1 and phase-2, and started in 2005. The phase-1 STF construction which was aimed quick start-up of superconducting (SC) RF technology, was completed in 2008. Their high-lights are high power RF operation of 1.3GHz SC cavities in the short-cryostat and infrastructure construction and operation for supporting the SC accelerator module. The new phase, STF phase-2 construction began to start in 2009. The phase-2 plan is aiming to realize ILC RF unit and to demonstrate its performance together with preparation and study of industrial production. Phase-2 also includes the compact bright X-ray source development referred as ‘Quantum Beam Technology Program’ which is founded by the MEXT (Ministry of Education, Culture, Sports, Science and Technology, in Japan) as an intermediate milestone. The industrialization of cavity fabrication and cost reduction is also one of the targets of this phase-2 construction.

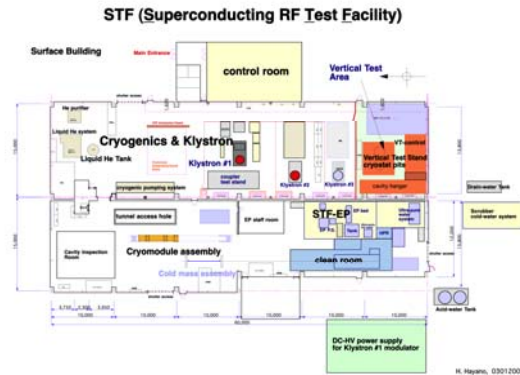


Figure 1: STF building floor; there are cryogenic plant, three RF power stations, cavity vertical test stations, EP facility, clean room, cryomodule assembly. There is 100m accelerator tunnel in 10m depth under this building.

3.7.1 Introduction

The reference design report (RDR) of the ILC was completed and published in 2007[1]. The baseline ILC configuration was determined as one polarised electron injector, central 6km damping rings, two 11 km main linacs with 31.5MV/m gradient,

positron line helical undulator at 150GeV, and 14mrad crossing final focus with single IR. The main linac RF unit consists of the following components. The bouncer modulator and the pulse transformer for the 10MW multi-beam klystron are the baseline design of RF power source. Beam is injected after filling time of 500 μ s from the start of RF filling into the cavities. The klystron has two RF output ports connected to the 4 branch of the linear distribution system of the cryomodule. The circulator of each cavity input ensures the matching condition of waveguide system. There are 9 cavities in the two cryomodules of both side, and 8 cavities and SC quadrupole magnet are in the central cryomodule. Total 26 cavities are in one RF unit. Average operation gradient for these cavities are 31.5MV/m, and loaded beam current is 9mA during about 1ms beam pulse train with 5Hz repetition. This RDR unit configuration is illustrated in Figure 2. The demonstration of this RF unit is the milestone of the STF phase-2 construction. In phase-2 plan, we will construct 12m-long RDR cryomodules including total 26 superconducting cavities and 1 SC quadrupole magnet. It has ILC structure electron beam generated by the photo-cathode RF gun and conditioned by the following two SC capture cavities. Phase-2 plan also includes the compact bright X-ray source development referred as ‘Quantum Beam Technology Program’ which is founded by the MEXT as an intermediate milestone. The industrialization of cavity fabrication and cost reduction is also one of the targets of this phase-2 construction.

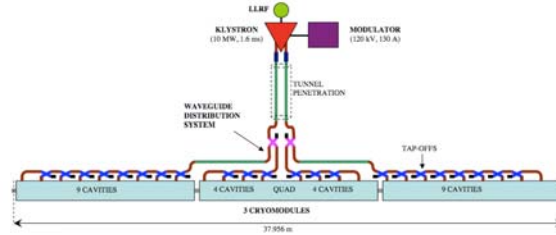


Figure 2: RF unit configuration of ILC main linac.

3.7.2 Cryomodule Test of STF Phase-1

The STF phase-1 test cryomodule consists from the two units of 5m horizontal cryostats (type A and type B) which are the half length of ILC design, and each of them can accommodate 4 cavities. The type A 5m cryomodule is designed to accommodate TESLA-style cavities, and the type B 5m cryomodule is for low-loss (LL) cavity. The cool-down test was carried for the one TESLA-style cavity in the cryomodule A, then one LL cavity in the cryomodule B in the next, during 2007-2008. During high power test and heat load measurement of LL cavity, four TESLA-like cavities were assembled into the cryomodule A. The installation of this cryomodule-A was done in May 2008 and cool-down test was performed from June to December 2008. In the meantime, the cavity development was changed its priority to TESLA-style cavity which is to be used for Phase-2 cavity. LL-cavity development is kept for a candidate of high gradient cavity as a possible option.

3.7.3 STF Phase-1 Experiment Results

The cool-down experiment of one TESLA-like cavity module and one LL cavity module were described in the other report [2]. The cryomodule of 4 TESLA-like

cavities was cooled down twice, in the term June to July 2008 and September to December 2008. The first cool-down is for cryomodule heat load measurement without connection of warm-side input coupler. In parallel, low-level performance measurement of the cavity, such as tuner performance and HOM performance were done. The second cool-down is for the high power RF test of the cavities, Low-Level RF vector-sum control and various power distribution test together with cryomodule heat load measurement.

One of the cavities out of four reached to 31.5MV/m, ILC operation gradient. Other three were stayed around 20MV/m, as shown in Fig.3. First, the study was performed using this high gradient cavity for the gradient demonstration and LD (Lorentz Detuning) measurement and compensation by feeding RF power into the specified cavity only. The field amplitude and phase were feedback controlled using piezo actuator LD compensation. The waveform of this demonstration is shown in Fig.4 (top). The other important demonstration is to show the small LD design of tuner and helium vessel. The LD measurement results shown in Fig.4 (bottom) demonstrated 300Hz detuning during pulse flat-top at 30.2MV/m. It is half detuning amount compared with TESLA cavity, and indicates that only a half stroke of piezo compensation is required.

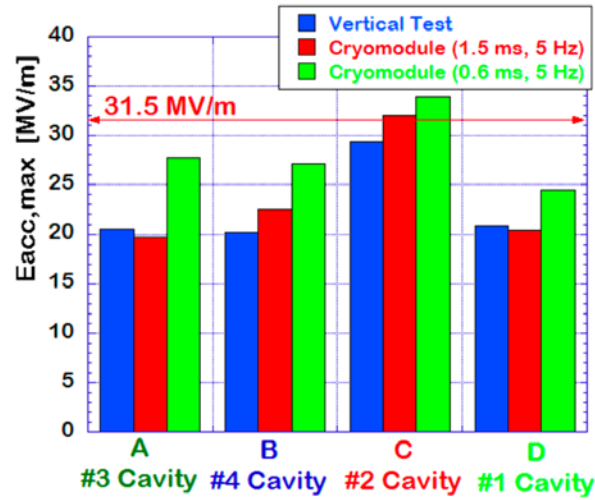


Figure 3: Reached gradient performance of 4 TESLA-style cavities in the cryomodule.

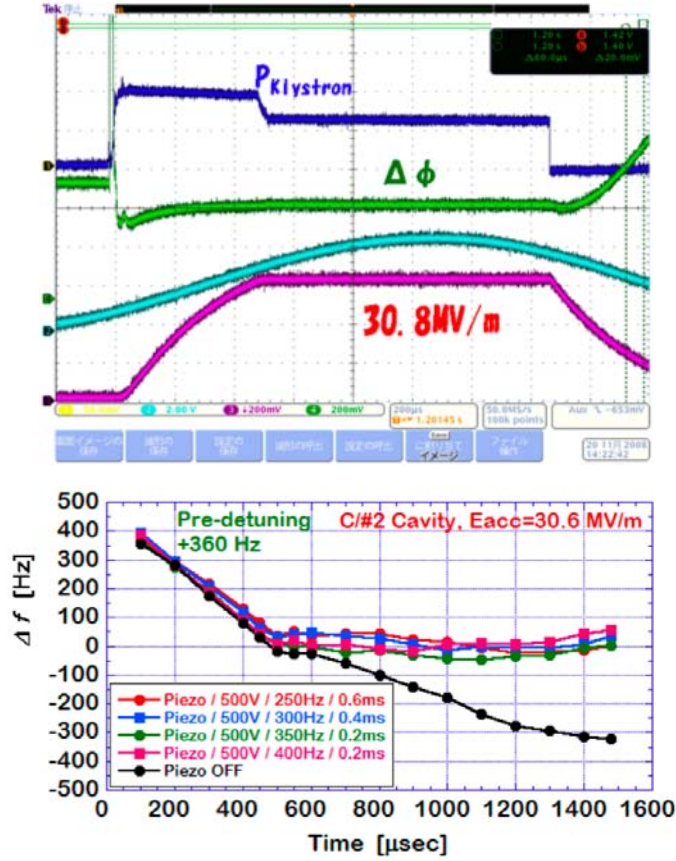


Figure 4: The waveform of the best performed TESLA-shape cavity with Piezo control on and feedback control on (top). The measured Lorentz detuning without piezo (black) and with piezo using various parameters (bottom).

After power test of each cavity, the waveguide was connected to feed RF power to four cavities together. Vector-sum control of Low-Level RF (LLRF) was demonstrated. As shown in Fig.5, stability of amplitude was performed as 0.04% (rms) and phase 0.02degree (rms). Since these four cavities have different QL, each cavity phase behaved differently during pulsed operation, in the mean time summed signal was controlled in flat. These stability performances are well below the specification ILC. Several trials for LLRF and power distribution were performed, such as simulated beam loading signal mixture, special filtering technique and IF-mixture ADC detection, QL control by waveguide short and phase shifter, etc. [3].

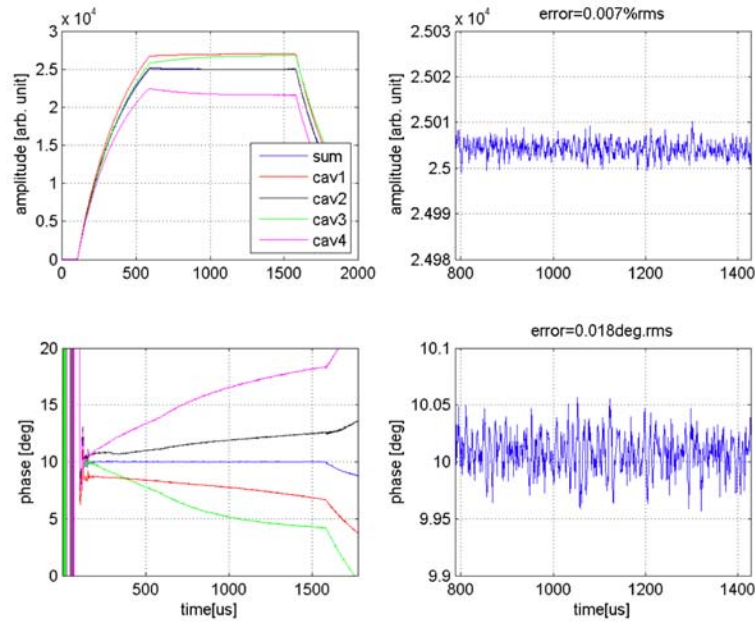


Figure 5: Waveforms of amplitude (top row) and phase (bottom row) during vector-sum feedback control for four TESLA-style cavities.

3.7.4 Infrastructure Developments

The new electro-polishing (EP) facility and vertical test stand (VT) became in operation after commissioning using FNAL cavity AES001, in summer 2008. The EP and VT are now routinely operated once in two week alternately. So far MHI-05 to MHI-09 (5 cavities) were processed and vertical tested. The EP system still in upgrading, such as rinse system for H₂O₂, Ethanol and degreaser, pre-EP function, TOC and particle monitoring during ultra-sonic rinsing and HPR. Also neutralization water filling sequence was upgraded to avoid ‘stain’ in the cavity surface.

The temperature mapping system is under developing for the vertical test cavities. The 352 temperature sensors are installed around each cell and end group HOMs. The temperature rise is summarized as a map plot as shown in Fig.6. We can identify the heat spot easily and easy to think the connection with followed surface inspection. Together with temperature mapping system, X-ray detectors using PIN photo-diode are installed to compose X-ray mapping system. They are installed in around iris parts with small interval spacing. When a cavity has field emission, strong X-ray emitted position can be detected, and emission source point can be estimated.

The development and upgrading of cavity surface inspection camera is being done by the collaboration with Kyoto University. Newly developed high performance CMOS camera and LED illumination combination makes it possible to catch defect images by 3.7μm/pix resolution. The current illumination of EL panel was found to have short life and not so bright. The introduction of LED strip illumination has 10 times brighter and much longer life. Also, in order to inspect various style of cavity like EP-jig installed or helium jacket installed, the camera cylinder rotation is required instead of cavity rotation. They were developed and in operation (Fig. 7).

In parallel, we started the research of surface analysis of cavity inner surface, in order to understand the source of field emission. We used the niobium sample pieces for laboratory EP and analyzed by X-ray photo-electron spectroscopy (XPS) to see what the residuals on the surface is. Also we installed the sample pieces into single cell cavity and applied EP process to the cavity. The samples from this single cell are analyzed by XPS. We see the sulfur residuals in case aged EP acid was used.

Local grinding study is also carried out, in order to eliminate defects such as welding beads and pits which were clearly enhanced by successive EP process. The diamond powder sheet with a few 10 μ m diamond was used for the grinding. Combination with grinding and EP process makes cavity surface smoother. The application test of this local grinding is ongoing.

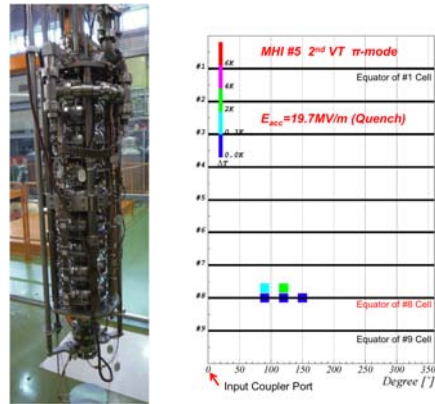


Figure 6: Temperature mapping inspection in the cavity vertical test. Picture of sensor installation (left) and temperature rise mapping result (right) are shown.



Figure 7: The upgraded inspection camera system for cavity inner surface observation.

3.7.5 Phase-2 Developments

During the cavity fabrication and design preparation for the cryostat and refrigerator, the S1-Global experiment was planned. The idea of the S1-Global is to

realize ILC operational gradient 31.5MV/m in the one cryomodule (8 cavities) by collaboration of world top-level performance cavities, as shown in Fig.8. Two high performance cavities from DESY, another two from FNAL, and KEK installs 4 cavities in the connected cryomodules. It will be operating in 2010 at STF.

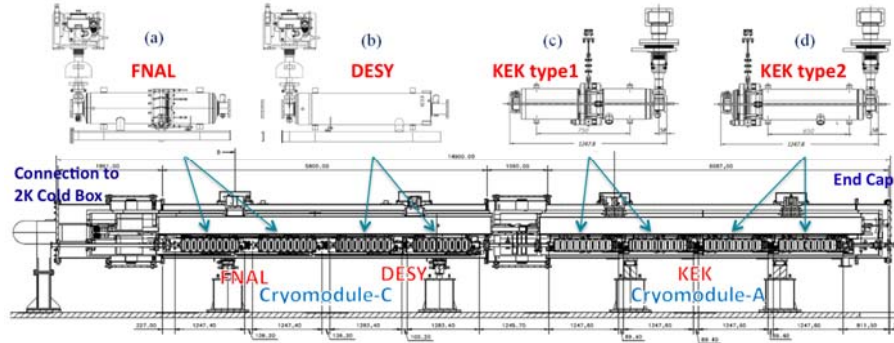


Figure 8: S1-Global cryomodule experiment.

The planned phase-2 accelerator is illustrated in Fig. 9. They consist of three ILC cryomodules driven by the 10MW multi-beam-klystron, photocathode RF gun, and two 9-cell cavities capture module. On a way of phase-2 construction, the compact X-ray source development is included in the commissioning of the beam source of phase-2 accelerator as shown in Fig. 10. The beam operation of X-ray source is scheduled in fall of 2011 to summer 2012.

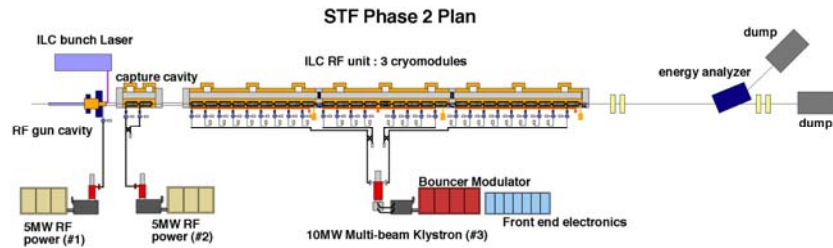


Figure 9: STF phase-2 accelerator diagram.

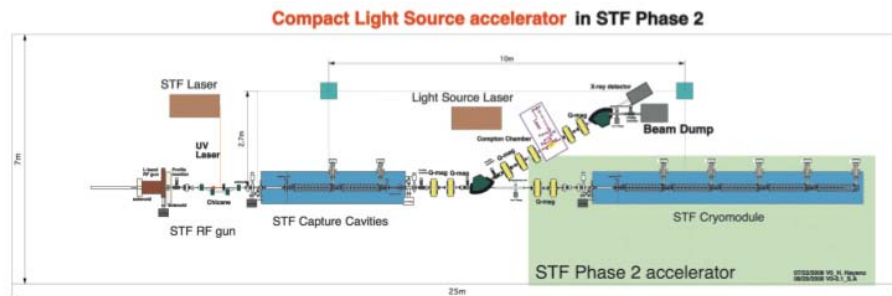


Figure 10: Compact X-ray source development on a way of the STF phase-2 construction.

After finished the X-ray generation experiment, the first ILC cryomodule will be installed in STF tunnel by the end of 2012. The second run of the phase-2 accelerator is

scheduled from January 2013 to July 2013. In the meantime, the rest of cryomodules will be in preparation. Also the rest 17 cavities will be fabricated and processed in parallel way, in order to catch up the second and third cryomodule installation. The current concerns are to build carry-in hatch in STF tunnel, expansion of clean-room to accommodate 9 cavities chain, expansion of cryomodule assembly tool, and to clear high-pressure vessel regulation for cavity and cryomodule. Overall schedule is shown in Fig. 11. The construction schedule of the last two cryomodules is still under discussion, and not yet decided.

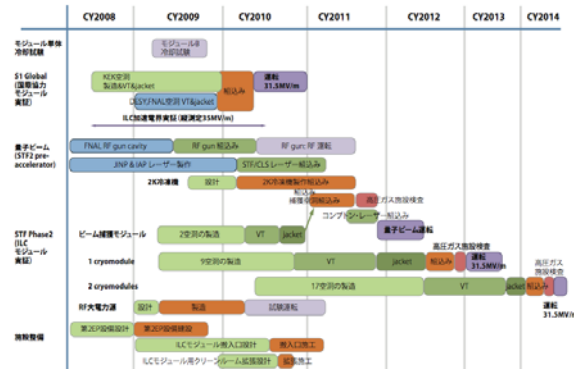


Figure 11: Plan and schedules for the overall STF phase-2 in coming several years.

On a way of STF phase-2 construction, the cavity fabrication pilot plant for the industrialization and cost reduction study is planned, in parallel to phase-2. They consist of electron beam welder (EBW), press machine, trimming machines, chemical process room clean room and lots of instrumentations. The cavity from this plant will be tested in the third cryomodule for the acceleration performance.

3.7.6 Acknowledgements

The author would like to thank all the members of STF group for their effort to develop ILC superconducting accelerator technology. The support of Accelerator Laboratory director, K. Oide, trustee of the executive board, Y. Kamiya, F. Takasaki, and director general of KEK, A. Suzuki, are gratefully appreciated.

3.7.7 References

1. ILC Reference Design Report, ILC-Report-2007-001 (2007); <http://www.linearcollider.org/cms/?pid=1000437>
2. Hitoshi Hayano, "KEK-STF status," Proc. of the 5th Japanese Accelerator Society meeting, 2008.
3. STF group, "STF phase 1 activity report", KEK report 2009-3, April 2009.

3.8 A Facility for Accelerator Research and Education at Fermilab

Mike Church and Sergei Nagaitsev, Fermilab
Mail to: church@fnal.gov

Fermilab is currently constructing the “SRF Test Accelerator at the New Muon Lab” (ILCTA). ILCTA consists of a photo-emitted RF electron gun, followed by a bunch compressor, low energy test beamlines, SCRF accelerating structures, and high energy test beamlines. The initial primary purpose of ILCTA will be to test superconducting RF accelerating modules for the ILC and for Fermilab’s “Project X” – a proposal for a high intensity proton source. The unique capability of ILCTA will be to test these modules under conditions of high intensity electron beams with ILC-like beam parameters. In addition ILCTA incorporates a photoinjector which offers significant tunability and especially the possibility to generate a bright electron beam with brightness comparable to state-of-the-art accelerators. This opens the exciting possibility of also using ILCTA for fundamental beams research and tests of new concepts in beam manipulations and acceleration, instrumentation, and the applications of beams.

Figure 1 is a photograph of the interior of ILCTA as it exists today. Building infrastructure – cryogenics, electrical power, RF power, water cooling, electronics racks, shielding, etc. are currently being installed. A single SC cavity is currently under cooldown and test, and a single SCRF cryomodule (type “TTF III+”) is in the building and commissioning will commence this winter. The electron gun will be installed and commissioned starting in 2/10. Beamline construction will start in CY11 and we expect to start delivering beam in late CY12.



Figure 1: Current interior of ILCTA, looking downstream from the injector end.

The injector beamline is shown in Figure 2. It consists of a 1.3 GHz RF photo-emitted electron gun, followed by 2 SCRF accelerating cavities, a bunch compressor and beam diagnostics. The primary injector beamline will operate at ~ 40 MeV and is ~ 22 m in length. It will be capable of producing ILC-like beam structure: bunch charge = 3.2 nC, 3 MHz bunch repetition rate, bunch train length = 1 ms, 5 Hz bunch train repetition rate, and peak current in excess of >10 kA. Single bunch charge can be as

high as 20 nC. In addition, there is floor space for 2 reconfigurable 40 MeV test beamlines for a variety of experiments.

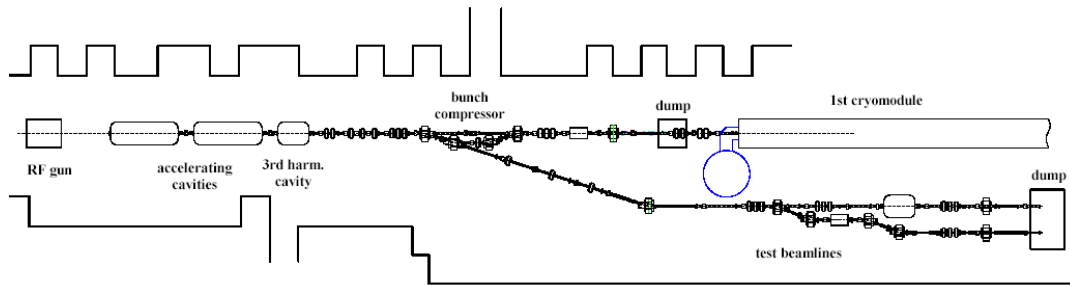


Figure 2: Injector beamline layout.

The acceleration section will initially consist of 3 ILC-type SCRF cryomodules (a single ILC “RF unit” powered by a single 10 MW klystron), capable of accelerating beam to ~ 600 MeV. A building expansion, about to start, will allow for a total of 6 cryomodules and up to ~ 1500 MeV beam energy. A plan for the high energy downstream beamlines is shown in Figure 3. There will be floor space and infrastructure available for up to 3 high energy test beamlines (18 – 34 m in length) and a storage ring up to ~ 10 m in diameter. High energy dumps will absorb the 80 KW of beam power.

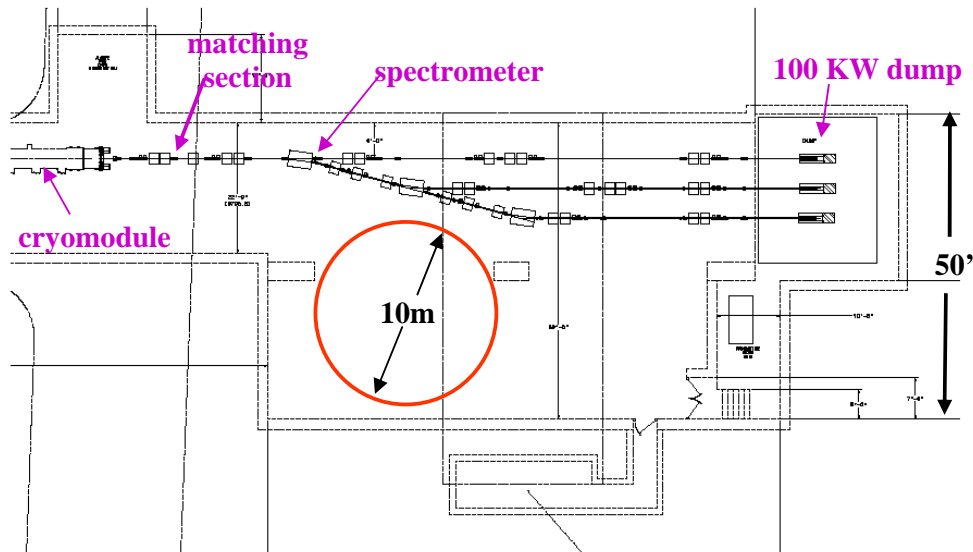


Figure 3: High energy beamline layout.

In May 2009, Fermilab hosted a workshop [1] to explore future directions of accelerator research at Fermilab. Half the agenda was devoted to fielding proposals for accelerator research experiments that might be performed at ILCTA. Researchers from 7 different institutions presented a total of 19 proposals, ideas, and suggestions for interesting experiments that could be conducted here. This was the first introduction of ILCTA to the accelerator physics community at large. We refer the reader to reference [1] for further proposals and background.

In summary, in addition to providing realistic tests of a new generation of RF cryomodules, the new ILCTA facility offers excellent opportunities to advance accelerator science and technology on several fronts. ILCTA will become a truly open users' facility with unique capabilities to advance accelerator research by groups from various institutions, to enhance accelerator education and to promote accelerator technology development for industrial applications.

References

1. Future Directions for Accelerator R&D at Fermilab, May 11–13, 2009, Lake Geneva, Wisconsin, USA, <http://apc.fnal.gov/ARDWS/index.html>

3.9 Final Focus Test Facility ATF2 Status

P. Bambade[†], A. Seryi^{*} and T. Tauchi

On behalf of the ATF2 Team^{**} for the ATF Collaboration
High Energy Accelerator Research Organization (KEK)
1-1 Oho, Tsukuba, Ibaraki, Japan

[†]KEK, LAL, Univ Paris-Sud, IN2P3/CNRS, Orsay, France

^{*}SLAC, Menlo Park, California

Mail to: Seryi@slac.stanford.edu

Abstract

ATF2 is a final-focus test beam line which aims to focus the low emittance beam from the ATF damping ring to a vertical size of about 37 nm and to demonstrate nanometre level beam stability. Several advanced beam diagnostics and feedback tools are used. In December 2008, construction and installation were completed and beam commissioning started, supported by an international team of Asian, European and American scientists. In this paper, the present status and performance of the recently deployed ATF2 systems are briefly described, based on the first experience with beam measurements and tuning during winter, spring and early autumn of 2009. The near and longer term plans are outlined as well.

3.9.1 Test Facility

An important technical challenge of future linear collider projects such as ILC [1] or CLIC [2] is the collision of extremely small beams of a few nanometres in vertical size. This challenge involves three distinct issues: creating small emittance beams, preserving the emittance during acceleration and transport and finally focusing the beams to nanometres before colliding them. The Accelerator Test Facility (ATF) at KEK [3] was built to create small emittance beams, and has succeeded in obtaining emittances that almost satisfy ILC requirements. The ATF2 facility [4], which uses the beam extracted from the ATF damping ring (DR), was constructed to address the last two issues: focusing the beams to nanometre scale vertical beam sizes and providing nanometre level stability. While the optics of the FFTB (Final Focus Test Beam) which ran at SLAC [5] in nineteen nineties was based on non-local chromaticity correction, the ATF2 optics, in the same way as ILC, is based on a scheme of local chromaticity correction [6] which is now also used for the CLIC design.

The main parameters of ATF2 are given in Table 1 with the corresponding values for the ILC and CLIC projects. The layout within the ATF facility and the design optical functions are shown in Figures 1 and 2, respectively. The two main project goals are to achieve a 37 nm vertical beam size at the optical focal point (referred to as IP, interaction point), by 2010 and nanometre level beam stability at that point by 2012.

Before entering into the ATF2 final focus, the beam is extracted from the DR into a reconfigured version of the old ATF extraction line and transported in a matching and diagnostic section where beam parameters can be measured with wire scanners and where anomalous dispersion, betatron mismatch and coupling can be corrected. The ATF2 beam line extends over about 90 meters from the beam extraction point in the ATF DR to the IP (see Figure 3). It contains 7 dipoles, 3 septa, 49 quadrupoles, 5 sextupoles and a number of corrector magnets [7]. The Final Doublet (FD) shown in Figure 4 is a system which requires special attention in terms of its integration, alignment and stability [8,9].

To measure the beam orbit and maintain the beam size with feedback, the beam line magnets are equipped with sub-micron resolution cavity Beam Position Monitors (BPM) and are placed on mechanical movers. There are 32 C-band (6.5 GHz) and 4 S-band (2.8 GHz) high resolution cavity BPMs. In addition to these dipole cavities there are 4 C-band and 1 S-band reference cavities to monitor beam charge and beam arrival phase [10-12]. In the diagnostics and final focus section every quadrupole and sextupole magnet is instrumented with such a BPM.

Measuring transverse beam sizes at the IP of single line ATF2 requires a dedicated laser interferometer-based Beam Size Monitor (BSM), also called Shintake monitor [13]. The BSM measures the beam size at the IP using inverse Compton scattering between the electron beam and a laser interference fringe pattern [13]. In such a monitor, the energy of the generated gamma rays is typically rather small compared to that of bremsstrahlung photons composing the main background (emitted when beam tail electrons interact with apertures and start showering). In the monitor designed for ATF2 [14], the signal is separated from this high energy background by analysing the longitudinal shower profile measured with a multilayered detector (located a few metres after the IP after a dipole magnet) [15]. The laser wavelength used is 532 nm, the 2nd harmonic of the Nd:YAG laser, providing a suitable fringe pitch to measure the target vertical size of 37 nm. Four laser beam crossing modes are available to provide a broad dynamic range of up to several microns for the initial beam tuning down to the nominal beam size or less. In addition, a laser wire mode can be used for horizontal beam size measurements.

The successful tuning of the ATF2 beam line relies on many automated software tools prepared and tested throughout the collaboration. To facilitate broad participation in the corresponding tasks, a "Flight Simulator" software environment was designed as a middle layer between the existing lower level ATF control system based on EPICS and V-system and the higher-level beam dynamics modelling tools [16]. This is a "portable" control system for ATF2 that allows code development and checkout offsite and additionally provides the framework for integrating that code into the operational ATF2 control system. The software developed through the flight simulator is developed mainly through the Lucretia [17] package while various "add-on" packages are also supported to enable usage of MAD8, PLACET and SAD optics programs. It is used in the ATF2 control room alongside tools developed through the existing V-System interface.

Table 1: Comparison of ATF2 parameters with ILC and CLIC specifications.

Parameters	ATF2	ILC	CLIC
Beam Energy [GeV]	1.3	250	1500
L^* [m]	1	3.5 - 4.5	3.5
$\gamma\epsilon_{x/y}$ [m.rad]	5E-6 / 3E-8	1E-5 / 4E-8	6.6E-7 / 2E-8
IP $\beta_{x/y}$ [mm]	4 / 0.1	21 / 0.4	6.9 / 0.07
IP η' [rad]	0.14	0.0094	0.00144
σ_E [%]	~ 0.1	~ 0.1	~ 0.3
Chromaticity	$\sim 1E4$	$\sim 1E4$	$\sim 5E4$
Number of bunches	1-3 (goal 1)	~ 3000	312
Number of bunches	3-30 (goal 2)	~ 3000	312
Bunch population	1-2E10	2E10	3.7E9
IP σ_y [nm]	37	5.7	0.7

ATF2 construction was completed in 2008 and first beam testing began in December that year, focusing on the first goal. In addition, a number of studies and hardware development towards the second goal have proceeded in parallel. Since the ATF2 project relies on many in kind contributions and is commissioned and operated by scientists from several institutions in a number of countries spread out geographically over three continents, it is considered a model for the organization of the international collaborations which will be needed to build and operate future large scale accelerator projects such as the ILC. Planning and coordination are of crucial importance. The organization of the ATF collaboration and commissioning efforts are described in [3]. The commissioning strategy is designed to use the large international contribution efficiently. Training and transfer of knowledge, important to strengthen the accelerator community and prepare for future large projects, are emphasized. Beam operation time is divided giving 50% for ATF2, 30% for DR and injector related R&D, and 20% for maintenance and upgrades, in order to ensure richness of the overall program while providing sufficient time for the commissioning.

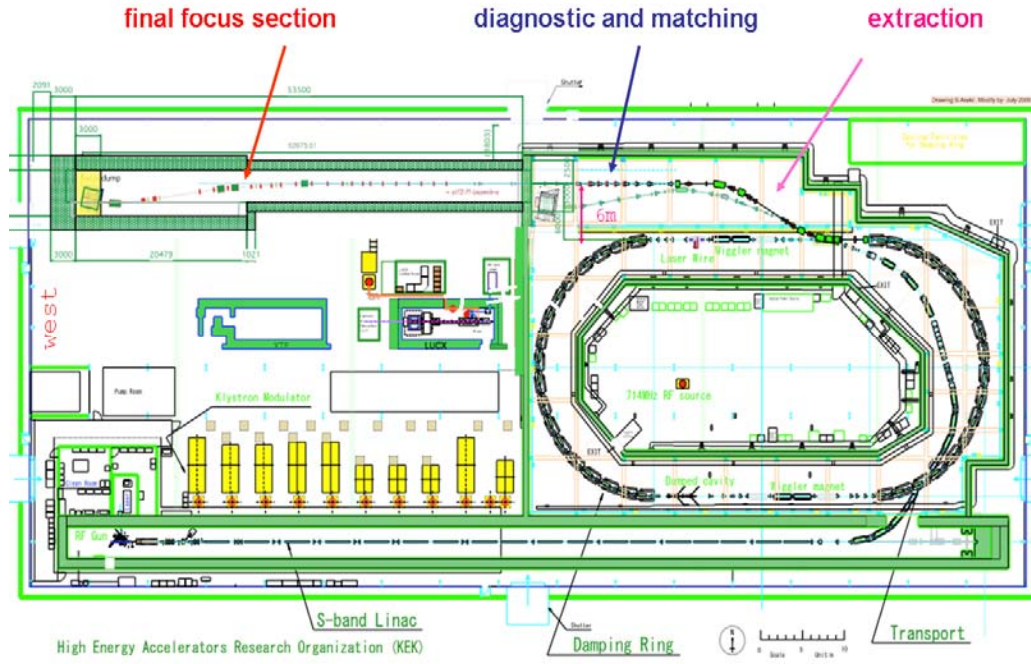


Figure 1: Layout of ATF damping ring and ATF2 final focus facility.

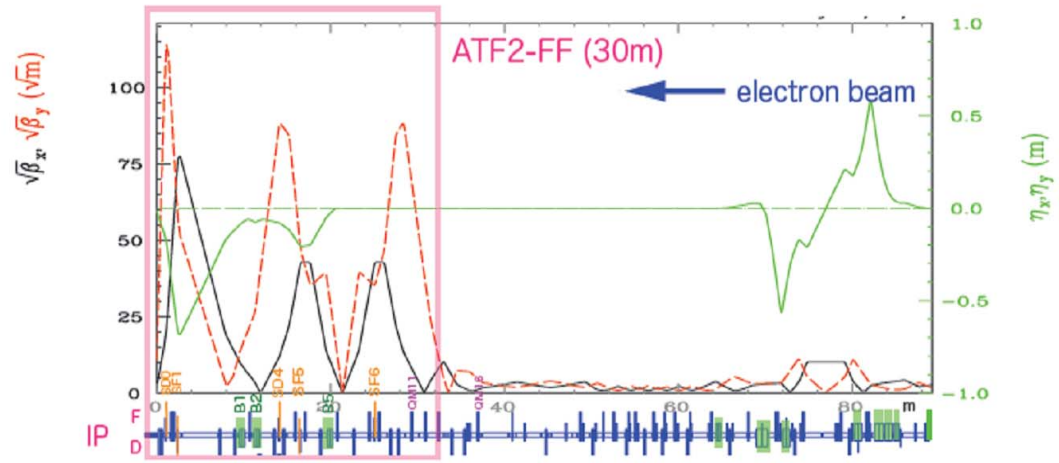


Figure 2: Optics of ATF2, starting from the ATF damping ring extraction point (on the right).



Figure 3: View of the latter part of the ATF2 beam line.

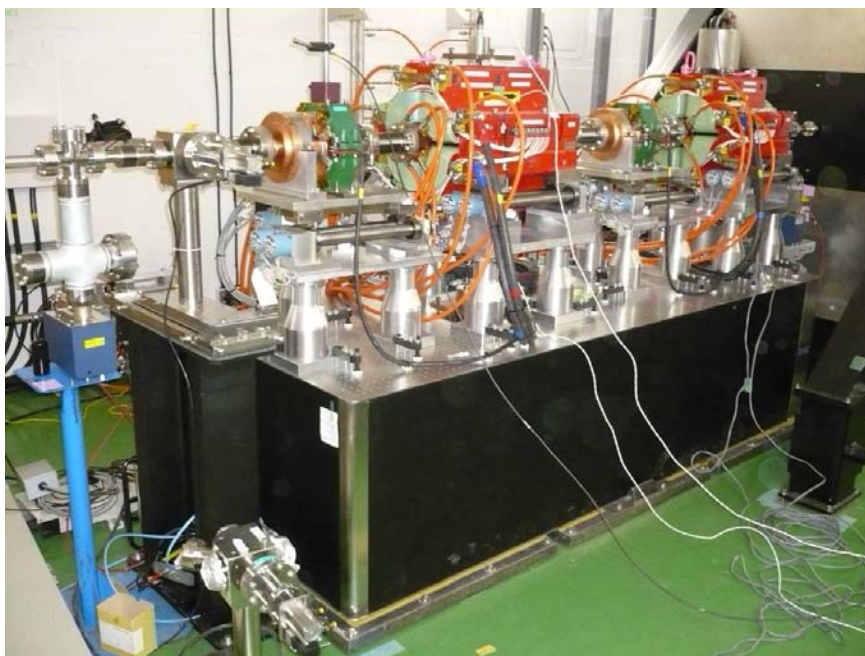


Figure 4: View of the Final Doublet installed on its rigid mechanical support system.

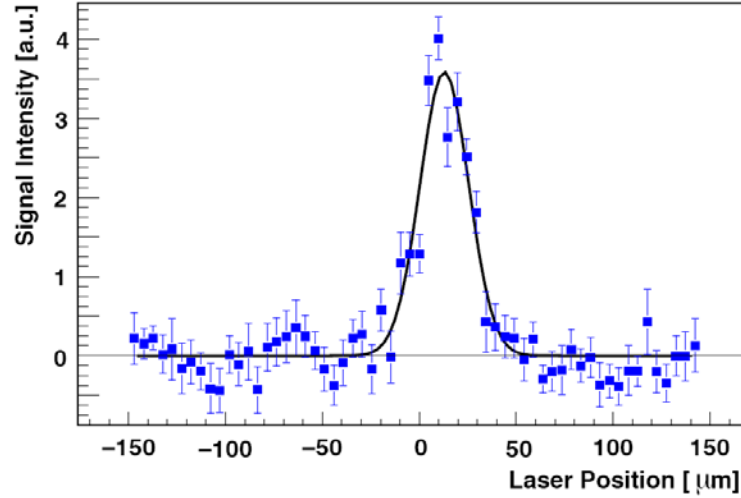


Figure 5: Convoluted horizontal size measured by BSM in laser wire mode in March 2009.

3.9.2 Highlights of ATF2 First Results

Since the beginning of commissioning at the end of December 2008, five commissioning runs were performed till early summer of 2009, each two or three weeks long, and further runs started in autumn of 2009. The December 2008 pilot run was performed with large β^* optics and a semi-ballistic trajectory with only some of the magnets turned on. The focus was to establish the beam to its dump, minimizing beam losses to pass a radiation inspection required at KEK. The very first tests of the hardware and tuning software, including commissioning and background characterization of the BSM, started during this run.

The BSM system was installed at the end of the beam line during summer 2008 [18]. After a first checkout with beam in December 2008, commissioning started in 2009 with the laser wire mode. This mode of operation was successfully and reproducibly established during winter and spring runs. Figure 5 shows an example of signal intensity as a function of laser position in the horizontal plane. The relative accuracy of the signal intensity measurement, obtained analysing the longitudinal profile of the shower in the multilayered photon detector, ranges from 10 to 20%. The line shows a Gaussian fit to the data. The measured convoluted horizontal size was 13 microns, consistent with the design waist size of the laser wire and with the beam size of about 10 microns available during the runs and confirmed by measurements with a wire scanner near the IP [19].

The February-March 2009 run was also performed with large β^* optics (8 cm horizontally and vertically), but with all ATF2 magnets switched on for the first time and an optical configuration with basic features similar to the nominal optics [20]. For such values of the β -functions, 20 and 800 times larger than nominal, beam sizes in the FD are reduced by the square root of the corresponding factors, which eased requirements for backgrounds while producing IP beam spots with $\sigma_{x,y} \sim 12.5, 1\text{-}2 \mu\text{m}$, within the measurable range of the BSM in laser wire mode and just below the resolution limit of the tungsten post-IP wire scanner. Hardware commissioning

continued, and the laser wire mode of the BSM was commissioned. Beam tuning and control tools for extraction line dispersion and coupling correction, extraction line and IP wire scans, Twiss parameter and emittance reconstruction as well as BBA were checked and started to be used in the regular setup procedure.

The April and May 2009 runs continued deployment and checks of tuning and control tools as well as further tests and characterisation of the BSM and of the cavity and strip line BPMs. Measurements of optical functions and beam parameters were also done in these runs, to establish the tuning strategy for the beam at the IP. The optical configuration used in these runs also had enlarged β^* values, 8 cm horizontally and 1 cm vertically, corresponding to IP beam spots of $\sigma_{x,y} \sim 12.5, 0.5 \mu\text{m}$. In this configuration, the chromaticity is not yet predominant and sextupole magnets have little influence. They were turned on when testing alignment procedures and optical corrections.

Achievement of low beam emittance in DR and preservation of the beam emittance during extraction is of critical importance for ATF2. Beam vertical emittances of less than 10 pm were consistently achieved in the DR during spring 2009 [21]. After extraction to ATF2, several effects can however enlarge it, especially anomalous dispersion and coupling remaining from the DR or generated in the extraction process. In the March 2009 run and during earlier tests in 2007-2008 [22] before reconfiguring the extraction line for ATF2, large growth factors were often observed. In April and May, systematic BBA in selected quadrupole magnets of the extraction line, followed by careful corrections for residual dispersion and coupling, enabled the reproducible measurement of vertical emittance values in the 10 to 30 pm range. Figure 6 shows results for the DR and extraction line emittances over period of time. One can see that vertical emittances of below 10pm in the ring and about 11pm in the extraction line were consistently measured recently.

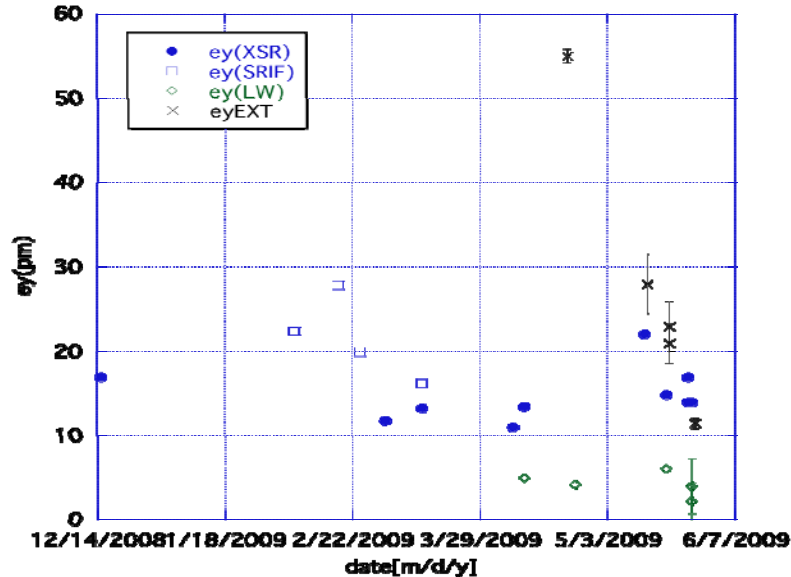


Figure 6: Emittances measured in the ATF Damping Ring and in ATF2 extraction line, where the recent measurements show vertical emittance of below 10pm in the ring as measured by the laser wire, and emittance of 11pm measured in the extraction line.

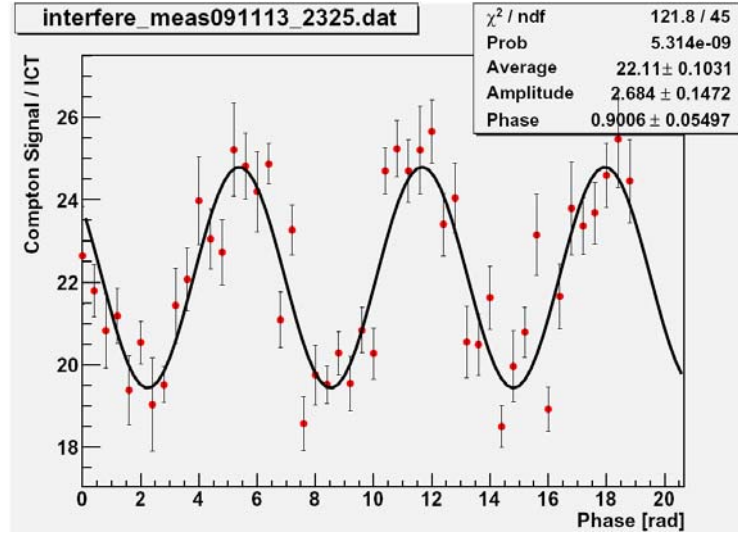


Figure 7: First measurement of the vertical beam size by the BSM working in the interferometer mode done in November 2009. The measurement corresponds to $3.3\mu\text{m}$ vertical beam size (the laser fringe pitch of the interferometer mode employed for this measurement is $10.2\mu\text{m}$).

During the summer shutdown in 2009, a number of improvements and hardware upgrades were made, especially in the BSM and BPM systems.

For the BPM system, the performance of the cavity BPMs was extensively studied in order to achieve stability and reproducibility at the sub 1% level in signal amplitude and phase over a month long period. Also, the offline RF tone calibration scheme was improved using more realistic signals. The electronics of the strip line BPMs was upgraded by adding high pass filters to suppress residual kicker noise picked up on the electrodes, which had been shown to degrade performances. A number of adjustments were also made to gains at different stages of the electronics readout chain and signal polarities were checked. Calibration work and studies will continue during the beam running to ensure optimal performances for both kinds of BPMs.

For the BSM system, a new three times more powerful laser has been installed that will enhance the signal significance with respect to the background. Additional collimation in front of the photon detector was installed to reduce the background from bremsstrahlung emitted upstream. Moreover, wire scanner, screen and knife edge monitors were newly installed in the IP chamber of the BSM to make it easier to overlap the electron and laser beams.

The hardware upgrades resulted in improvements of systems' performance and in November 2009 the first observation of the vertical beam size by the BSM working in the interferometer mode has been achieved [23]. The measurements are illustrated in Figure 7 where the depth of the Compton signal modulation corresponds to $3.3\mu\text{m}$ vertical beam size for the laser fringe pitch of the interferometer mode of $10.2\mu\text{m}$, known from the laser optics.

3.9.3 ATF2 Outlook and Plans

The present ATF2 efforts of the ATF collaboration are focused on the first ATF2 goal. The priority for the ongoing runs during autumn and early winter of 2009 is to measure sub-micron vertical beam sizes using the interference mode of the BSM. This will involve continued operation with the large β^* optics (8 cm horizontally and 1 cm vertically) in order to confirm its properties in more detail followed by a squeeze of the beta-function to smaller values.

During 2010, the goal will be to reduce the β^* parameters enough towards the nominal values for vertical beam sizes smaller than 100 nm to be measured. Preparations towards this goal are on-going in parallel with the above tasks. In particular, a new system with multiple OTR (Optical Transition Radiation) stations is being prepared in the diagnostic section to supplement the existing wire scanners and enable speedier and more precise 2D profile measurements. The improved Twiss parameter, emittance and coupling determinations which will result should help to minimise the extracted vertical emittance. A re-design of the strip line BPM electronics is also being evaluated to improve the accuracy and reproducibility of trajectory measurements in the extraction line. Finally, two additional tasks related to the BSM are needed to achieve the first goal in 2010: improved automation of the BSM data acquisition along with integration into the overall software environment for beam size tuning at the IP, and evaluation of BSM beam induced backgrounds, in particular as a function of β^* .

The ATF collaboration also pursues several other hardware developments of particular relevance to future linear colliders, especially in the context of the second ATF2 goal: characterization of the site and beam line stability [24], the MONALISA interferometer system [25] for accurate monitoring of the FD position with respect to that of the BSM, the FONT (Feedback On Nanosecond Timescale) project [26], the nanometre resolution IP-BPM project [27], the fast nanosecond rise time kicker project [28] and a new cavity-BPM optimised to monitor angular variations of the beam near the IP with high accuracy [29]. A laser wire system operated in the old ATF extraction line during 2005-2008 with the aim to demonstrate 1 μm resolution beam size measurements [30] has also been moved to a new location in the ATF2 diagnostics section for further testing and development in coming years. In the future, this system could be expanded to replace some or all present wire scanners. Future linear colliders are expected to rely extensively on laser wire systems, so it is important to gain experience operating a multiple system in realistic conditions.

Plans to upgrade the performance of ATF2 on the time scale of a few years, after the main goals of ATF2 have been achieved, are also discussed. In particular, optical configurations with ultra-low β^* values (two to four times smaller than nominal in the horizontal and vertical planes), relevant to both the CLIC design and to some of the alternative ILC beam parameter sets [1], are actively studied [31]. There is also a proposal to upgrade the FD with superconducting magnets [32] built according to ILC direct wind technology, to allow stability studies with beam of direct relevance to the ILC setup. An R&D programme to develop a tuneable permanent magnet suitable for the FD is also pursued in parallel, with as initial goal the construction of a prototype for initial beam testing in the upstream part of the ATF2 beam line [33]. Since possibilities to achieve the smallest vertical beam sizes are limited, especially in the case of reduced

β^* values, both by the field quality in the magnets of the presently installed FD [31, 34] and by their aperture (to avoid excessive bremsstrahlung photon background in the BSM), these proposals are naturally connected in the sense that an upgraded FD should also aim to both enlarge the aperture and improve the field quality.

Longer term, more tentative, plans being discussed also include, after 2012, the possibility of a photon facility, with laser and optical cavities for the planned photon linear collider and generation of a photon beam. Strong QED experiments with laser intensities of $> 10^{22}$ W/cm² could then also be considered, e.g. to pursue experimental studies of the predicted Unruh radiation [35].

3.9.4 Conclusion

The ATF collaboration has completed the construction of ATF2 and has started its commissioning. Important experience operating the new cavity BPM and BSM instrumentation in real conditions has been gained and first beam measurements have been performed in a magnetic configuration with reduced optical demagnification. Both horizontal and vertical emittances were successfully tuned and measured in the extraction line, with values approaching the design values of 2 nm and 12 pm, respectively. First checks of the first order optics along the beam line and at the IP were also done. Hardware developments for the second ATF2 goal are being pursued in parallel with the present commissioning work for the first goal. The collaboration is also preparing several near and long terms plans for ATF2. In the next few years, information very valuable for any future collider with local chromaticity correction and tuning of very low emittance beams can be expected. In the previous experience at the FFTB, the smallest vertical beam sizes which were achieved were about 70 nanometres. The work described here continues to address this largely unexplored regime in a systematic way.

3.9.5 Acknowledgements

This work is supported by: DOE Contract DE-AC02-76SF00515; Grant-in-Aid for Creative Scientific Research of JSPS (KAKENHI 17GS0210); USA-Japan Collaboration Research Grant of MEXT; Agence Nationale de la Recherche of the French Ministry of Research (Programme Blanc, Project ATF2-IN2P3-KEK, contract ANR-06-BLAN-0027); The “Toshiko Yuasa” France Japan Particle Physics Laboratory; Science and Technology Facilities Council, UK and EuCARD project co-funded by the European Commission within the Framework Programme 7, under Grant Agreement no 227579.

** B. Parker, J.-P. Delahaye, D. Schulte, R. Tomas, F. Zimmermann, A. Wolski, E. Elsen, E. Gianfelice-Wendt, M. Ross, M. Wendt, T. Takahashi, M. Alabau Pons, A. Faus-Golfe, S. Bai, J. Gao, R. Apsimon, P. Burrows, G. Christian, B. Constance, C. Perry, J. Resta-Lopez, C. Swinson, D. Uner, P. Coe, M. Warden, A. Reichold, S. Araki, A. Aryshev, M. Fukuda, H. Hayano, Y. Honda, K. Kubo, T. Kume, S. Kuroda, M. Masuzawa, T. Naito, T. Okugi, R. Sugahara, T. Tauchi, N. Terunuma, J. Urakawa, K. Yokoya, Y. Iwashita, T. Sugimoto, A.-Y. Heo, E.-S. Kim, H.-S. Kim, P. Bambade, Y. Renier, C. Rimbault, M. Verderi, H. Guler, B. Bolzon, N. Geffroy, A. Jeremie, J.Y.Huang, S.H.Kim, Y.J.Park, W.H.Hwang, G. Blair, S. Boogert, G. Boorman, L.

Deacon, P. Karataev, S. Molloy, J. Amann, P. Bellomo, B. Lam, D. McCormick, J. Nelson, E. Paterson, M. Pivi, T. Raubenheimer, A. Seryi, C. Spencer, M.-H. Wang, G. White, W. Wittmer, M. Woodley, Y. Yan, F. Zhou, D. Angal-Kalinin, J. Jones, D. Okamoto, T. Sanuki, A. Lyapin, A. Scarfe, Y. Kamiya, S. Komamiya, T. Nakamura, M. Oroku, T. Suehara, Y. Yamaguchi, T. Yamanaka, H. Yoda, BNL; CERN; Cockcroft Institute, Univ. of Liverpool; DESY; Fermilab; Hiroshima Univ.; IFIC Valencia; IHEP Beijing; JAI, Oxford; KEK; Kyoto ICR; Kyungpook Nat. Univ.; LAL, LLR, Univ. Paris-Sud, IN2P3/CNRS, Orsay, France; LAPP, Annecy; PAL, Korea; JAI, Royal Holloway; SLAC; Cockcroft Institute, STFC, Daresbury Laboratory; Tohoku Univ.; UCL, London; Cockcroft Institute, Univ. of Manchester; The Univ. of Tokyo

3.9.6 References

1. ILC RDR, ILC-REPORT-2007-001
2. R. Tomàs, “CLIC Overview”, to appear in Phys. Rev. ST Accel. Beams, and references therein
3. ATF collaboration, <http://atf.kek.jp/collab/ap/>
4. ATF2 Proposal, SLAC-R-771, 2005
5. V. Balakin *et al.*, Phys. Rev. Lett. 74, 2479 (1995)
6. P. Raimondi and A. Seryi, Phys. Rev. Lett. 86, 3779 (2001)
7. R. Sugahara *et al.*, “Construction of the magnet system for the ATF2 beam line”, Proceedings of 6th annual meeting of the Particle Accelerator Society of Japan, August 5-7, 2009, Tokai, Ibaraki, Japan; KEK Preprint 2009-22
8. A. Jérémie, “Installation of FD in September”, 7th ATF2 Project Meeting, KEK, Dec. 2008, <http://ilcagenda.linearcollider.org/conferenceDisplay.py?confId=3003>
9. B. Bolzon *et al.*, “Impact of flowing cooling water on ATF2 FD vibrations”, ATF-Report 09-01
10. S. Molloy *et al.*, Proceedings of PAC09, TH6REP028
11. A. Lyapin *et al.*, Proceedings of PAC09, TH6REP025.
12. J. Y. Huang *et al.*, Proceedings of APAC07, WEC3H102
13. T. Shintake, Nucl. Instr. Meth. A311, 453 (1992)
14. T. Yamanaka *et al.*, IEEE NSS08 Conf. Record, 3308 (2008); T. Suehara, Doctor Thesis, The University of Tokyo (2008)
15. M. Oroku *et al.*, IEEE NSS08 Conf. Record, 2330 (2008); Y. Yamaguchi *et al.*, Proceedings of the 5th Annu. Meet. of PASJ, WPBDA33 (2009)
16. G. White *et al.*, Proceedings of EPAC08, TUPP016
17. P. Tenenbaum *et al.*, SLAC-PUB-11215 (2005)
18. T. Kume *et al.*, Proceedings of PAC09, TH5RFP084
19. T. Yamanaka *et al.*, Proceedings of PAC09, TH6REP062
20. S. Bai *et al.*, “Optical configurations with variable β^* at different IP locations in ATF2”, ATF- Report 08-05
21. K. Kubo *et al.*, Proceedings of PAC09, FR1RAC05
22. M. Alabau Pons *et al.* “Experimental studies and analysis of the vertical emittance growth in the ATF extraction line in 2007-2008”, ATF-Report 08-15
23. T. Yamanaka, *et al.*, First measurements of the vertical size by BSM, private communication, November 2009.
24. M. Masuzawa *et al.*, Proceedings of IWAA06, IWAA-2006-FR002
25. M. Warden *et al.*, Proceedings of IWAA08
26. P. Burrows *et al.*, Proceedings of PAC09, WE6PFP077
27. Y. Inoue *et al.*, Phys. Rev. ST Accel. Beams 11, 062801 (2008)
28. T. Naito *et al.*, Proceedings of PAC09, TU6RFP036

29. D. Okamoto *et al.*, Proceedings of PAC09, TH6REP022
30. A. Aryshev *et al.*, Proceedings of PAC09, TH6REP023
31. R. Tomàs *et al.*, Proceedings of PAC09, WE6PFP024
32. B. Parker *et al.*, Proceedings of PAC09, MO6PFP044
33. Y. Iwashita *et al.*, Proceedings of PAC09, MO6PFP024
34. G. White *et al.*, Proceedings of PAC09, FR5PFP021
35. T. Tauchi, Seminar at Oxford, March 2009,
http://www.pp.rhul.ac.uk/~blair/laserwire_Oxf_Mar09/tauchi_atf2-unruh-oxford-9mar09.pdf

3.10 Fourth International Accelerator School for Linear Colliders

Barry Barish and Weiren Chou
 mail to: barish@ligo.caltech.edu, chou@fnal.gov

The Fourth International Accelerator School for Linear Colliders took place from September 7 to 18, 2009 at the Jixian Hotel, Huairou near Beijing, China. (<http://www.linearcollider.org/school/2009/>) This school continued the successful series: 2006 in Japan, 2007 in Italy and 2008 in the U.S. This year's school was jointly organised by the ILC GDE, the International Linear Collider Steering Committee (ILCSC) and the ICFA Beam Dynamics Panel. The Institute of High Energy Physics (IHEP) hosted the school.

The school was aimed at PhD students, postdocs and young researchers, especially young experimentalists. The response to the school was overwhelming. We received 244 applications from 41 countries; most of the candidates presented strong credentials. However, the school could only accommodate a limited number. Through a difficult and rigorous selection process, the Curriculum Committee accepted 71 students from 18 countries. The committee members carefully read the CV and recommendation letter of each applicant, and discussed among themselves before making the decision to admit or reject an applicant. For personal reasons two admitted students did not come. Thanks to the IHEP Foreign Affairs Office, all the students received a visa. Only an Iranian student did not receive the visa until the day the school started. He still came but was a few days late. The sixty-nine students who attended the school were a talented and highly motivated group. They successfully met the challenge of an intensive 10-day education program and did well in the final examination.

The curriculum consisted of lectures, homework assignments and a final exam. The first two days were plenary sessions with introductory lectures: general introduction, ILC, CLIC and the muon collider. After that the students divided into two parallel classes. Class A, accelerator physics, had 41 students and included four lectures: sources, linacs, damping rings and beam delivery system. Class B, RF technology, had 28 students and included three lectures: room temperature RF, superconducting RF, high power and low level RF. There was a half-day joint lecture on linac basics for both classes. Many lecturers are ILC GDE members. They not only gave lectures during the day, but also gave tutorials and helped students with their homework in the evenings. They designed the examination problems and graded them. The final exam on the last day lasted four-and-a-half hours. All 69 students took the final exam. The lecture slides, homework and exam problems can be found on the school web site.

The exam problems were different for Class A and B but were equally challenging. Most students did well as shown in the figures of exam scores. The top 9 students were

honored at the banquet and each was awarded a certificate and a book (*Reviews of Accelerator Science and Technology*, volume 1, edited by A. Chao and W. Chou, and published by World Scientific in 2008).

In addition to lectures, the students paid a site visit to IHEP. This gave them an opportunity to learn about real accelerators. The students visited the BEPC II linac, the ring and tunnel, the control room, the superconducting RF research center and the BES III detector.

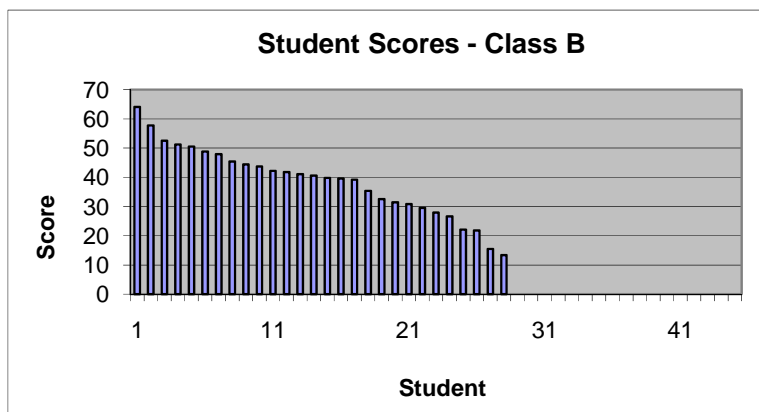
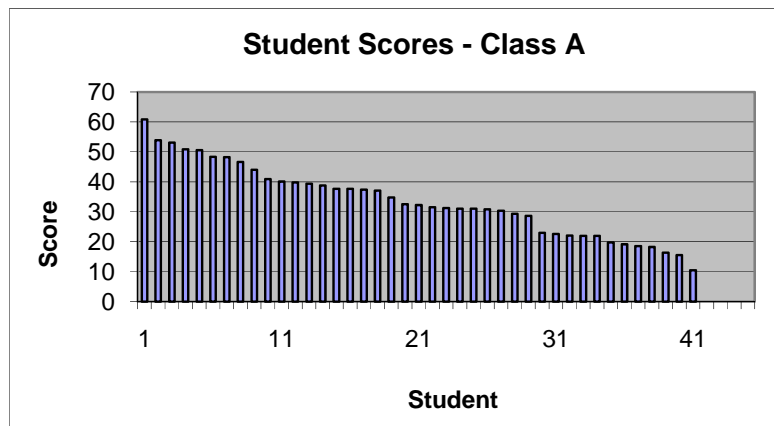
Throughout the school period, the students were encouraged to make new friends since this was a once-in-a-lifetime opportunity for many of them to meet with other young talented people from different origins who shared the same interest (accelerators) and career goals (linear colliders). Some of the friendships nurtured at the school will last a lifetime.

The IHEP was responsible for the organization of this school and Fermilab's Conference Office (Cynthia Sazama, Suzanne Weber and Jean Guyer) provided valuable assistance. The Local Committee was chaired by Jiuqing Wang, Deputy Director of IHEP. Tongzhou Xu, head of the IHEP Foreign Affairs Office played a pivotal role in making the school a success. Jinjun Zhang was stationed at the school from the beginning to the end and was the liaison between the school and the hotel. Jie Gao, Tiejun Deng, Jiyuan Zhai, Peggy Pan and many others from IHEP spent an enormous amount of time and effort and did an outstanding job. They arranged everything for the school: visa applications, airport pickups, housing assignments, meals, coffee breaks, reception, banquet, photos, excursion and the IHEP site visit. All logistics was well taken care of so the teachers could concentrate on teaching and the students could focus on studying and learning. When one of the students fell sick and needed emergency medical care, the IHEP people took her to the hospital and arranged for surgery. She quickly recovered and returned to continue her participation in the school. We were very impressed by the talent and dedication of the IHEP staff.

The school received generous sponsorship from a number of funding agencies and institutions all over the world: U.S. DOE Office of Science, NSF, Fermilab, SLAC, FRA, ILC GDE, CERN, DESY, IN2P3, INFN, Oxford University, KEK, KNU, IHEP, CAS, NSFC and CCAST.

We carried out a student survey on the last day of school. The results were given to the lecturers and committee members for improvements for future schools.

Based on the interest, demand and success of the first four schools, it was decided to continue in 2010. The fifth school will take place from October 18 to 29, 2010 in Europe and be hosted by CERN.



4 Workshop and Conference Reports

4.1 47th ICFA Advanced Beam Dynamics Workshop on *the Physics and Applications of High Brightness Electron Beams*

J. B. Rosenzweig

UCLA Dept. of Physics and Astronomy, 405 Hilgard Ave., Los Angeles, CA 90095

Mail to: rosen@physics.ucla.edu

4.1.1 Introduction

The 47th ICFA Advanced Beam Dynamics workshop, also endorsed by the ICFA sub-panel on Advanced and Novel Accelerators, entitled “*The Physics and Applications of High Brightness Electron Beams*”, was held in Maui, Hawaii, November 16-19, 2009. This workshop represents the latest workshop in the joint tradition of the “Arcidosso” and High Brightness Beam series, and is the direct heir to the last workshop in the series [1-3], held in Erice, Sicily.

The workshop mission was slightly changed in this year’s gathering. It is given in the following statement:

High brightness electron beams are playing an increasingly critical role in two frontier fields that are now yielding results that provoke considerable excitement and activity across the scientific community: radiation generation methods and advanced acceleration schemes. Such cutting edge radiation production methods include variations on the revolutionary 4th generation device, the free-electron laser, as well as inverse Compton scattering of intense lasers. These diverse approaches are thus able to create high peak and high average power light sources, with applications in ultrafast sciences and the Å level, as well as in nuclear and high-energy physics. Likewise, high brightness beams are at the center of many future accelerator schemes, e.g. based on high gradient electron and laser wakefields. Indeed, laser wakefield accelerators are now entering the proof-of-application phase, where unique light sources based on advanced acceleration schemes are enabled. The goal of this workshop is to provide a comparative study of the generation, manipulating, modeling and measuring of high brightness electron beams, and the multitude of underlying, interdisciplinary methods linking the physics of these beam systems to the physics of advanced applications.

This mission’s modified emphasis was reflected in the list of invited speakers, which varied from state-of-the-art standard technology to a series of contribution on frontier approaches employing lasers, plasmas and wakefields and even Bose-Einstein condensates. The workshop program is discussed further below.

4.1.2 Organization and Attendees

The 2009 workshop on “*The Physics and Applications of High Brightness Electron Beams*” was co-chaired by J. Rosenzweig (UCLA), L. Palumbo (Univ. Roma 1). The program committee, which produced an exciting and forward-looking agenda, was chaired by M. Ferrario (INFN-LNF). The workshop’s location in the mid-Pacific was designed to encourage a larger participation from Asian scientists, and this effort was met with success. The workshop had 105 registered attendees from across the beam physics community, among them 10 students with partial support from the workshop. The workshop received financial contributions from ANL, LBNL Sincrotrone Trieste, SLAC, UCLA, and the Univ. of Tokyo. The conference secretariat was headed by Carly Nguyen of UCLA, and also included Francesca Casarin and Daniela Ferrucci of INFN-LNF. The web site, which gives further information on the workshop organization, is available at:

<http://pbpl.physics.ucla.edu/HBEB/index.html>.

As with any successful workshop, there were enjoyable social interactions, particularly at an authentic Hawaiian luau on Wednesday evening.

4.1.3 Scientific Program

The scientific program consisted of invited talks in the morning sessions and working groups in the afternoons. The invited speaker list, impressive in its variation of theme across beam physics and applications fields, is given here for emphasis:

- David Dowell (SLAC) "LCLS injector performance and impact on lasing"
- Frank Stephan (DESY-Zeuthen) "High Brightness Beams at PITZ"
- Thorsten Kamps (HZB / BESSY II) "Superconducting injector development"
- Rami Kishek (University of Maryland) "Intense space charge effects of relevance to FEL injectors"
- Victor Malka (CNRS-ENSTA-X) "Controlled Electron beam injection by colliding laser pulses"
- Luca Cultrera (INFN-LNF) "Overview of advanced cathodes for HBB"
- Charles Brau (Vanderbilt) "Novel high brightness beyond photocathodes"
- Hiromitsu Tomizawa (Spring-8) "Advanced Laser Pulse Shaping"
- Pietro Musumeci (UCLA) "Photoinjector blow out regime experiments"
- Alessandro Cianchi (Univ. Rome, Tor Vergata) "Velocity bunching at SPARC"
- Patric Muggli (University of Southern California) "Generation of train of short electron pulses for wakefield experiments"
- Henrik Loos (SLAC) "Beam diagnosis at the fs frontier"
- Diktys Stratakis (Brookhaven National Laboratory) "Tomographic phase space mapping of high brightness beams"
- Kwang-Je Kim (Argonne National Laboratory) "X-ray FEL oscillators"
- Chun-xi Wang (Argonne National Laboratory) "Emittance compensation theory and experimental results in HB photoinjector"

- Chiping Chen (Massachusetts Institute of Technology) "Thermal beam equilibria in periodic focusing fields"
- Eric Esarey (Lawrence Berkeley National Laboratory) "Overview of plasma accelerator simulations"
- Andrea Rossi (INFN-Milano) "Brightness characterization of electron beams from plasma injectors"
- Dao Xiang (SLAC) "Echo harmonic-techniques for introducing nm beam structures"
- Wim Leemans (LBNL) "Overview of LWFA Experiments"
- F.Sannibale (LBNL) "High average power, high brightness electron beam sources"
- Rynosuke Kuroda (AIST) "Overview of Thomson/Compton Sources"
- Mark Hogan (SLAC) "Plasma and dielectric wakefield acceleration experiments at SLAC"
- James Rosenzweig (UCLA) "Sub-fs electron pulses for FEL and PWFA applications"
- Matthias Fuchs (Ludwig-Maximilians University) "Soft x-ray undulator radiation from laser accelerated electrons"
- Carl Schroeder (LBNL) "Prospects for a table top FEL"
- Ben Cowan (Tech-X Corporation) "Laser-structure accelerators"
- O. J. Luiten (Univ. Eindhoven) "The coolest beam in the world"

The working groups and their leaders were:

- WG1. Electron sources, including photoinjectors and plasma-laser sources, Phillippe Piot (NIU)
- WG2. Manipulation and diagnostics of high brightness electron beams, Enrica Chiadroni (INFN-LNF)
- WG3. Theory and modeling, simulation challenges, Carl Schroeder, LBNL.
- WG4. Applications of high brightness beams in advanced accelerators and light source, Chuanxiang Tang (Tsinghua Univ.)

The working group leaders presented detailed summaries of break-out session talks and discussions on the final afternoon. These talks, as well as the invited and break-out session oral contributions, are available on the workshop website.

4.1.4 Publications

A complete collection of papers submitted to the HBEB2009 workshop will be posted on JACoW (<http://www.jacow.org>) without peer review. The workshop organizing committee has also recommended that all contributors to the workshop consider submitting an extended version of their HBEB2009 paper to PRST-AB. Authors should submit to PRST-AB using the procedure found through links on the PRST-AB home page. Papers will be peer-reviewed through the normal refereeing procedure, and if accepted for publication they will be published as regular PRST-AB articles and as part of the HBEB2009 Conference Edition, guest edited by J. Rosenzweig.

Publication will be timely; articles will be published as soon as they are ready with no delay waiting for other papers presented at the conference. In addition, the HBEB2009 Table of Contents and the workshop website will be updated each time a paper is published.

4.1.5 References

1. *The Physics of High Brightness Beams*, Edited by James Rosenzweig and Luca Serafini, World Scientific, 2000.
2. *The Physics and Applications of High Brightness Electron Beams*, Edited by James Rosenzweig, Gil Travish and Luca Serafini, World Scientific, 2003.
3. *The Physics & Applications of High Brightness Electron Beams*, Edited by Luigi Palumbo, James Rosenzweig, and Luca Serafini, World Scientific, 2006.

4.2 Workshop on Top-Up Operations at Synchrotron Light Sources

Rohan Dowd

Australian Synchrotron, 800 Blackburn Rd. Clayton, Australia

Mail to: rohan.dowd@synchrotron.org.au

Top-up is fast becoming the standard operational goal for synchrotron light sources. New light source facilities are designed with top-up in mind and many older facilities have invested in hardware upgrades to enable it. The advantages of top-up operations are clear to both the accelerator and user communities. Aside from the higher average photon flux, operating in top-up generates a more even thermal load on both the accelerator and beamline components, leading to greater stability. This improved stability comes at the price of increased availability and stability requirements of the injector systems and requires many technical challenges to be overcome. The Australian Synchrotron is looking to move to top-up operations and is currently in the process of identifying steps needed to enable this.

A workshop on top-up operations at synchrotron light sources was held in Melbourne on October 7-9. The event was jointly hosted by the Australian Synchrotron and the University of Melbourne and consisted of a series of concurrent talks interspersed with generous discussion periods. The goal of the workshop was to bring together world experience in top-up operations and identify the technical and operational issues that need to be addressed by any facility before top-up operation can be implemented.

Speakers from 12 different light source facilities presented 13 talks over the 3 day workshop, which was attended by 41 people from around the world. The talks given were:

1. "Top-Up Experience at Spring-8" Kouichi Soutome, Accelerator Division, JASRI/Spring-8
2. "Four good reasons for topup: stability, resolution, speed and flexibility" David Paterson, Principal Scientist, XFM Beamline, Australian Synchrotron
3. "Overview of the Australian Synchrotron Accelerators" Mark Boland, Principal Scientist, Accelerator Physics, Australian Synchrotron
4. "MAX-IV Bulk Shielding" Magnus Lundin, Physicist, MAX-lab

5. “APS Top-Up Experience” Louis Emery, Group Leader Accelerator Operations and Physics, APS
6. “Novel Injection Schemes” Peter Kuske, BESSY-II
7. “Improving the Dynamic Aperture by Passive and Active Multipole Shimming at BESSY” Johannes Bahrtdt, BESSY-II
8. “NSRRC Experience with Top-Up” Gwo-Huei Luo, Deputy Director, NSRRC
9. “Diamond Top-Up Implementation” Vince Kempson, Head Accelerator Operations, Diamond
10. “Residual Orbit Corrections for Top-Up at SOLEIL” Alexandre Loulergue, SOLEIL
11. “SSRL’s Move to Top-Up” Jeff Corbett, SSRL, SLAC
12. “Simulation and Experimental Results of SSRF Top-Up Operations” Haohu Li, Associate Leader Accelerator Physics, SSRF
13. “NLSL-II Top-Up Requirements and Plans” Timur Shaftan, Group Leader Injection System, NLSL-II

A program and copy of talks can be found at:

<http://www.topup.synchrotron.org.au>.

The main topics identified and discussed were:

1. Motivations for Top-Up. Discussion of the increased photon beam flux and stability for beamlines and increased storage ring orbit stability.
2. Current stability requirements for Top-up. To what accuracy should the current be maintained at the same level? How does this impact on the requirements for the injector systems? Top-up filling schemes and stability of injector delivered current were also discussed.
3. Orbit stability and injection efficiency. Techniques for minimizing the residual oscillations from injection. Preserving dynamic aperture by compensating for insertion devices.
4. Novel injection schemes. Current ‘conventional’ injection schemes are not ideal for Top-Up. Proposed design of new injection kicker and septum arrangements.
5. Safety requirements. Injected beam phase space modeling techniques to verify safety of injection with beamline shutters open. Shielding and dose constraints at different facilities.

The workshop was considered by the participants as a great success in building a common base of knowledge of the issues surrounding top-up for synchrotron light sources. Another workshop has been proposed as a satellite meeting for IPAC2010.

5 Recent Doctoral Theses

5.1 Coupling Impedance and Collective Effects in the RCS Ring of the China Spallation Neutron Source

Na Wang

Graduate University of Chinese Academy of Sciences and
Institute of High Energy Physics, Beijing, China

Mail to: wangn@ihep.ac.cn

Graduation Date: July 4, 2009

Supervisor: Prof. Qing Qin (Institute of High Energy Physics)

Abstract

The rapid cycling synchrotron (RCS) of the China spallation neutron source (CSNS) is a high intensity proton accelerator. The study on the coupling impedance and the collective effects in the ring plays an important role in the stability of the machine performance and in achieving the final beam power. A thorough evaluation of the coupling impedance is necessary in controlling the total impedance of the ring, which can accordingly prevent the occurrence of the beam instability and reduce the beam loss. Therefore, in this thesis, we perform an in-depth and systematic research of the impedance and collective effects in the CSNS/RCS ring.

First, we investigate theoretically the impedance with a non-relativistic beam. The general formulae of the resistive wall impedance of the two-layer and multi-layer tubes in the non-relativistic condition are obtained. Then the non-relativistic corrections of the impedance of the metal tubes are derived. We calculate the impedance of the extraction kicker with non-relativistic beam based on the calculation in the relativistic limit. The expressions of the longitudinal and transverse impedance of the extraction kicker are given.

By using both the analytical and numerical methods, we calculate the impedance of the main vacuum components in the RCS ring, and finally the impedance model of the whole ring is established. According to the impedance budget, the threshold and growth rate of possible collective effects are estimated. A simulation of the impedance-induced instability is performed with the code ORBIT.

The electron-proton instability is an important subject among the studies of the collective effects. It is expected to be a potential threat limiting the machine performance of the RCS ring. Based on the theoretical models, the threshold of the electron-proton instability is analyzed. Pertaining to the property of the CSNS/RCS ring, we developed the electron-cloud simulation code of the Beijing Electron Position Collider Upgrade (BEPCII) to investigate the electron cloud issues in the lower-energy proton rings. By using the code, we simulate the electron-cloud formation and electron-induced beam instability in the CSNS RCS ring. The results show that the electron cloud is not likely to cause beam instabilities under normal operating conditions.

6 Forthcoming Beam Dynamics Events

6.1 46th ICFA Advanced Beam Dynamics Workshop: *HB2010*

The 46th ICFA Advanced Beam Dynamics Workshop will take place from September 27 to October 1, 2010 in Morschach near Lake Lucerne, Switzerland.

The fifth meeting in a series of workshops focused on High-Intensity, High-Brightness Hadron Beams will be hosted by the Paul Scherrer Institut, PSI. HB2010 continues the tradition of successful workshops held in Batavia (2002), Bensheim (2004), Tsukuba (2006) and Nashville (2008). The program covers experimental and theoretical advancements associated with high-intensity and/or high-brightness hadron beams, beam dynamics studies, reviews of planned projects, and practical experience gained with operating accelerators. The workshop is intended to provide a venue for detailed discussion and close interaction among experts in the field of accelerator science and technology.

The meeting will be held in Morschach, embedded in a beautiful landscape 200 m above Lake Lucerne. We plan to offer a visit to PSI and its accelerator facilities on October 1. The workshop website:

<http://hb2010.web.psi.ch>

will be regularly updated to include the latest information as it becomes available.

Contact:

HB2010 Chair, Mike Seidel, PSI, Switzerland, hb2010@psi.ch



6.2 48th ICFA Advanced Beam Dynamics Workshop on Future Light Sources: *FLS2010*

The 48th ICFA Advanced Beam Dynamics Workshop will take place from March 1 to 5, 2010 at SLAC, California, USA.

The workshop series on future light sources is the flagship event of the ICFA sub-panel on Future Light Sources. It intends to review and discuss modern accelerator-based light sources for wavelengths ranging from the Infrared to X-rays. The workshop program will consist of plenary talks and working group sessions. Working groups will be dedicated to critical issues of scientific needs for future light sources, ERL, FEL, storage ring, and novel light source concepts, as well as to the essential technologies of high brightness electron sources, synchronization, high resolution beam diagnostics, X-ray beamline optics and detectors.

Attendance will be limited to 150 people. Additional information and registration details are available at the workshop website:

<http://www-conf.slac.stanford.edu/icfa2010/>

Contacts:

Workshop Chairperson: [John Galayda](#)

Program Committee Chairpersons: [John Corlett](#), [Tor Raubenheimer](#)

6.3 2nd ICFA Mini-Workshop on Deflecting/Crabbing RF Cavity Applications in Accelerators

This workshop will take place at the Cockcroft Institute (UK) from Tuesday April 21 through Friday April 23, 2010.

Deflecting/crabbing mode cavities have been proposed, designed and implemented for a number of accelerator applications such as beam luminosity increase for “head-on” collisions in high energy colliders, emittance exchange techniques and particle beam diagnostic. In recent years a number of high-energy synchrotron light sources have started serious R&D programs to utilize superconducting deflecting cavities for the production of short x-ray pulses based on Zholents’ proposed scheme. Following the success of KEKB, CERN is pursuing the use of crab cavities for the LHC with a potentially significant luminosity increase.

The purpose of this workshop is to bring together researchers in various accelerator communities and discuss advances in the deflecting/crabbing RF cavity for accelerator applications.

Topics of interest are:

1. High energy colliders (LHC, KEK-B, ILC, CLIC ...);
2. Generation of short x-ray pulses in synchrotron light sources;
3. Beam manipulations, emittance exchange and diagnostics;
4. Deflecting cavity design optimization;
5. Novel deflecting cavity design.

Please contact Ali Nassiri (nassiri@aps.anl.gov) if you have any question on the workshop.

The workshop web site has been set up with more information on programs, registration, accommodation, transportation, UK visa application, local weather and attractions:

<http://www.cockcroft.ac.uk/events/cavity>

Please forward this announcement to anyone whom you think might be interested.

Organizing Committee:

Ali Nassiri (co-chair), Derun Li, Frank Zimmermann, Graeme Burt, Huaibi Chen, Kenji Hosoyama, Kwang-Je Kim, Peter McIntosh (co-chair), Robert Rimmer, and Zhentang Zhao.

6.4 New Books on Accelerators

6.4.1 Innovation Was Not Enough – A History of the Midwestern Universities Research Association (MURA)

Miguel A. Furman, LBNL
Mail to: mafurman@lbl.gov

A book describing the history of the Midwestern Universities Research Association (MURA) has been written by L. Jones, F. Mills, A. Sessler, K. Symon and D. Young, who were deeply involved with MURA. The book has been recently published by World Scientific. A description may be found at:

<http://www.worldscibooks.com/physics/6937.html>

An earlier book on the history of accelerators, "*Engines of Discovery: A Century of Particle Accelerators*", by E. Wilson and A. Sessler, is available at Amazon.com.

6.4.2 Reviews of Accelerator Science and Technology

Junji Urakawa, KEK
Mail to: urakawa@post.kek.jp

A book describing the medical applications of accelerators has been edited by A. Chao and W. Chou: "*Reviews of Accelerator Science and Technology, Volume 2*." This topic is of enormous importance to human health and has a deep impact on our society. The book has been recently published by World Scientific. A description may be found at:

<http://www.worldscibooks.com/physics/7676.html>

Volume 1 of *Reviews of Accelerator Science and Technology* edited by A. Chao and W. Chou was published in 2008.

7 Announcements of the Beam Dynamics Panel

7.1 ICFA Beam Dynamics Newsletter

7.1.1 Aim of the Newsletter

The ICFA Beam Dynamics Newsletter is intended as a channel for describing unsolved problems and highlighting important ongoing works, and not as a substitute for journal articles and conference proceedings that usually describe completed work. It is published by the ICFA Beam Dynamics Panel, one of whose missions is to encourage international collaboration in beam dynamics.

Normally it is published every April, August and December. The deadlines are 15 March, 15 July and 15 November, respectively.

Categories of Articles

The categories of articles in the newsletter are the following:

1. Announcements from the panel.
2. Reports of beam dynamics activity of a group.
3. Reports on workshops, meetings and other events related to beam dynamics.
4. Announcements of future beam dynamics-related international workshops and meetings.
5. Those who want to use newsletter to announce their workshops are welcome to do so. Articles should typically fit within half a page and include descriptions of the subject, date, place, Web site and other contact information.
6. Review of beam dynamics problems: This is a place to bring attention to unsolved problems and should not be used to report completed work. Clear and short highlights on the problem are encouraged.
7. Letters to the editor: a forum open to everyone. Anybody can express his/her opinion on the beam dynamics and related activities, by sending it to one of the editors. The editors reserve the right to reject contributions they judge to be inappropriate, although they have rarely had cause to do so.

The editors may request an article following a recommendation by panel members. However anyone who wishes to submit an article is strongly encouraged to contact any Beam Dynamics Panel member before starting to write.

7.1.2 How to Prepare a Manuscript

Before starting to write, authors should download the template in Microsoft Word format from the Beam Dynamics Panel web site:

<http://www-bd.fnal.gov/icfabd/news.html>

It will be much easier to guarantee acceptance of the article if the template is used and the instructions included in it are respected. The template and instructions are expected to evolve with time so please make sure always to use the latest versions.

The final Microsoft Word file should be sent to one of the editors, preferably the issue editor, by email.

The editors regret that LaTeX files can no longer be accepted: a majority of contributors now prefer Word and we simply do not have the resources to make the conversions that would be needed. Contributions received in LaTeX will now be returned to the authors for re-formatting.

In cases where an article is composed entirely of straightforward prose (no equations, figures, tables, special symbols, etc.) contributions received in the form of plain text files may be accepted at the discretion of the issue editor.

Each article should include the title, authors' names, affiliations and e-mail addresses.

7.1.3 Distribution

A complete archive of issues of this newsletter from 1995 to the latest issue is available at

<http://icfa-usa.jlab.org/archive/newsletter.shtml>.

This is now intended as the primary method of distribution of the newsletter.

Readers are encouraged to sign-up for electronic mailing list to ensure that they will hear immediately when a new issue is published.

The Panel's Web site provides access to the Newsletters, information about future and past workshops, and other information useful to accelerator physicists. There are links to pages of information of local interest for each of the three ICFA areas.

Printed copies of the ICFA Beam Dynamics Newsletters are also distributed (generally some time after the Web edition appears) through the following distributors:

Weiren Chou	chou@fnal.gov	North and South Americas
Rainer Wanzenberg	rainer.wanzenberg@desy.de	Europe ⁺⁺ and Africa
Susumu Kamada	susumu.kamada@kek.jp	Asia ^{**} and Pacific

⁺⁺ Including former Soviet Union.

^{**} For Mainland China, Jiu-Qing Wang (wangjq@mail.ihep.ac.cn) takes care of the distribution with Ms. Su Ping, Secretariat of PASC, P.O. Box 918, Beijing 100039, China.

To keep costs down (remember that the Panel has no budget of its own) readers are encouraged to use the Web as much as possible. In particular, if you receive a paper copy that you no longer require, please inform the appropriate distributor.

7.1.4 Regular Correspondents

The Beam Dynamics Newsletter particularly encourages contributions from smaller institutions and countries where the accelerator physics community is small. Since it is impossible for the editors and panel members to survey all beam dynamics activity worldwide, we have some Regular Correspondents. They are expected to find interesting activities and appropriate persons to report them and/or report them by themselves. We hope that we will have a “compact and complete” list covering all over the world eventually. The present Regular Correspondents are as follows:

Liu Lin	Liu@lnls.br	LNLS, Brazil
Sameen Ahmed Khan	Rohelakan@yahoo.com	SCOT, Oman
Jacob Rodnizki	Jacob.Rodnizki@gmail.com	Soreq NRC, Israel
Rohan Dowd	Rohan.Dowd@synchrotron.org.au	Australian Synchrotron

We are calling for more volunteers as Regular Correspondents.

7.2 ICFA Beam Dynamics Panel Members

Name	eMail	Institution
Rick Baartman	baartman@lin12.triumf.ca	TRIUMF, 4004 Wesbrook Mall, Vancouver, BC, V6T 2A3, Canada
Marica Biagini	marica.biagini@lnf.infn.it	LNF-INFN, Via E. Fermi 40, Frascati 00044, Italy
Yunhai Cai	yunhai@slac.stanford.edu	SLAC, 2575 Sand Hill Road, MS 26, Menlo Park, CA 94025, U.S.A.
Swapn Chattopadhyay	swapan@cockcroft.ac.uk	The Cockcroft Institute, Daresbury, Warrington WA4 4AD, U.K.
Weiren Chou (Chair)	chou@fnal.gov	Fermilab, P.O. Box 500, Batavia, IL 60510, U.S.A.
Wolfram Fischer	wfisher@bnl.gov	Brookhaven National Laboratory, Bldg. 911B, Upton, NY 11973, U.S.A.
Yoshihiro Funakoshi	yoshihiro.funakoshi@kek.jp	KEK, 1-1 Oho, Tsukuba-shi, Ibaraki-ken, 305-0801, Japan
Miguel Furman	mafurman@lbl.gov	Center for Beam Physics, LBL, 1 Cyclotron Road, Berkeley, CA 94720-8211, U.S.A.
Jie Gao	gaoj@ihep.ac.cn	Institute for High Energy Physics, P.O. Box 918, Beijing 100049, China
Ajay Ghodke	ghodke@cat.ernet.in	RRCAT, ADL Bldg. Indore, Madhya Pradesh, 452 013, India
Ingo Hofmann	i.hofmann@gsi.de	High Current Beam Physics, GSI Darmstadt, Planckstr. 1, 64291 Darmstadt, Germany
Sergei Ivanov	ivanov_s@mx.ihep.su	Institute for High Energy Physics, Protvino, Moscow Region, 142281 Russia
Kwang-Je Kim	kwangje@aps.anl.gov	Argonne Nat'l Lab, Advanced Photon Source, 9700 S. Cass Avenue, Argonne, IL 60439, U.S.A.
In Soo Ko	isko@postech.ac.kr	Pohang Accelerator Lab, San 31, Hyoja-Dong, Pohang 790-784, South Korea
Alessandra Lombardi	alessandra.lombardi@cern.ch	CERN, CH-1211, Geneva 23, Switzerland
Yoshiharu Mori	mori@kl.rii.kyoto-u.ac.jp	Research Reactor Inst., Kyoto Univ. Kumatori, Osaka, 590-0494, Japan
Mark Palmer	mark.palmer@cornell.edu	Wilson Laboratory, Cornell University, Ithaca, NY 14853-8001, USA
Chris Prior	c.r.prior@rl.ac.uk	ASTeC Intense Beams Group, STFC RAL, Chilton, Didcot, Oxon OX11 0QX, U.K.
Yuri Shatunov	yu.m.shatunov@inp.nsk.su	Acad. Lavrentiev, prospect 11, 630090 Novosibirsk, Russia
Junji Urakawa	junji.urakawa@kek.jp	KEK, 1-1 Oho, Tsukuba-shi, Ibaraki-ken, 305-0801, Japan
Jiu-Qing Wang	wangjq@mail.ihep.av.cn	Institute for High Energy Physics, P.O. Box 918, 9-1, Beijing 100049, China
Rainer Wanzenberg	rainer.wanzenberg@desy.de	DESY, Notkestrasse 85, 22603 Hamburg, Germany

*The views expressed in this newsletter do not necessarily coincide with those of the editors.
The individual authors are responsible for their text.*